# Color and Appearance in Dentistry

Alvaro Della Bona
*Editor*

Springer

# Color and Appearance in Dentistry

Alvaro Della Bona
Editor

# Color and Appearance in Dentistry

Springer

*Editor*
Alvaro Della Bona
Dental School
Universidade de Passo Fundo
Passo Fundo, RS
Brazil

ISBN 978-3-030-42625-5 ISBN 978-3-030-42626-2 (eBook)
https://doi.org/10.1007/978-3-030-42626-2



This Springer imprint is published by the registered company Springer Nature Switzerland AG
The registered company address is: Gewerbestrasse 11, 6330 Cham, Switzerland

*For my parents, Carlos and Zelima,*
*who taught me to appreciate love,*
*joy, and kindness.*

*For my wife Carla and children,*
*Izadora and Diogo,*
*who gave me the gift to continue*
*sharing those feelings.*

# Preface

This book is a result of international collaboration with subsequent scientific research publications in distinguished international journals, followed by evidence-based information illustrated by clinical procedures. Therefore, writing this book was a long, cumulative process involving learning, researching, clinical experience, and, most importantly, collaboration with outstanding experts from the University of Granada, Spain.

Interacting with university and industry experts and dental clinicians from around the world created the foundation for this text, which endeavors to explain the color science and its application in Dentistry, to assist in teaching and training color determination in Dentistry, to guide on visual and instrumental dental shade matching, offering guidelines on color management and communication in Dentistry, and glancing on future developments using artificial intelligence (AI) in Dentistry.

Therefore, this book was designed to enhance understanding of Color and Appearance in Dentistry for students, researchers, and clinicians.

Passo Fundo, RS, Brazil — Alvaro Della Bona

# Acknowledgements

This book was only possible because of the outstanding expertise from Dr. María del Mar Pérez Gómez, Dr. Razvan Ionut Ghinea, Dr. Ana María Andreea Ionescu, Dr. Oscar Emilio Pecho Yataco, Dr. Juan de la Cruz Cardona Pérez, Dr. Luis Javier Herrera Maldonado, Me. Francisco Carrillo Pérez, and the support of our families.

The authors are very grateful to their mentors for providing knowledgeable guidance, sage advice, thought-provoking discussion, and critical thinking.

# Contents

# About the Editors

**Alvaro Della Bona, DDS, MMedSci, PhD, FADM** Doctor of Dental Science (DDS) at the University of Passo Fundo, RS, Brazil (1987). Preceptorship in Restorative Dentistry at the University of Texas Health Science Center at San Antonio, TX, USA (1992). Master of Medical Science (MMedSci) in Restorative Dentistry at the University of Sheffield, UK (1994). in Dental Biomaterials at the University of Otago, New Zealand (1996). Doctor of Philosophy (PhD) in Materials Science & Engineering at the University of Florida, USA (2001). Postdoctoral in Tissue Engineering at the University of Michigan, USA (2013). Postdoctoral in Hybrid Ceramic 3D Printing at the University of Colorado, USA (2020). University of Passo Fundo, RS, Brazil. Past-President of the Academy of Dental Materials (ADM).

# Color Science and Its Application in Dentistry

1

María del Mar Pérez Gómez, Razvan Ionut Ghinea, Ana María Andreea Ionescu, Oscar Emilio Pecho Yataco, and Alvaro Della Bona

## Contents



## 1.1 Color Measurements and Whiteness Indexes

A common ultimate goal of color measurement or shade specification in dentistry is the reproduction of important appearance characteristics of oral structures by prosthetic materials. Within the dental clinical setting, whenever an indirect restoration is planned for an area that is readily observed and the restoration would be easily assessed for harmony to adjacent existing natural structure, it would be ideal to quantify valid color information fast and reliably using the patient's existing natural

M. del M. Pérez Gómez (✉) · R. I. Ghinea · A. M. A. Ionescu
Optics Department, Faculty of Science, University of Granada, Granada, Spain
e-mail: mmperez@ugr.es; rghinea@ugr.es; anaionescu@ugr.es

O. E. Pecho Yataco · A. Della Bona
Dental School, Postgraduate Program in Dentistry, University of Passo Fundo, Passo Fundo, RS, Brazil
e-mail: dbona@upf.br


A. Della Bona (ed.), *Color and Appearance in Dentistry*,
https://doi.org/10.1007/978-3-030-42626-2_1

structure, which has characteristics throughout the visible spectrum. Such information is used to facilitate the complex color scenario that comprise the restoration, which can have similar colors under various illumination conditions, within at least acceptable limits but, more preferably, within limits of perceived color difference**.**

Color measurements in dentistry often involve nonhomogeneous layers of both natural and prosthetic materials with varying inherent color and translucency. In addition, teeth often present interesting texture and curved surface. By contrast, color and reflectance standards are flat and opaque, mainly due to the complicating effects of both translucency and non-planar surfaces on color measurement.

### 1.1.1 CIE Standard Observers

The color of an object depends on its spectral reflectance, the spectral power distribution of the light source, and, finally, the observer. When performing a color measurement it is important to standardize all the observation/measurement conditions in order to obtain reproducible and trustful results that can be comparable with previous studies.

#### 1.1.1.1 CIE 1931 Standard Colorimetric Observer

The CIE 1931 standard colorimetric observer is defined for a 2° foveal field of observation (2° field corresponds to an area of the macula lutea that has a practically constant density of photoreceptors) and a dark surround.

The CIE 1931 2° observer was derived from results of two investigations on color matching of test stimuli with mixtures of three RGB primary stimuli, conducted by WD Wright and J Guild. The results of these studies led to the first $\bar{r}(\lambda), \bar{g}(\lambda), \bar{b}(\lambda)$ color-matching functions (CMF), which characterize the CIE 1931 2° standard observer. However, these first matching functions presented negative lobes, which referred to the fact that in some parts of the spectrum a match can be obtained only if one of the matching stimuli is added to the test stimulus.

The negative lobes present in the CMFs made calculations difficult and, therefore, in 1931, the International Commission on Illumination decided to transform from the real RGB primaries to a set of imaginary primaries *X Y Z*, with the difference that, in this latter case, the new CMFs that characterize the observer do not have negative lobes. In addition, an equienergy stimulus was characterized by equal tristimulus values ($X = Y = Z$), one of the tristimulus provide photometric quantities and the volume of the tetrad on set by the new primaries should be as small as possible.

Therefore, *X Y Z* tristimuli values are calculated as the integral over the visible spectrum (380 nm–780 nm):

$$X = k \int_{380\text{nm}}^{780\text{nm}} \phi_{\lambda}(\lambda)\bar{x}(\lambda)\,\mathrm{d}\lambda$$

$$Y = k \int_{380\text{nm}}^{780\text{nm}} \phi_\lambda(\lambda)\bar{y}(\lambda)\mathrm{d}\lambda$$

$$Z = k \int_{380\text{nm}}^{780\text{nm}} \phi_\lambda(\lambda)\bar{z}(\lambda)\mathrm{d}\lambda$$

where $k$ is a constant; $\phi(\lambda)$ is the color stimulus function of the light seen by the observer and $\bar{x}(\lambda), \bar{y}(\lambda), \bar{z}(\lambda)$ are the CMF of the CIE 1931 standard colorimetric observer.

However, according to the CIE recommendations, the $X\,Y\,Z$ tristimuli values can be calculated as numerical summation at wavelength intervals ($\Delta\lambda$) by applying the following equations:

$$X = k\sum_k \phi_\lambda(\lambda)\bar{x}(\lambda)\Delta\lambda$$

$$Y = k\sum_k \phi_\lambda(\lambda)\bar{y}(\lambda)\Delta\lambda$$

$$Z = k\sum_k \phi_\lambda(\lambda)\bar{z}(\lambda)\Delta\lambda$$

In the case of a non-self-luminous object, the spectral reflection of the surface is described by the spectral reflectance factor $R(\lambda)$ and the spectral transmission is described by the spectral transmittance factor $T(\lambda)$. Taking into account these considerations, the relative color stimulus function $\phi(\lambda)$ for reflecting or transmitting objects is given by:

$$\phi(\lambda) = R(\lambda)\cdot S(\lambda) \text{ or } \phi(\lambda) = T(\lambda)\cdot S(\lambda.)$$

where $R(\lambda)$ is the spectral reflectance factor; $T(\lambda)$ is the spectral transmittance factor of the object (preferably evaluated for one of the standard geometric conditions recommended by CIE), and $S(\lambda)$ is the relative spectral power distribution of the illuminant (preferably, one of CIE standard illuminants).

In this case, the constant $k$ is chosen so that the tristimulus value $Y = 100$ for objects that have $R(\lambda) = 1$ or $T(\lambda) = 1$ at all wavelengths:

$$k = \frac{100}{\sum_\lambda S(\lambda)\cdot\bar{y}(\lambda)d(\lambda)}$$

The color-matching functions of the CIE 1931 standard colorimetric observer are given as values from 360 nm to 830 nm at 1 nm intervals [1] (Fig. 1.1). This observer should be used if the field subtended by the sample is between 1° and 4° at the eye of the observer. In technical applications, this observer is often addressed as 2° standard colorimetric observer.

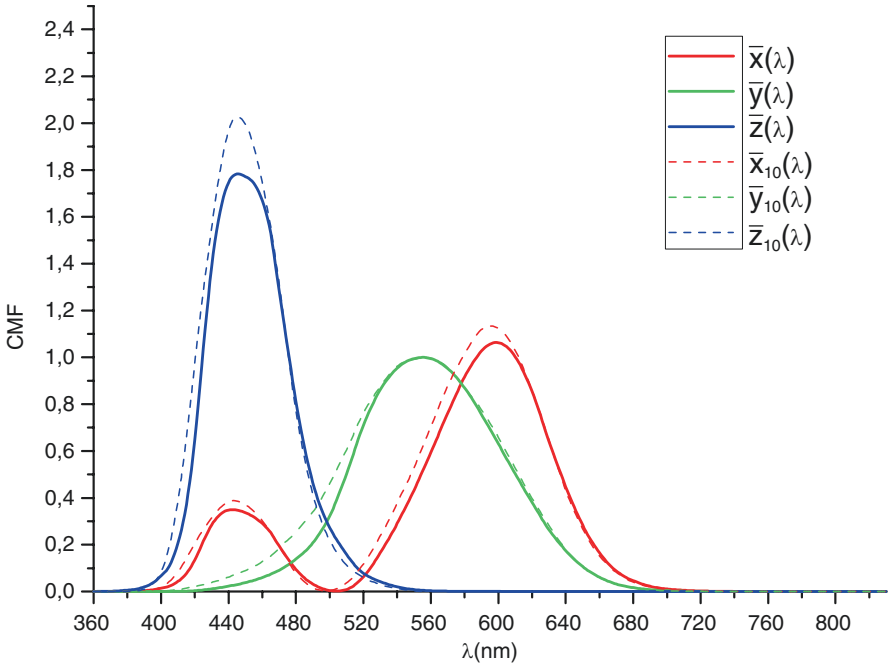


**Fig. 1.1** $\bar{x}(\lambda), \bar{y}(\lambda), \bar{z}(\lambda)$ color-matching functions (CMF) of the CIE 1931 standard colorimetric observer (continuous line) and the $\bar{x}_{10}(\lambda), \bar{y}_{10}(\lambda), \bar{z}_{10}(\lambda)$ color-matching functions of the [2] standard colorimetric observer (dotted line)

#### 1.1.1.2 CIE [2] Standard Colorimetric Observer

As specified before, the CIE 1931 2° standard observer is recommended only for small stimuli, which is 1°–4° at the eye of the observer. However, the description of a larger stimulus that falls on a larger area of the macula lutea, or it is seen partially parafoveally, is required. In this sense, the International Commission on Illumination standardized a large-field colorimetric system [2] based on the visual observations conducted on a 10° visual field.

The adoption of a 10° colorimetric observer was based on the works of Stiles and Burch in 1959, which used different sets of monochromatic primaries, and the CMFs were obtained directly from the observations, and no appeal to heterochromatic brightness measurements or to any luminous efficiency function was required.

The color-matching functions of the 10° system are distinguished from the 2° system by a 10 subscript. The color-matching functions of the [2] standard colorimetric observer are given as values from 360 nm to 830 nm at 1 nm intervals [1] (Fig. 1.1).

The tristimulus values are calculated similar to the case of the 2° standard observer:

$$X = k_{10} \cdot \int_{380\text{nm}}^{780\text{nm}} \phi_\lambda(\lambda)\bar{x}_{10}(\lambda)\mathrm{d}\lambda$$

$$Y = k_{10} \cdot \int_{380\text{nm}}^{780\text{nm}} \phi_\lambda(\lambda)\bar{y}_{10}(\lambda)\mathrm{d}\lambda$$

$$Z = k_{10} \cdot \int_{380\text{nm}}^{780\text{nm}} \phi_\lambda(\lambda)\bar{z}_{10}(\lambda)\mathrm{d}\lambda$$

and the $k_{10}$ constant for non-self-luminous objects is defined by the following equation:

$$k_{10} = \frac{100}{\sum_\lambda S(\lambda)\cdot\bar{y}_{10}(\lambda)d(\lambda)}$$

Apart from the recommendations regarding the field sustained by the sample, there are additional factors that have to be taken into account when using the [2] standard colorimetric observer. The precision of the system is greater than that of the CIE 1931 trichromatic system since it has been determined with a higher number of observers but the larger stimulus area rod intrusion had to be considered as well. Further, in the case of using the 10° observer without any rod-correction, the luminance levels have to be high enough. While in the case of a 2° field one can calculate with photopic adaptation down to about 10 cd/m$^2$, this is not the case for the larger field size. In this sense, CIE [1] recommends the following: "The large-field color matching data as defined by the [2] standard colorimetric observer are intended to apply to matches where the luminance and the relative spectral power distributions of the matched stimuli are such that no participation of the rod receptors of the visual mechanism is to be expected." This condition of observation is important as "rod intrusion" may upset the predictions of the standard observer. For daylight, possible participation of rod vision in color matches is likely to diminish progressively above, approximately, 10 cd/m$^2$ and be entirely absent at about 200 cd/m$^2$.

### 1.1.2 CIE Color Space

The color of a stimulus can be specified by a triplet of tristimulus values ($X$, $Y$, $Z$). In order to provide a convenient two-dimensional representation of the color, chromaticity diagrams were developed. In the transformation from tristimulus values to chromaticity coordinates, a normalization that removes luminance information is performed. This transformation is defined by:

$$x = \frac{X}{X+Y+Z}$$

$$y = \frac{Y}{X+Y+Z}$$

$$z = \frac{Z}{X+Y+Z}$$

Chromaticity coordinates attempt to represent a three-dimensional phenomenon with just two variables. To fully specify a colored stimulus, one of the tristimulus values must be reported in addition to two of the chromaticity coordinates. Usually, the *Y* tristimulus value is reported since it represents the luminance information. Therefore, this color space is often called the CIE *Yxy* space.

The CIE *Yxy* space is well suited to describe color stimuli. However, the practical use of colorimetry very often requires information about whether two samples will be indistinguishable by visual observation or not. MacAdam showed that the chromaticity difference that corresponds to a just noticeable color difference will be different in different areas of the *xy* chromaticity diagram, and also, at one point in the diagram, equal chromaticity differences in distinct directions represent visual color differences of distinct magnitudes [3]. Many attempts were made to transform the *xy* diagram in such a form that the MacAdam ellipses become circles, but it should be mentioned that there is still no perfect transformation available.

Nowadays, the use of the chromaticity diagrams has become largely obsolete, and CIELAB and CIELUV color spaces are the most frequently used. One of the main characteristics of these two color spaces is that they extend tristimulus colorimetry to three-dimensional spaces with dimensions that approximately correlate with the perceived lightness, chroma, and hue of a colored stimulus. This is achieved by incorporating features to account for chromatic adaptation and nonlinear visual responses. The main aim in the development of these spaces was to provide uniform practices for the measurement of color differences, something that cannot be done reliably in tristimulus or chromaticity spaces. The International Commission on Illumination recommended, in 1976, the use of both spaces, since there was no clear evidence to support one over the other at that time. However, over time, CIELAB has been greater implemented in color applications than the CIELUV color space. This is also true for dental color studies.

### 1.1.2.1 CIE 1976 ($L^*a^*b^*$) Color Space—CIELAB

The CIE 1976 ($L^*a^*b^*$) color space, or simply CIELAB, is defined by the following equations [1]:

$$L^* = 116 \cdot f\left(Y/Y_n\right) - 16$$

$$a^* = 500 \cdot \left[ f\left( X/X_n \right) - f\left( Y/Y_n \right) \right]$$

$$b^* = 200 \cdot \left[ f\left( Y/Y_n \right) - f\left( Z/Z_n \right) \right]$$

where

$$f\left( X/X_n \right) = \left( X/X_n \right)^{1/3} \text{ if } \left( X/X_n \right) > \left( 24/116 \right)^3$$

$$f\left( X/X_n \right) = \left( 841/108 \right) \cdot \left( X/X_n \right) + 16/116 \text{ if } \left( X/X_n \right) \le \left( 24/116 \right)^3$$

and

$$f\left( Y/Y_n \right) = \left( Y/Y_n \right)^{1/3} \text{ if } \left( Y/Y_n \right) > \left( 24/116 \right)^3$$

$$f\left( Y/Y_n \right) = \left( 841/108 \right) \cdot \left( Y/Y_n \right) + 16/116 \text{ if } \left( Y/Y_n \right) \le \left( 24/116 \right)^3$$

and

$$f\left( Z/Z_n \right) = \left( Z/Z_n \right)^{1/3} \text{ if } \left( Z/Z_n \right) > \left( 24/116 \right)^3$$

$$f\left( Z/Z_n \right) = \left( 841/108 \right) \cdot \left( Z/Z_n \right) + 16/116 \text{ if } \left( Z/Z_n \right) \le \left( 24/116 \right)^3$$

In these equations, $X$, $Y$, and $Z$ are the tristimulus values of the sample and the $X_n$, $Y_n$, and $Z_n$ are the tristimulus values of the reference white. These signals are combined into three response dimensions corresponding to the light–dark, red–green, and yellow–blue responses of the opponent theory of color vision. Finally, appropriate multiplicative constants are incorporated into the equations to provide the required uniform perceptual spacing and proper relationship between the three dimensions.

The CIE $L^*$ coordinate is a correlate to perceive lightness ranging from 0, for black, to 100, for a diffuse white ($L^*$ can sometimes exceed 100.0 for stimuli such as specular highlights in images). The CIE $a^*$ and CIE $b^*$ coordinates correlate approximately with red–green and yellow–blue chroma perceptions. They take on both negative and positive values. Both $a^*$ and $b^*$ have values of 0 for achromatic stimuli (white, gray, black). Their maximum values are limited by the physical properties of materials, rather than the equations themselves. The CIELAB $L^*$, $a^*$, and $b^*$ dimensions are combined as Cartesian coordinates to form a three-dimensional color space (Fig. 1.2).

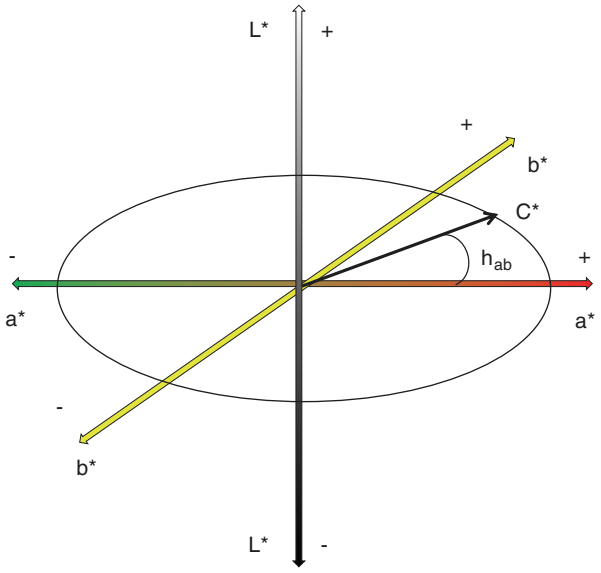


**Fig. 1.2** Schematic representation of the CIELAB color space

In some applications the correlates of the perceived attributes of lightness, chroma, and hue are of more practical interest. In this case, the CIELAB color space is represented using three cylindrical coordinates (lightness—$L^*$; chroma—$C^*_{ab,}$ and hue angle—$h_{ab}$) (Fig. 1.2). The CIE $L^*$ coordinate is calculated as described before, while chroma and hue angle are calculated as follows:

$$C^*_{ab} = \sqrt{\left(a^{*2} + b^{*2}\right)}$$

$$h_{ab} = \arctan\left(b^* / a^*\right)$$

### 1.1.3 Color-Difference Formulas

In the CIELAB color space, the color difference between two object color stimuli of the same size and shape, viewed in identical white to middle-gray surroundings, by an observer photopically adapted to a field of chromaticity not too different from that of average daylight, is quantified as the Euclidean distance between the points representing them in the space. This difference is expressed in terms of the CIELAB $\Delta E^*_{ab}$ color-difference formula, and calculated as:

$$\Delta E^*_{ab} = \sqrt{\Delta L^{*2} + \Delta a^{*2} + \Delta b^{*2}}$$

The CIELAB $\Delta E^*_{ab}$ color-difference formula is widely adopted and it was used in multiple fields and applications. It represented a great step forward toward

harmonization of color-difference evaluation and also color description in the technical world.

The CIELAB color space was designed with the goal of having color differences being perceptually uniform throughout the space, but this goal was not strictly achieved. Soon after its implementation, the CIELAB $\Delta E^*_{ab}$ color-difference formula was reported to present inhomogeneities. To improve the uniformity of color-difference measurements, modifications of the CIELAB $\Delta E^*_{ab}$ equation have been made based upon various empirical data, but in almost all cases a poor correlation between the dataset of visual judgments and the Euclidean distances was found, hence raising the need of equation optimization [4].

Keeping CIELAB coordinate system as a start, several changes were applied to components of the color-difference formula by adapting weighting functions to the three component differences. The Color Measurement Committee (CMC) of the Society of Dyers and Colorists proposed a new color-difference formula denominated CMC(l:c), which became an ISO standard for textile applications in 1995 [5]. Other CIELAB-based formula, named BFD(l:c), which is similar in structure to the CMC(l:c) formula, was proposed by Luo and Rigg, in 1987 [6]. Later, the CIE Technical Committee tried to find an optimization of the CIELAB color-difference formula mainly based on new experiments under well-controlled reference conditions. The resulting recommendation followed the general form of the CMC(l:c) formula and it was called CIE94 color-difference formula ( $\Delta E^*_{94}$ ) [7]. Luo et al. in 2001 [8], proposed a new color-difference metric named CIEDE2000 color difference, which became a CIE recommendation for color-difference computation in 2004 [1]. The CIEDE2000 formula stands as the last, in a long series, of developments improving the CIELAB formula, and outperforms the older CMC(l:c), BFD(l:c), and CIE94 formulas [5].

CIEDE2000 total color-difference formula [8] corrects for the non-uniformity of the CIELAB color space for small color differences under reference conditions. Improvements to the calculation of total color difference for industrial color-difference evaluation were made through corrections for effects of lightness dependence, chroma dependence, hue dependence, and hue–chroma interaction on perceived color difference. The scaling along the $a^*$ axis is modified to correct for a non-uniformity observed with gray colors. The resulting recommendation is as follows [1]:

$$\Delta E_{00} = \sqrt{\left(\frac{\Delta L'}{K_L S_L}\right)^2 + \left(\frac{\Delta C'}{K_C S_C}\right)^2 + \left(\frac{\Delta H'}{K_H S_H}\right)^2 + R_T \left(\frac{\Delta C'}{K_C S_C}\right)\left(\frac{\Delta H'}{K_H S_H}\right)}$$

$$L' = L^*$$

$$a' = a^* \left(1 + G\right)$$

$$b' = b^*$$

$$G = 0.5\left(1 - \sqrt{\frac{\bar{C}_{ab}^{*\,7}}{\bar{C}_{ab}^{*\,7} + 25^7}}\right)$$

The weighting functions $S_L$, $S_C$, $S_H$ adjust the total color difference for variation in perceived magnitude with variation in the location of the color-difference pair in $L'$, $a'$, and $b'$ coordinates.

$$S_L = 1 + \frac{0.015\left(\bar{L}' - 50\right)^2}{\sqrt{20 + \left(\bar{L}' - 50\right)^2}}$$

$$S_C = 1 + 0.045\bar{C}'$$

$$S_H = 1 + 0.015\bar{C}'T$$

$$T = 1 - 0.17\cos\left(\bar{h}' - 30\right) + 0.24\cos\left(2\bar{h}'\right) + 0.32\cos\left(3\bar{h}' + 6\right) - 0.20\cos\left(4\bar{h}' - 63\right)$$

Visual color-difference perception data show an interaction between chroma difference and hue difference in the blue region that is observed as a tilt of the major axis of a color-difference ellipsoid from the direction of constant hue angle. To account for this effect, a rotation function is applied to weighted hue and chroma differences:

$$R_T = -\sin\left(2\Delta\Theta\right)R_C$$

$$\Delta\Theta = 30\exp\left\{-\left[\left(\bar{h}' - 275\right)\Big/25\right]^2\right\}$$

$$R_C = 2\sqrt{\frac{\bar{C}'^7}{\bar{C}'^7 + 25^7}}$$

The parametric factors $K_L$, $K_C$, $K_H$, are correction terms for variation in experimental conditions. Under reference conditions they are all set to 1. The reference conditions are defined by the International Commission on Illumination as [1]:

- Illumination: source simulating the spectral relative irradiance of CIE standard illuminant D65;
- Illuminance: 1000 lx;
- Observer: normal color vision;
- Background field: uniform, neutral gray with $L^* = 50$;
- Viewing mode: object;
- Sample size: greater than four degrees subtended visual angle;

– Sample separation: minimum sample separation achieved by placing the sample pair in direct edge contact;
– Sample color-difference magnitude: 0–5 CIELAB units;
– Sample structure: homogeneous color without visually apparent pattern or non-uniformity.

Few years after the CIEDE2000 ($\Delta E_{00}$) color-difference formula was published, comparisons between CIELAB and CIEDE2000 formulas were already available in dental literature [9, 10]. In addition, some studies showed significant correlations between $\Delta E^*_{ab}$ and $\Delta E_{00}$ values of resin composites [10–12], metal-ceramic and all-ceramic restorations [13], and natural tooth color space [14, 15]. The majority of reported correlations showed the values obtained from these formulas are proportional, but the two color-difference formulas cannot be used interchangeably to evaluate the color differences in dentistry.

A recent study [14, 15] determined the relationship between the results provided by classic $\Delta E^*_{ab}$ and CIEDE2000 formulas in the natural tooth color space using the Bland and Altman approach. The results obtained showed that in the natural tooth color space, the scale factor between both formulas values changes from 0.46 to 0.90, suggesting it is difficult an accurate scale factor between both values. Furthermore, the $\Delta E_{00}/\Delta E^*_{ab}$ ratio increases with the increase in $\Delta L^*$ and the decrease in $\Delta b^*$. Additionally, CIEDE2000 formula reflected the color differences perceived by the human eye better than the CIELAB formula [14–17]. It was reported that CIEDE2000 (2:1:1) formula showed the best estimate to visual perception when compared to CIELAB and CIEDE2000 (1:1:1) formulas [16, 17]. CIELAB and CIEDE2000 (2:1:1) formulas were also used to evaluate the influence of gender on visual shade matching. Only CIEDE2000 (2:1:1) formula showed a statistical difference between genders [18].

### 1.1.4 Whiteness Indexes

In spectral terms, a white material is the one that has a constant and high (near to 100%) reflectance across the entire visible wavelength range. Whiteness is generally considered to be a one-dimensional perception defined by Ganz as an attribute of color of high luminous reflectance and low purity situated in a relatively narrow region of the color space along dominant wavelengths of 570 nm and 470 nm, approximately. In terms of CIELAB color space, this type of spectral behavior is translated into a very high lightness ($L^*$) and very low (ideally zero) chroma ($C^*_{ab}$).

For a three-dimensional color space, three color coordinates are necessary for a complete identification of any white. However, a one-dimensional color index can be more efficient for identifying the properties of white materials. Since colors perceived as white are in a three-dimensional color space, most observers are able to arrange white samples in one-dimensional order according to whiteness.

In the literature, numerous whiteness indices have been proposed for various industrial needs. Yet, only those relevant to dental applications are considered in

this text. One of them is the CIE whiteness index (WIC), which was proposed by CIE in 1986 for the neutral hue preference [19].

$$\mathrm{WIC} = Y + 800\left(x_n - x\right) + 1700\left(y_n - y\right)$$

where $x$, $y$ are chromaticity coordinates defined as the ratio of individual tristimulus value and the sum of all three tristimulus values. $x_n$ and $y_n$ are chromaticity coordinates of the perfect white for the chosen standard observer (2° or 10°), and always under illuminant D65. The WIC formula gives relative, but not absolute, evaluations of whiteness. The higher the value of WIC, the greater the whiteness of the object.

Another whiteness index is based on the Euclidean distance of test color from the perfect white diffuser in the CIELAB color space [20].

$$W^* = \left(100 - L^*\right)^2 + a^{*2} + b^{*2}$$

A modified version of CIE whiteness index (WIO) was proposed specifically for quantifying tooth whiteness based on visual perception of the Vita 3D Shade Guide [21]:

$$\mathrm{WIO} = Y + 1075.012\left(x_n - x\right) + 145.516\left(y_n - y\right)$$

It was found that the WIO index outperformed other whiteness and yellowness indices for tooth whiteness assessment and was as reliable as the average human observer. In a study of colorimetric analysis of shade guides, it was demonstrated that the WIO gave the best fit with the instrumental color measurements.

A new CIELAB-based whiteness index for dentistry, $\mathrm{WI_D}$, was proposed based on correlations with visual perception of shade guide tabs and dental materials [22].

$$\mathrm{WI_D} = 0.511L^* - 2.324a^* - 1.100b^*$$

$\mathrm{WI_D}$ showed an improved correlation to the associated visual perception data compared to all other CIELAB and CIE 1931 XYZ-based whiteness or yellowness indexes tested under laboratory and clinical conditions. The results [22] showed that only WIO index was comparable to $\mathrm{WI_D}$ index. Further evaluations were done, including validation experiments under laboratory and typical clinical conditions, showing that the $\mathrm{WI_D}$ index outperformed previous indices, being the most adequate CIELAB-based index to evaluate whiteness in dentistry. Considering the popularity of CIELAB in dentistry and that color-measuring devices used in dental practice use this color space for color specification, the proposed whiteness index represents a significant step forward on measuring and evaluating whiteness in dentistry. Therefore, changes ($\Delta\mathrm{WI_D}$) on tooth whitening treatments can be calculated as [23, 24]:

$$\Delta\mathrm{WI_D} = \mathrm{WI_D}\left(\mathrm{treament}\right) - \mathrm{WI_D}\left(\mathrm{baseline}\right)$$

## 1.2 Optical Properties and Measuring Methods

### 1.2.1 Optical Properties

Scattering and absorption are the main processes light suffers when traveling throughout a tissue or biomaterial.

#### 1.2.1.1 Scattering

The scattering of the optical radiation in tissues or biomaterials occurs due to variations in the refractive index at microscopic level (cell membranes, cellular organelles, etc.). Similar to absorption, a scattering coefficient ($\mu_s$) can be defined as:

$$I = I_0 e^{-\mu_s x}$$

where $I$ is the undispersed component of the light beam after crossing a non-absorbing sample with a thickness $x$. The inverse amount of the scattering coefficient ($1/\mu_s$) is named scattering penetration and it is equal to the average optical path that a photon passes between two consecutive dispersions. It is also possible to define the optical thickness of a sample as the product between the dispersion penetration and the sample thickness ($\mu_s x$—dimensionless measure).

When an incident photon with a direction described by the unit vector $\vec{e}_s$ suffers a scattering, the probability that its new direction of displacement is described by another unitary vector $\vec{e}_s'$ is given by the normalized phase function $f\left(\vec{e}_s \cdot \vec{e}_s'\right)$. For tissues, it can be considered that the distribution probability is a function that depends only on the angle formed by the direction of the incident photon and the scattered photon ($\theta$). Thus, this probability can be expressed in a very convenient way as a function of the cosine of the dispersion angle ($\vec{e}_s \cdot \vec{e}_s' = cos\theta$):

$$f\left(\vec{e}_s \cdot \vec{e}_s'\right) = f\left(\cos\theta\right)$$

Therefore, the anisotropy of a material or tissue can be characterized by using the mean value of the cosine of the scattering angle. The parameter used is called anisotropy factor (factor):

$$g = \int_{-1}^{1} \cos\theta \left[ f\left(\cos\theta\right)\theta \right] d\cos\theta$$

#### 1.2.1.2 Absorption

The absorption coefficient ($\mu_a$) is defined as:

$$dI = \mu_a I dx$$

where $dI$ is the differential variation of the intensity of a collimated luminous beam that travels an infinitesimal dx path in a homogeneous medium having the absorption coefficient $\mu_a$. The inverse amount of the absorption coefficient ($1/\mu_a$) is named

absorption penetration and is equal to the average optical path that a photon passes between two consecutive absorptions. If the medium has a thickness ($x$), then:

$$I = I_0 e^{-\mu_a x}$$

### 1.2.1.3 Transmittance

The transmittance ($T$) is defined as the ratio between the intensity of the light beam transmitted by the analyzed material ($I$) and the intensity of the incident light beam ($I_0$):

$$T = \frac{I}{I_0}$$

Reflection and transmission greatly influence the chromatic appearance, and scattering and absorption are the main optical phenomena that affect the way optical radiation propagates through the material. Even if the effect of both phenomena is important, scattering is considered to have a greater influence on the propagation of optical radiation, since even for very thin samples (<1 mm) there is a high probability that photons will suffer multiple dispersions before crossing the sample as a result of the atomic interaction with the elements of the analyzed material. The relative probability to occur these interaction processes depends on the wavelength of the incident radiation. Therefore, when the incident radiation is polychromatic (consisting of several wavelengths), these properties are to be reported spectrally (depending on wavelength).

### 1.2.1.4 Radiative Transport Equation

Propagation of optical radiation through tissues (as natural tooth) could be described using fundamental electromagnetic theory. In this case, the tissue should be considered as a medium with a position-dependent permittivity so that field variations can be described using Maxwell's equations. This approach is not possible due to the high complexity of the tissue structure as well as to the lack of precise knowledge of its permittivity. The problem can be simplified by ignoring phenomena related to wave propagation, such as polarization and interference, as well as phenomena related to microscopic particles, such as inelastic collisions.

Thus, according to this theory, the radiance $L\left(r,\vec{s}\right)$ of a light beam in the position $r$ propagating in the direction described by the unit vector $\vec{s}$ is diminished due to absorption and scattering and amplified by radiation propagating in the direction of $\vec{s}'$ but scattered in the direction of $\vec{s}$. The equation describing this phenomenon is as follows:

$$\vec{s}\cdot\nabla L\left(r,\vec{s}\right) = -\left(\mu_a+\mu_s\right)L\left(r,\vec{s}\right) + \mu_s\int_{4\pi} p\left(\vec{s},\vec{s}'\right)L\left(r,\vec{s}'\right)d\omega'$$

where $\mu_a$ is the asorption coefficient, $\mu_s$ is the scattering coefficient, $d\omega'$ is the differential solid angle in $\vec{s}'$ direction, and $p\left(\vec{s},\vec{s}'\right)$ is the phase function.

The phase function describes the angular distribution for a single scattering and generally depends on the angle formed between $\vec{s}$ and $\vec{s}'$. In general, the phase function is not known, being characterized by the anisotropy factor ($g$):

$$g = \int_{4\pi} p\left(\vec{s},\vec{s}'\right)\left(\vec{s}\cdot\vec{s}'\right)d\omega'$$

Solving of the radiative transport equation has a high degree of difficulty, which has led over time to propose different approximations for the radiance and/or phase function. Thus, the type of approximation that can be applied to calculate the distribution of a light beam through the biological tissues depends on the type of irradiation (diffuse or collimated) and the presence of a variation of the refractive index.

#### 1.2.1.5 Translucency and Opacity

Translucency and opacity are related to the ability of a material to transmit light. The hiding power or opacity of materials has been described by its contrast ratio (CR). The opacity of a dental material was first described by Paffenbarger and Judd, in 1937 [25], and refined in 1979 for "esthetic dental filling materials" [26]. Subsequently, direct composite materials were described by CR based on luminous reflectance. The popular CR was defined as the ratio of the luminous reflectance of a translucent material on a black backing to the luminous reflectance of the same material on a white backing. Thus, it is important to note that luminous reflectance is the $Y$ tristimulus value in reflectance, as defined by CIE.

$$CR = \frac{Y_B}{Y_W}$$

The thickness required to produce a certain CR can be calculated when the relationship between thickness and CR is known [26]. This method offers the possibility of establishing a critical CR for a given application and then solving for the thickness required to obtain this critical value of translucency.

The translucency parameter (TP) has been used to assess the translucency of dental materials and it is defined as the CIELAB color difference for a material, at a particular thickness, on optical contact with ideal black and white backings [27]. As previously mentioned, CIE currently recommends the use of CIEDE2000 color-difference formula to improve correction between perceived and computed color differences; however, the majority of translucency studies in dental literature still uses TP associated to CIELAB color-difference formula ($\Delta E^*_{ab}$). Thus, in this case, TP values are determined by calculating the color difference between readings from the same specimen over the black ($B$) and the white ($W$) backgrounds using CIELAB color-difference formula ($\mathrm{TP}_{ab}$).

$$\mathrm{TP}_{ab} = \left[\left(L^*_B - L^*_W\right)^2 + \left(a^*_B - a^*_W\right)^2 + \left(b^*_B - b^*_W\right)^2\right]^{1/2}$$

where the subscripts "$B$" and "$W$" refer to color coordinates over the black and the white backgrounds, respectively.

Following CIE current recommendations, the translucency parameter can be calculated using CIEDE2000 color-difference formula ($TP_{00}$) [28]:

$$TP_{00} = \left[ \left( \frac{L_B' - L_W'}{K_L S_L} \right)^2 + \left( \frac{C_B' - C_W'}{K_C S_C} \right)^2 + \left( \frac{H_B' - H_W'}{K_H S_H} \right)^2 + R_T \left( \frac{C_B' - C_W'}{K_C S_C} \right) \left( \frac{H_B' - H_W'}{K_H S_H} \right) \right]^{1/2}$$

where the subscripts "*B*" and "*W*" refer to lightness ($L'$), chroma ($C'$), and hue ($H'$) of the specimens over the black and the white backgrounds, respectively.

#### 1.2.1.6 Opalescence and Fluorescence

Opalescence is one of the most interesting color features of teeth. This is characterized by bluish and amber shades that appear with greater or lesser intensity in the translucent incisal edge of anterior teeth. Its presence in dental reconstructions brings natural beauty to them. Most dental ceramic and resin-based composite systems allow the dental professional to simulate natural dental opalescence to adapt restorations to their natural environment.

Opalescence is caused by the scattering of the visible spectrum of light, giving the material a bluish appearance in reflected color, and an orange/brown appearance in transmitted color, because shorter light wavelengths are more scattered than longer wavelengths. Thus, blue light is scattered throughout the translucent tooth enamel and it is reflected back as a bluish-white light, which is clearly visible as the incisal halo. Structurally, tooth enamel hydroxyapatite crystals (0.16 μm long and 0.02–0.04 μm wide) act as scattering particles causing the opalescence, brightening the tooth and rendering depth and vitality to the structure. As opalescence is more evident in the incisal third of dental crowns, many clinicians, incorrectly, assume that could be specific areas of opalescence in tooth enamel. This, however, is caused by counter opalescence, a phenomenon in which light penetrates an opalescent object and it is reflected from within. Such opalescence is responsible for the orange or orange-pink coloration, commonly seen in the mamelons and incisal edge of the anterior teeth [29].

The most popular index to evaluate opalescence of tooth tissues and esthetic restorative materials is the OP-RT, which is calculated from the difference in yellow-blue ($\Delta b^*$) and red-green ($\Delta a^*$) coordinates between the reflected and transmitted colors measured by spectrophotometers [30].

$$OP - RT = \left[ \left( CIE^*_{a_R} - CIE^*_{a_T} \right)^2 + \left( CIE^*_{b_R} - CIE^*_{b_T} \right)^2 \right]^{1/2}$$

where the subscripts *R* and *T* indicate the reflected and transmitted mode, respectively.

OP-RT values of human and bovine tooth enamel have been reported [30, 31]. As required, enamel color was measured in reflectance and transmittance modes. Two spectrophotometers were used to determine their configuration influence on the OP-RT values of bovine enamel, and one spectrophotometer was used for human

enamel samples because of their reduced dimensions. Sample thickness varied between 0.7 and 1.1 mm for bovine enamel and from 0.9 to 1.3 mm for human enamel. Mean OP-RT value of bovine enamel varied between 10.6 and 19.0 based on the spectrophotometers configuration. A mean OP-RT value of 22.9 was found for human enamel. No significant correlation was found between sample thickness and OP-RT values for both bovine and human enamel.

OP-RT values of restorative materials (ceramics and resin-based composite) were reported as well [29]. Mean OP-RT values of cured direct resin-based composites have a large variation (5.7–23.7) and are usually significant different before (~25.6) and after (~12.4) light activation (polymerization). Those values are much higher than the ones for unfilled resin (3.5). In addition, mean OP-RT values of ceramic systems vary between 1.6 and 7.1. Thus, considering that most of these OP-RT values are lower than the value of tooth enamel, manufacturers should design dental restorative systems to adjust the composition of filler and matrix phases to facilitate the reproduction of natural teeth opalescence.

Fluorescence is defined as the absorption of UV light (100–400 nm invisible light) by an object and its spontaneous emission in longer wavelengths (430–450 nm visible light). Thus, dental practitioners should consider fluorescent emission of human teeth as part of a successful esthetic rehabilitation.

Bluish-white fluorescence of human teeth is resultant from a broad emission band with a diffuse peak at 410–420 nm when subjected to near UV excitation of ~340 nm. In human teeth, fluorescence mostly occurs in dentine because of its greater amount of organic content [32]. As to the endogenous fluorophores in enamel and dentine, studies using UV excitation indicated that light is emitted from the organic matrix embedded in the inorganic calcium apatite matrix [33]. In addition, three distinct fluorescence peaks (350–360 nm, 405–410 nm, and 440–450 nm) were found in enamel and dentine. Another study reported blue fluorescence from dentine at 440 ± 10 nm, with a peak width of about 100 nm [34]. Yet, as chroma of dentine increases, fluorescence decreases. Thus, dentine presents a more intense and a greater index of fluorescence than enamel. Not surprising, fluorescence at the gingival area is significantly greater than at the incisal area. However, there is no significant difference in fluorescence between male and female teeth, nor between upper and lower teeth, nor even between tooth types (incisors, canines, premolars, and molars) taken from the same individual [32].

The fluorescence of human teeth and dental materials can be determined with a color-measuring spectrophotometer or spectroradiometer. Spectral reflectance can be measured over a white standard tile using a standard illuminant D65. A UV filter is inserted or removed to exclude or include the UV component of the illumination. From the spectral reflectance values, the subtraction spectrum is calculated by the inclusion and exclusion of the UV component, and the color difference by the UV component is defined as the fluorescence parameter ( $\Delta E^*_{ab}$ − FL):

$$\Delta E^*_{ab} - \mathrm{FL} = \left[ \left( L^*_i - L^*_e \right)^2 + \left( a^*_i - a^*_e \right)^2 + \left( b^*_i - Lb^*_e \right)^2 \right]^{1/2}$$

where subscripts *i* and *e* indicated UV included and excluded, respectively

Fluorescence properties of resin-based restorative systems vary depending on material, shade, and polymerization. The mean fluorescence parameter value for a resin-based composite was reported to be 2.5 before polymerization and 0.7 after polymerization [35].

### 1.2.2 Methods of Measuring Optical Properties

The optical properties of biological tissues or biomaterials are described in terms of the absorption coefficient, $\mu_a$, the scattering coefficient, $\mu_s$, the scattering function $p(\theta, \psi)$, where $\theta$ is the deflection angle of scatter and $\psi$ is the azimuthal angle of scatter, and the real refractive index of the media. The $p(\theta, \psi)$ is appropriate when discussing only a single or few scattering events, such as during confocal reflectance microscopy, which includes optical coherence tomography. In thicker biomaterials and biological tissues where multiple scattering occurs and the orientations of scattering structures are randomly oriented, the $\psi$ dependence of scattering is averaged and hence ignored, and the multiple scattering averages $\theta$, such that and average parameter, $g = \cos\theta$, called the anisotropy of scatter, characterizes tissue scattering in terms of the relative forward versus backward direction of scatter.

To determine the optical properties of a biomaterial or a tissue is the initial step toward properly designing devices, interpreting diagnostic measurements or planning therapeutic protocols. Secondly, the optical properties are used in a light transport model to predict the light distribution and energy deposition. Thus, it is essential to use adequate methods to determine the optical parameters of tissues and biomaterials and they can be divided into two large groups, direct and indirect methods.

Direct methods include those based on some fundamental concepts and rules such as Bouguer–Beer–Lambert law, the single-scattering phase function for thin samples, or the effective light penetration depth for slabs. The parameters measured are the collimated light transmission, *Tc*, and the angular dependence of the scattered light intensity, $I(\theta)$, for thin samples or the fluence rate distribution inside a slab. These methods are advantageous in that they use very simple analytic expressions for data processing and reconstruction of optical parameters. Their disadvantages are related to the necessity to strictly fulfill experimental conditions dictated by the selected model, single scattering in thin samples, exclusion of the effects of light polarization, etc. In the case of slabs with multiple scattering, the recording detector must be placed far from both the light source and the medium boundaries.

Indirect methods obtain the solution of the inverse scattering problem using a theoretical model of light propagation in a theoretical model of light propagation in a medium. They are divided into iterative and non-iterative models. The former uses equations in which the optical properties are defined through parameters directly related to the quantities being evaluated. The latter are based on the two flux Kubelka–Munk (K-M) model and multi-flux models. In indirect iterative methods, the optical properties are implicitly defined through measured parameters. Quantities determining the optical properties of a scattering medium are listed until the

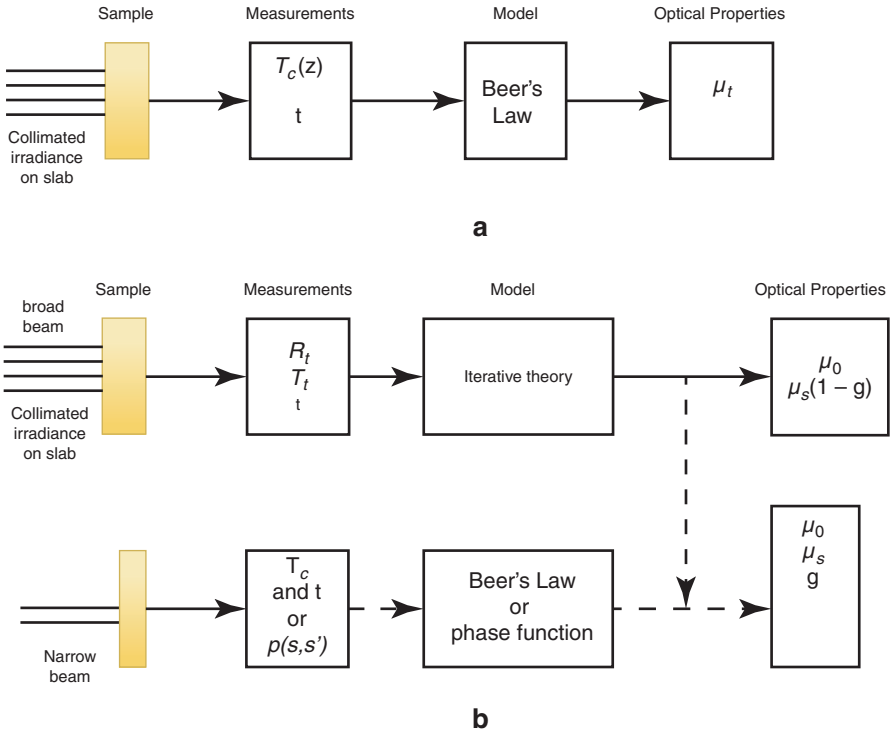


**Fig. 1.3** Schematic representation of (**a**) non-iterative method and (**b**) iterative method

estimated and measured values for reflectance and transmittance coincide with the desired accuracy. These methods are difficult, but the optical models currently in use maybe even more complicated than those underlying non-iterative methods, such as the diffusion theory, inverse adding-doubling (IAD), and inverse Monte Carlo (IMC) methods.

A schematic representation of methods to measure the optical properties of tissues is shown in Fig. 1.3.

### 1.2.2.1 Kubelka–Munk Theory

In 1948, Kubelka and Munk described a simplified mathematical model of the optical radiation interaction with the translucent isotropic materials. Taking into account that the main dental structures (dentine and enamel) and dental materials designed to replace them are translucent, the applicability of this theory in dentistry is obvious.

Based on the double-flux theory of a light beam crossing a translucent material, Kubelka and Munk mathematically processed the reflection and transmission of a sample (both homogeneous and inhomogeneous) placed and measured on different colored backgrounds [36]. They expressed the scattering ($S$) and absorption ($K$) of

a material where both parameters depend on the wavelength, considering the influence of sample thickness and background.

According to the Kubelka–Munk theory the reflectance ($R$) and transmittance ($T$) are described by the following expressions:

$$R = \frac{\sin h(Sbd)}{a\cos h(Sbd) + b\sin h(Sbd)}$$

$$T = \frac{b}{a\cos h(Sbd) + b\sin h(Sbd)}$$

where $S$ and $K$ represent the scattering and absorption Kubelka-Munk coefficients, and $a$ and $b$ are the optical Kubelka–Munk constants. The advantage of this theory lies in the fact that both scattering and absorption coefficients can be expressed according to the reflectance and the transmittance of the material:

$$S = \frac{1}{bd}\ln\left[\frac{1 - R(a-b)}{T}\right]$$

$$K = (a-1)S$$

where

$$a = \frac{1 + R^2 - T^2}{2R}$$

$$b = \sqrt{a^2 - 1}$$

If no transmittance measurements are available, the Kubelka–Munk $a$ and $b$ optical constants can be calculated from reflectance measurements of a sample over a black background and a white background:

$$a = \frac{\begin{array}{l} R(B) - R(W) - R_B + R_W - R(B)\cdot R(W)\cdot R_B + R(B)\cdot R(W)\cdot R_W \\ +R(B)\cdot R_B \cdot R_W - R(W)\cdot R_B \cdot R_W \end{array}}{2\cdot\left(R(B)\cdot R_W - R(W)\cdot R_B\right)}$$

$$b = \sqrt{a^2 - 1}$$

where $R_B$ represents the black background reflectance, $R_W$ the white background reflectance, $R(B)$ is the sample reflectance over a black background, and $R(W)$ is the sample reflectance over a white background [37].

Reflectivity (RI—reflectance of a sample of infinite thickness) can also be defined as:

$$RI = a - b$$

Thus, the Kubelka–Munk scattering ($S$) and absorption ($K$) coefficients are described by the following equations:

$$S\left(\mathrm{mm}^{-1}\right)=\frac{1}{b\cdot X}\operatorname{arctgh}\left(\frac{1-a\cdot\left(R\left(B\right)+R_B^{\mathrm{eff}}\right)+R\left(B\right)\cdot R_B^{\mathrm{eff}}}{b\cdot\left(R\left(B\right)-R_B^{\mathrm{eff}}\right)}\right)$$

$$\mathrm{K}\left(\mathrm{mm}^{-1}\right)=S\left(a-1\right)$$

where $X$ is the thickness of the measured sample, $R(B)$ is the reflectance of the sample over the black background, and $R_B^{\mathrm{eff}}$ is the effective reflectance of the black background when it is in contact with the measured sample. $R_B^{\mathrm{eff}}$ is calculated according to suggestions proposed by Mikhail et al. [38]:

$$R_B^{\mathrm{eff}}=\frac{R_B}{\left(1-k_1\right)\cdot\left(1-k_2\right)+R_B\cdot k_2}$$

where $k_1 = 0.039$ and $k_2 = 0.540$

The Kubelka–Munk transmittance ($T$) can be calculated as:

$$T=\frac{b}{a\cdot\sinh\left(bSX\right)+b\cdot\cosh\left(bSX\right)}$$

Both, the simplicity in implementing the Kubelka–Munk theory and the fact that it allows the determination of an analytical solution, are the main reasons why this theory is used in many areas, including dentistry. However, it should be noted that the Kubelka–Munk theory does not provide an explicit relationship between its coefficients ($S$, $K$) and the optical coefficients ($\mu_s$, $\mu_a$). The correlation between these parameters has been extensively studied by several authors [39–41]. Nowadays, these relationships are as follows:

$$K=2\mu_a$$

and

$$S=\frac{3}{4}\mu_s^{'}-x\mu_a$$

Thennadil [42] demonstrated that the contribution of the term that includes the absorption coefficient ($\mu_a$) to the Kubelka–Munk scattering coefficient ($S$) leads to impossible values from a physical standpoint, and, therefore, this relationship is reduced to

$$S=\frac{3}{4}\mu_s^{'}$$

It has been concluded that the use of this formula for the estimation of the optical properties of materials produces an approximate error of 3%.

### 1.2.2.2 Inverse Adding-Doubling Method

The principle of the adding method, as first proposed by van de Hulst [43], is illustrated in Fig. 1.4. For a very thin slab, one can write the radiance at the two surfaces from knowledge of the phase function, since the multiple scattering is negligible. If an identical slab is added, the radiance of the final double-thick slab can be calculated by considering the successive scattering back and forth between the component layers. Computation for thicker slabs can be carried out by adding other thin layers or, more efficiently, by doubling the total thickness with each iteration (Fig. 1.4).

When one-dimensional geometry is a reasonable representation, the adding-doubling method provides an accurate solution of transport equation for any phase function. It allows modeling of anisotropically scattering, internally reflecting, and arbitrarily thick layered media with relatively fast computations. The adding-doubling approximation is one simple method and it has been successfully used to determine the optical properties of turbid media, such as biological tissues.

Prahl et al. [44] proposed a method for determining the optical properties of turbid media based on the adding-doubling approximation, called inverse adding-doubling (IAD): inverse implies a reversal of the usual process of calculating reflection and transmission from optical properties, and adding-doubling indicates the method used to resolve the radiative transport equation. The adding-doubling method is sufficiently fast that iterated solutions are possible on current microcomputers and sufficiently flexible that anisotropic scattering and internal reflection at boundaries may be included.

Inverse adding-doubling (IAD) method involves direct measurements of reflectance and transmittance of the samples and a Monte Carlo simulation to determine the scattering and absorption coefficients. Reflection and transmission measurements, usually made with an integrating sphere, are converted to the optical properties of the sample (scattering and absorption coefficients) using the computer program named "iad," developed by Scott Prahl (https://omlc.org/software/iad/manual.pdf). This program has been extensively tested and validated for accuracy and precision and it has been widely used to determine the optical characteristics of

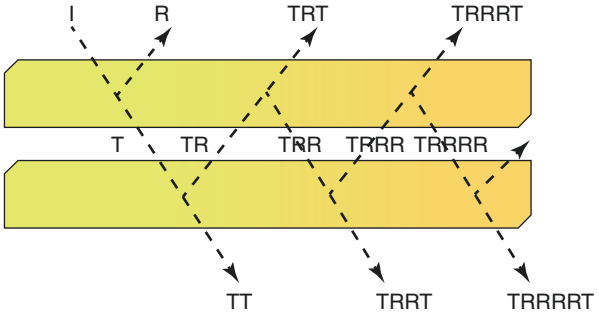


**Fig. 1.4** Schematic representation of the adding-doubling approximation method. *I* incident light, *R* refraction, *T* transmission

different biological tissues. The general idea is that measurements of reflection and transmission are fed into the program to extract the intrinsic optical properties of the sample to be studied. The program does it by repeatedly guessing the optical properties and comparing the expected observables with those that have been made.

To solve the radiative transport equation, the iad program must be supplied with the experimental values of total diffuse reflectance (MR) and transmittance (MT) together with the values of the scattering anisotropy factor ($g$) and the refraction index ($n$) of the sample. The program guesses a set of optical properties ($\mu_a$ and $\mu'_s$) and then calculates values for reflectance (MR) and transmittance (MT). This process is repeated until the calculated and measured values of reflectance (MR) and transmittance (MT) are within a specified tolerance (for the sum of both relative differences, the tolerance default value is 0.01%).

The Monte Carlo simulation is a statistical method that calculates the trajectories of a great number of photons and, as a result, presents the reflectance and transmission of a sample for a given set of optical parameters. The use of this simulation minimizes systematic errors, considers the scattering phase function, and also takes into account the measuring geometry. A limiting consideration is that the accuracy of calculated quantities increases only with the square root of the number of photon histories, making the Monte Carlo particle simulation a computationally costly method. Nevertheless, as computing power is progressively becoming cheaper, this technique is being more widely applied, for example, in tissue optics. The inverse Monte Carlo simulation was included in the iad program to achieve an accurate evaluation of the sample's optical properties. The measurements of the total diffuse reflectance (MR) and transmittance (MT) used in the IAD method to determine the optical absorption coefficient($\mu_a$) and reduced scattering coefficient ($\mu'_s$) are modeled by the Monte Carlo simulation technique, which uses as stochastic simulation of light interaction with biological media.

A schematic of the experimental setup for measuring the total diffuse reflectance and total diffuse transmittance is shown in Fig. 1.5.

A polarizer is used to reduce and direct the intensity of the incident laser beam in order to prevent undesirable diffuse reflections. A mirror system to divert the laser beam was added to fix the sample after the diffuse reflection measurements, so that the diffuse transmission measurements could be performed in the same spot of the sample.

The total diffuse reflectance $M_R$, in terms of percentage, is calculated using:

$$M_R = r_{\text{std}} \frac{R\left(r_s^{\text{direct}}, r_s\right) - R(0,0)}{R\left(r_{\text{std}}, r_{\text{std}}\right) - R(0,0)}$$

where $r_{\text{std}}$ is the reflection of the reference standard.

Total diffuse transmittance is measured under the same setup conditions (single-integrating-sphere setup using collimated light). Transmittance measurements ($T\left(t_s^{\text{direct}}, r_s\right)$) were referenced to 100% with the lasers illuminating the open and empty port ($T(0,0)$) and a dark measurement with an open port without illumination

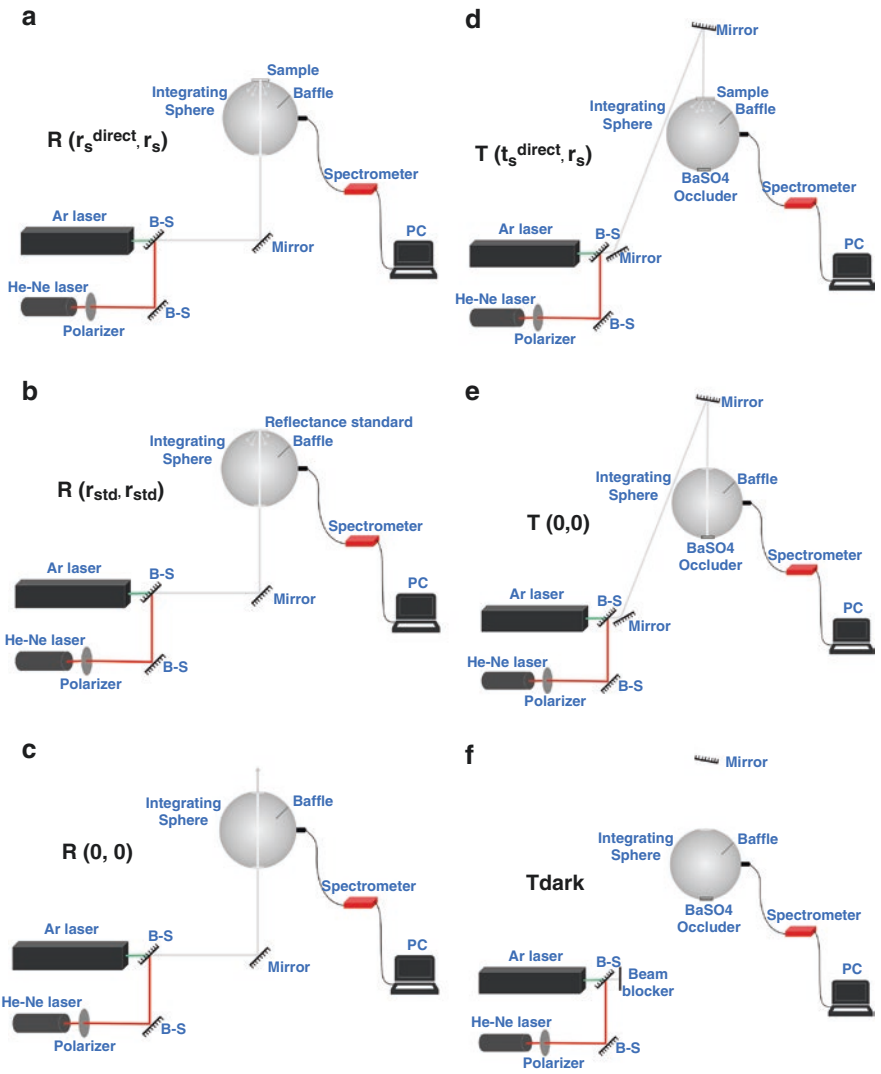


**Fig. 1.5** Schematic representation of the experimental setup. (**a**–**c**) Configuration for reflection measurements and (**d**–**f**) configuration for transmission measurements

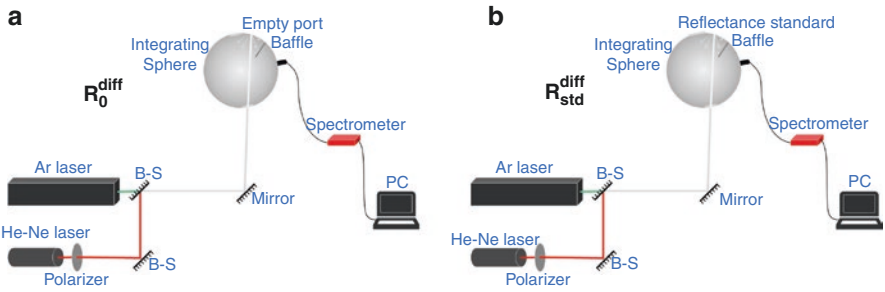


**Fig. 1.6** Schematic representation of the experimental setup used for the reference sphere calibration measurements. (**a**) measurements without the standard and (**b**) measurements with the standard

from the lasers ($T_{\text{dark}}$) (Fig. 1.5). The total diffuse transmittance, in terms of percentage, was calculated using

$$M_T = \frac{T\left(t_s^{\text{direct}}, r_s\right) - T_{\text{dark}}}{T\left(0,0\right) - T_{\text{dark}}}$$

One critical parameter in both reflection and transmission measurements is the sphere wall reflectance. In order to determine this parameter, two measurements are needed (Fig. 1.6). The integrating sphere rotated with respect to the incident beam so that light was directly incident upon the sphere wall between the sample port and the baffle. The reflectance sphere wall ($r_w$) was calculated according to the following equation:

$$\frac{1}{r_w} = a_w + a_d r_d \left(1 - a_e\right) + a_s r_{\text{std}} \left(1 - a_s\right) \frac{R_{\text{std}}^{\text{diff}}}{R_{\text{std}}^{\text{diff}} - R_0^{\text{diff}}}$$

where $a_w$ is the fractional sphere wall area, $a_d$ is the fractional detector area, $a_s$ is the fractional sample area, $a_e$ is the fractional entrance port area, $r_d$ is the detector reflectance, and $r_{\text{std}}$ is the reflectance of the reflectance standard.

## 1.2.3 Application of Color Science and Optical Properties to Dental Structures and Dental Materials

### 1.2.3.1 Color of Tooth

From the point of view of a human observer, the appearance of a tooth is a complicated psycho-physiological process, which is influenced by different factors, such as the spectral power distribution of the illuminant, the sensitivity of the observer and the spectral characteristic of the tooth, mostly reflectance and transmittance, which are mainly determined by its absorption, reflection, and transmission properties. As with any other translucent sample, when light reaches the surface of a tooth, five phenomena associated with the interaction of radiant energy with tooth may

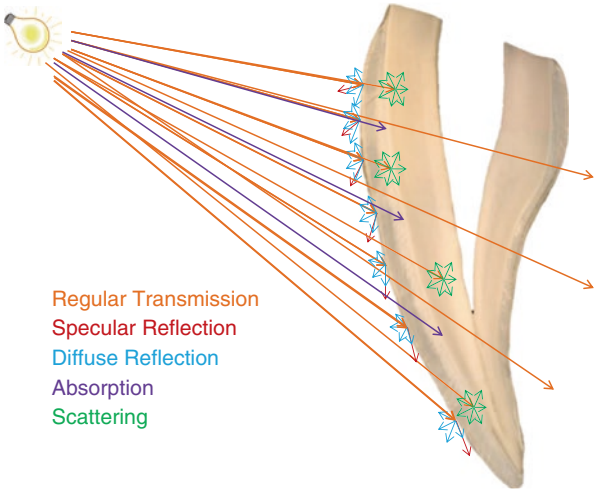


**Fig. 1.7** Five phenomena (regular transmission, specular reflection, diffuse reflection, absorption, and scattering) may occur in the interaction of incident radiation and tooth

occur: specular reflection at the tooth surface, diffuse reflectance, direct transmission through the tooth, and absorption and scattering of light within the different tooth structures (Fig. 1.7).

Tooth color is influenced by a combination of intrinsic color and the presence of extrinsic stains that may form on the tooth surface. Light scattering and absorption within enamel and dentine give rise to the intrinsic color of the teeth and since enamel is relatively translucent, the properties of dentine can play a major role in determining the overall tooth color.

The range and distribution of tooth color has been described in a number of studies [45] where factors such as location, gender, age, and ethnicity have been investigated. In general, the maxillary anterior teeth are slightly more yellow than mandibular anterior teeth, and the maxillary central incisors have greater value than the lateral incisors and canines [46, 47]. Although some studies have shown no differences in tooth color between males and females, few studies have reported differences in tooth color between genders with females showing lighter and less yellow incisors than males [46, 48–50]. In a study with Chinese urban population ($N = 405$), $L^*$ values were significantly higher (about 1.7 units) and $b^*$ values were significantly lower (about 0.9 units) for females [51]. Similarly, in a Spanish population ($N = 1361$) the females showed higher in $L^*$ values (2.53 units) and lower $b^*$ values (3.11 units) compared to males [49, 50].

In the midst of a vast array of genetically determined tooth colors, all teeth darken over the course of time. Indeed, many studies have showed the color of teeth become darker and more yellow with aging. In a group of 180 USA adults and teenagers whose maxillary central incisors were measured with a spectrophotometer, it was shown that for each year of life, the average tooth color decreased in $L^*$ value by 0.22 units and increased in $b^*$ value by 0.10 units [52]. Larger changes have been measured in a Spanish population using a spectrophotometer where tooth color decreased in $L^*$ value

by 0.6 units per year, $b^*$ values increased by 0.56 units per year, and $a^*$ values increased by 0.26 units per year [49, 50]. In addition, it has been shown that with increase in age, the mean value of $b^*$ increases faster in males than females [52].

Studies investigating the relationship of skin color to tooth shade and color are conflicting. Most studies show no relationship, but few studies reported an inverse relationship where people with medium- and dark-skin tones were more likely to have the highest value in tooth color in comparison to people with lighter skin tones regardless of their age or gender [53]. In contrast, others studies investigated the relationship of the color of maxillary incisors and facial skin across four different ethnic groups and found that $L^*$ value of tooth color had a positive correlation with $L^*$ value of skin color for subjects from Saudi Arabia, India, and East Asia [54]. In addition, it was found a negative correlation between the $L^*$ values of tooth and skin color for subjects of African origin. Such controversy is probably associated to differences in sample size and ethnic origin of population, as well as to the methods used to measure skin and tooth color. When considering the broad range of tooth colors measured and reported in the literature from many different study populations, it is evident that ethnicity does not pre-dispose an individual to a particular tooth color. Considering Saudi Arabian, Indian, African, and East Asian groups, the reported mean (standard deviation) values for $L^*$ were 79.26 (3.16), 80.59 (3.23), 78.95 (4.33), and 78.33 (2.10), respectively; for $a^*$ were 0.853 (0.99), 0.546 (0.95), 1.132 (1.51), and 0.955 (0.56), respectively; and for $b^*$ were 21.05 (3.84), 19.57 (4.01), 19.30 (4.95), and 17.52 (2.75), respectively [54]. Despite the statistical difference found among groups for each color parameter, the clinical relevance of the data indicates that the spread of tooth colors from one ethnicity will greatly overlap with those of another ethnicity, indicating that all ethnicities share a large proportion of tooth colors.

Considering tooth whiteness, the WIC formula has been used in some early dental studies to assess whiteness of porcelain teeth, human teeth, and VITA Shade Guide tables [55, 56], and the $W^*$ formula has been used in a few tooth bleaching studies to track whiteness changes after treatments. It was suggested that for a whiteness index to be valid, it must be used with the type of materials for which it was intended. Thus, it was reported that tooth colors appear to be outside the valid color range for using the WIC formula [21].

The index WIO has been used in several in vitro and in vivo tooth whitening studies, including tooth bleaching studies with hydrogen peroxide products and whitening studies with toothpastes containing optical whitening technologies [57, 58]. In vitro studies demonstrated that toothpastes containing blue covarine gave a statistically significant reduction in tooth yellowness and both, in vitro and clinical trials, reported improvement in tooth whiteness immediately after brushing. In addition, the higher concentration blue covarine toothpaste gave statistically significant greater tooth whitening benefits than the lower concentration blue covarine toothpaste [59].

#### 1.2.3.2 Optical Properties of Dental Structures and Dental Materials

Measuring and reporting optical properties of natural teeth and dental materials are of particular importance, since their interaction is the basis for an esthetic match between the restorative material and the adjacent or remaining dental structure.

Therefore, reported values for the various dental structures should be used in the development and manufacture of esthetic dental restorative materials.

The optical properties of esthetic restorative materials (resin composites, ceramics, etc.) and dental structures (enamel and dentin) have been extensively investigated. We can easily find reports on the anisotropy factor, absorption, scattering coefficients, and transmittance for different dental materials and dental structures. Relevant data from some of these studies are summarized below.

### The Anisotropy Factor (*g*)

It characterizes the phase function and it has been experimentally evaluated for different dental tissues (enamel and dentin) and dental materials (hybrids, resin-based composites, and ceramics) for two different thicknesses (0.5 mm and 1 mm) [60]. The anisotropy factor was calculated from the average cosine of the scattering angle, and four-dimensional measurements were made for four wavelengths of the visible spectrum: 457.9 nm, 488.0 nm, 514.5 nm, and 632.8 nm. The results demonstrate that the thicker samples have a low scattering profile compared to the thinner samples, regardless of the material. It was also observed that dental materials have an anisotropy factor ($g$) comparable to tissues they aim to replace (Table 1.1).

### Absorption Coefficient ($\mu_a$) and Scattering Coeffficient ($\mu_s$)

In other study [60], the absorption ($\mu_a$) and scattering ($\mu_s$) coefficients, as well as the reduced scattering coefficient ($\mu_s'$) of three types of dental materials (hybrid composite, nano-composite, and zirconia) were evaluated for four different wavelengths. The determination of the coefficients was performed using the iterative, inverse adding-doubling method that combines transmission and reflection measurements with an experimental setup containing an integrating sphere and a multi-frequency laser (Fig. 1.5). According to the results of this study, both the absorption ($\mu_a$) and scattering ($\mu_s$) coefficients exhibit a similar spectral behavior for the two composite materials but different from that obtained for the ceramic material (Table 1.2). It was concluded that these differences may be due to the anisotropy factor ($g$), which exhibits different values for ceramic compared to resin-based composites.

### Absorption (*K*) and Scattering (*S*) Coefficients, Transmittance (*T*), and Reflectivity (RI) According to the Kubelka–Munk Theory

The correct application of Kubelka–Munk theory (K-M theory) for the analysis of dental structures and dental materials was demonstrated by Ragain and Johnston [61]. They showed that Kubelka–Munk theory can reliably estimate the

**Table 1.1** Anisotropy factor ($g$) values for different dental materials and structures

| | Anisotropy factor ($g$) | | | | |
|---|---|---|---|---|---|
| $\lambda$(nm) | Enamel | Dentine | Nano-composite | Hybrid composite | Zirconia |
| 457.9 | 0.68 | 0.13 | 0.96 | 0.87 | −0.19 |
| 488.0 | 0.67 | 0.21 | 0.95 | 0.86 | −0.25 |
| 514.5 | 0.74 | 0.21 | 0.96 | 0.86 | −0.23 |
| 632.8 | 0.92 | 0.06 | 0.98 | 0.95 | −0.20 |

**Table 1.2** Values of the absorption ($\mu_a$), scattering ($\mu_s$), and reduced scattering ($\mu_s'$) coefficients for different dental materials

| | Nano-composite | | | Hybrid composite | | | Zirconia | | |
|---|---|---|---|---|---|---|---|---|---|
| $\lambda$(nm) | $\mu_a$ ($mm^{-1}$) | $\mu_s'$ ($mm^{-1}$) | $\mu_s$ ($mm^{-1}$) | $\mu_a$ ($mm^{-1}$) | $\mu_s'$ ($mm^{-1}$) | $\mu_s$ ($mm^{-1}$) | $\mu_a$ ($mm^{-1}$) | $\mu_s'$ ($mm^{-1}$) | $\mu_s$ ($mm^{-1}$) |
| 457.9 | 0.07 | 0.99 | 26.1 | 0.06 | 1.34 | 10.4 | 0.02 | 14.63 | 12.3 |
| 488.0 | 0.03 | 0.85 | 16.6 | 0.04 | 1.19 | 8.2 | 0.03 | 14.15 | 11.3 |
| 514.5 | 0.03 | 0.77 | 17.9 | 0.03 | 1.03 | 7.1 | 0.06 | 11.47 | 9.3 |
| 632.8 | 0.02 | 0.74 | 43.5 | 0.01 | 0.73 | 15.9 | 0.01 | 20.70 | 17.1 |

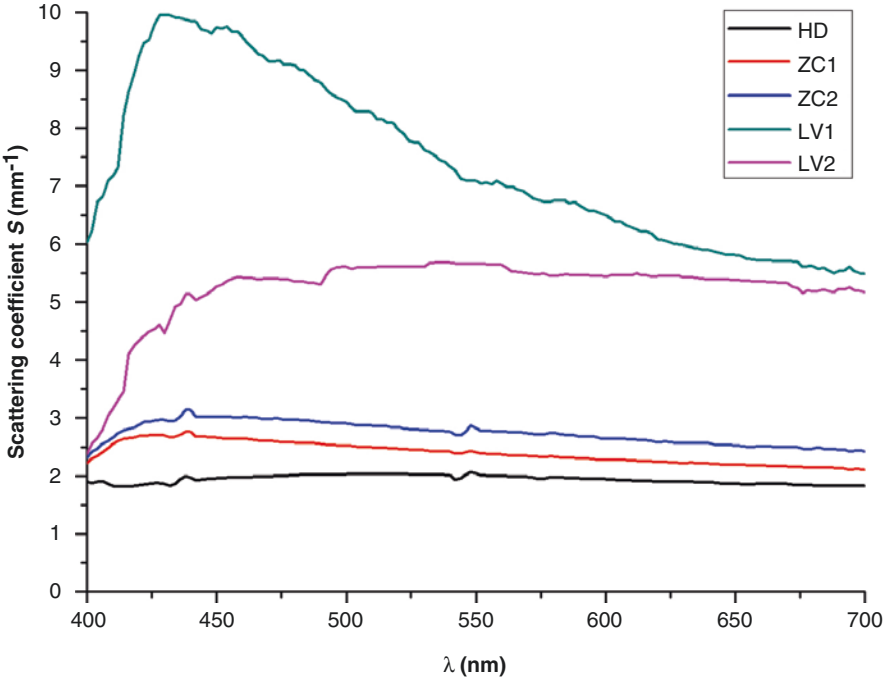


**Fig. 1.8** Spectral distribution of Kubelka-Munk scattering coefficient (*S*) for human dentine (HD) and two zirconia-based ceramic systems (ZC and LV)

diffuse reflection values of samples by comparing them with the diffuse reflectance values experimentally measured with a spectrophotometer. Since then, the Kubelka–Munk theory has been used to estimate the optical properties of various dental restorative materials. In one of such studies [62], the K-M theory was used to evaluate the scattering, absorption, and transmittance of human and bovine dentines, and two ceramic systems. The spectral behavior of the scattering coefficient (*S*) for both dentines (human and bovine) was found similar in all wavelengths. Although the ceramic systems and human dentine showed similar spectral behavior of the scattering coefficient (*S*), their values were statistically different (Fig. 1.8). Significant differences were found among the study groups

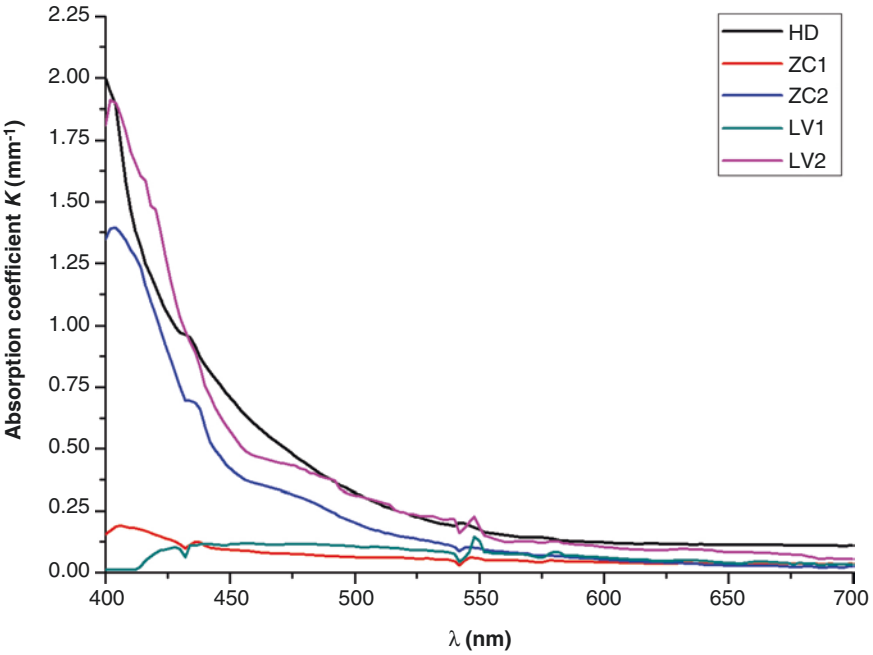


**Fig. 1.9** Spectral distribution of Kubelka-Munk absorption coefficient (*K*) for human dentine (HD) and two zirconia-based ceramic systems (ZC and LV)

for the absorption coefficient (*K*). However, in all cases, *K* values were greater for short wavelengths and the values were decreasing as the wavelength increases (Fig. 1.9). The spectral behavior of transmittance (*T*) showed a constant increase of values with increasing wavelengths, displaying the highest values for the longest wavelengths (Fig. 1.10). The spectral values obtained for human and bovine dentines were similar. Although the zirconia-based ceramic systems showed similar spectral behavior to human dentine, the values were statistically different. Both ceramic systems showed lower transmittance values compared to human and bovine dentines.

In addition, the Kubelka-Munk theory was used to estimate the optical properties of a range of shades from resin-based composites with wide applicability in clinical practice [16, 17]. It was found that the scattering coefficient (*S*) has a maximum value at the 450 nm wavelength. Thus, lower values of *S* were found for longer wavelengths. Translucent shades exhibit different spectral behavior compared to other shades (Fig. 1.11). The spectral behavior of the absorption coefficient (*K*) is marked by a decrease in *K* values as the wavelength increases, thus the smallest values of *K* are found for the longest wavelengths. As for other dental materials, the transmittance (*T*) increased with the wavelength and, as expected, greater *T* values were found for translucent materials.

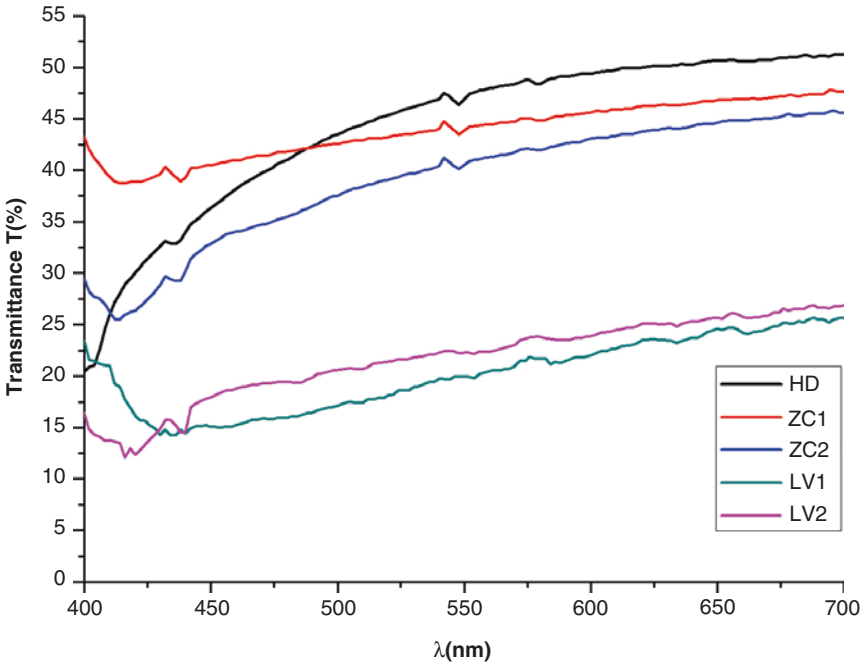


**Fig. 1.10** Spectral distribution of Kubelka–Munk transmittance (*T*) for human dentine (HD) and two zirconia-based ceramic systems (ZC and LV)

Last but not least, the Kubelka–Munk theory was used to evaluate the optical properties of 2-mm thick dentine sections from three teeth: incisor, canine, and molar [63]. Similar spectral behavior of scattering (*S*), transmittance (*T*), and reflectivity (RI) was found for the three types of dentine, despite significant different values. However, no significant difference was found for the absorption coefficient (*K*) among the three types of dentine (incisor, canine, and molar). Dentine from canine teeth showed the highest scattering and reflectivity values (Fig. 1.12), while dentine from molar teeth showed the highest absorption and transmittance values (Fig. 1.13). Therefore, the optical properties of human dentine are influenced by the type of tooth dentine.

Many studies evaluated the translucency of natural tooth structure and several conditions of dental materials using the translucency parameter (TP), contrast ratio (CR), and transmission (%*T*) [64]. Polymers from conventional and industrial polymerization showed a wide variation in translucency using wavelength-specific transmittance determinations. Direct and indirect dental composite materials, that is, resin-based composites cured by different polymerization processes, also showed a change in translucency (TP values). Changes due to depth of cure were also investigated using both TP and wavelength-specific transmittance measurements. Polymerization kinetics was evaluated using wavelength-specific transmittance measurements. The influence of bisphenol in the resin matrix composition was

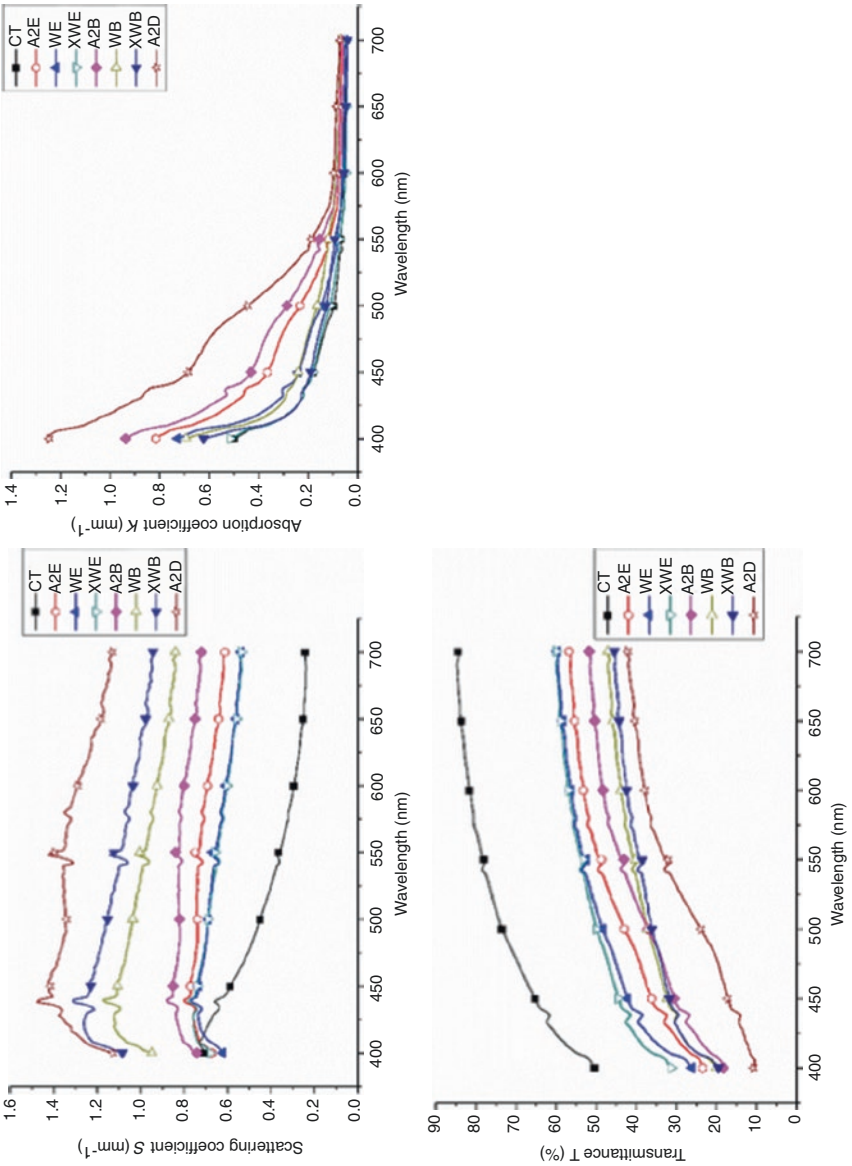


**Fig. 1.11** Spectral distribution of (**a**) the scattering coefficient ($S$), (**b**) the absorption coefficient ($K$), and (**c**) the transmittance ($T$) for different shades of the same resin-based composite material

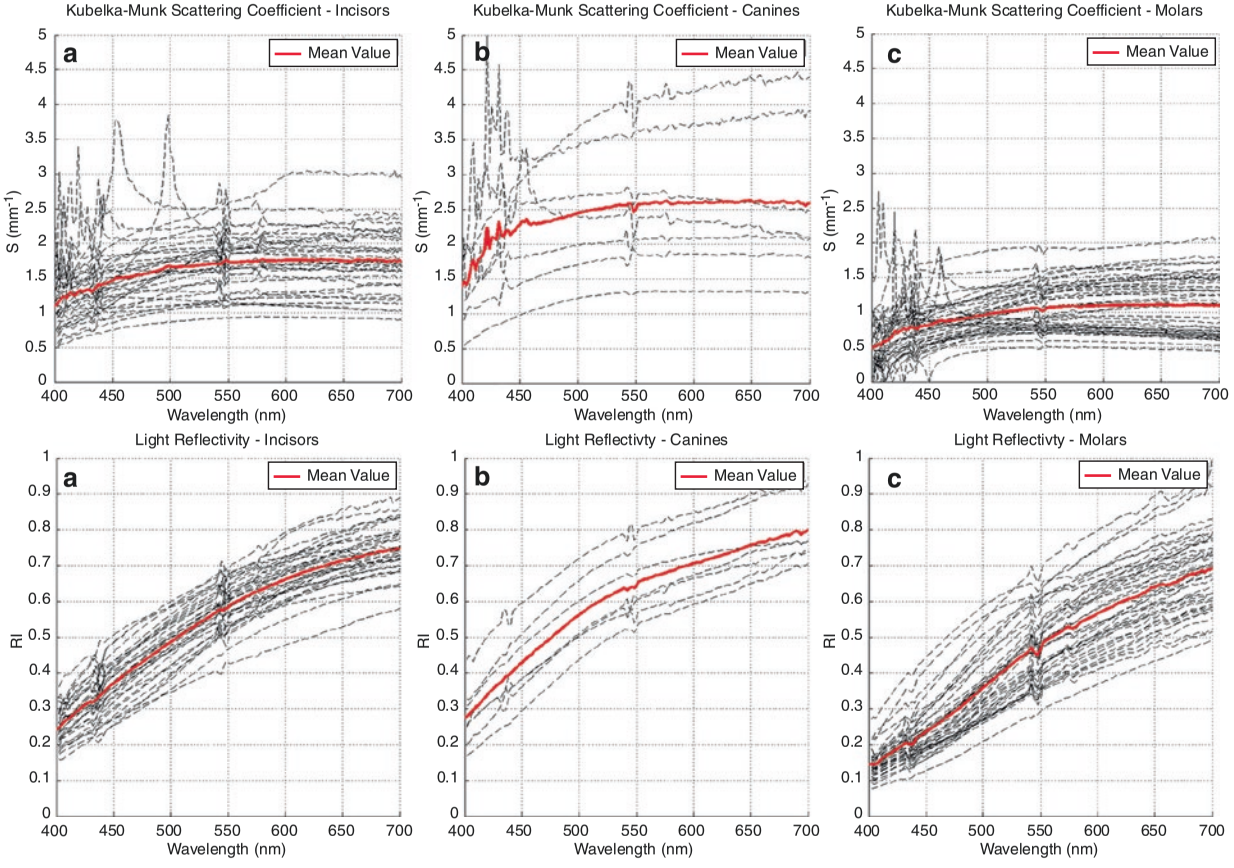


**Fig. 1.12** Spectral distribution of scattering (*S*) and reflectivity (RI) for dentine from (**a**) incisor, (**b**) canine, and (**c**) molar teeth. Mean value spectrum for each graph is shown in red

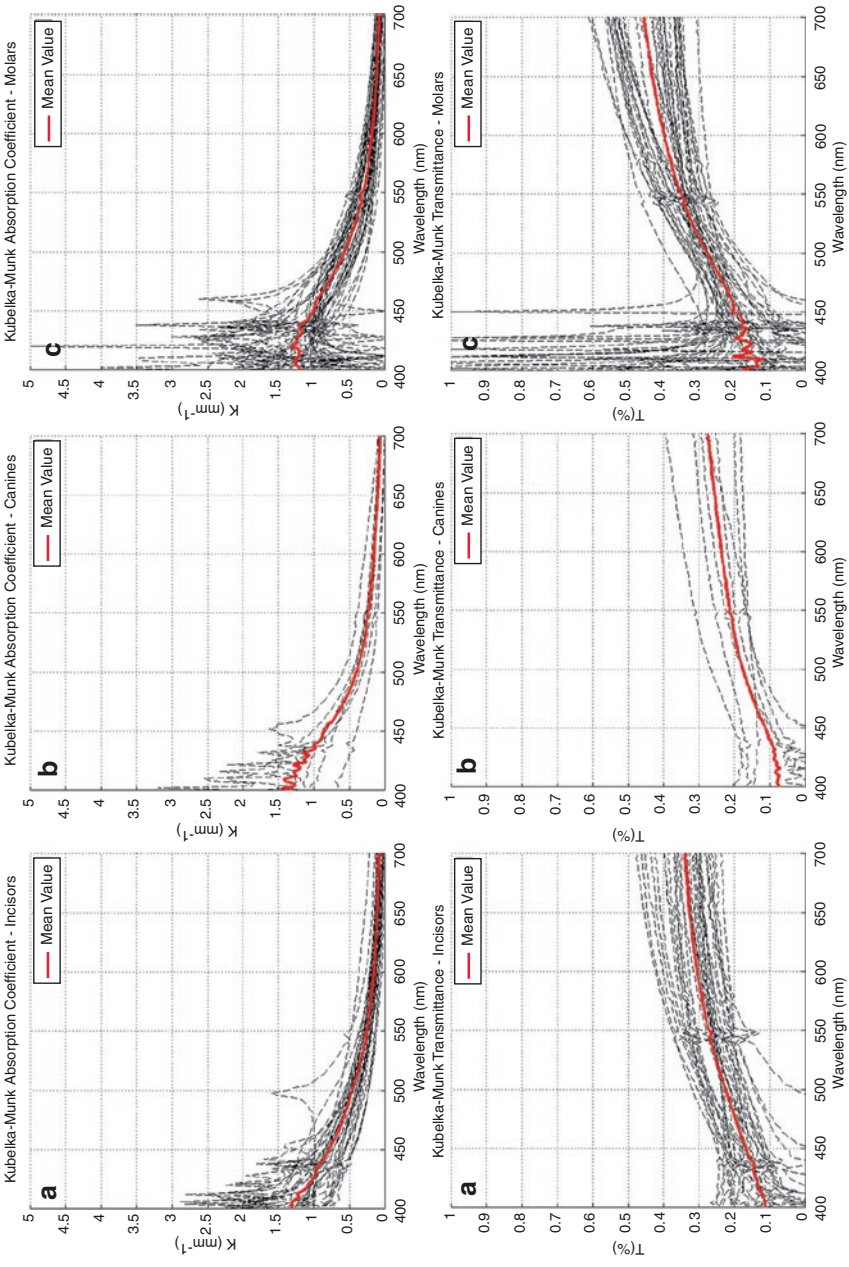


**Fig. 1.13** Spectral distribution of absorption coefficient ($K$) and transmittance ($T$) for dentine from (**a**) incisor, (**b**) canine, and (**c**) molar teeth. Mean value spectrum for each graph is shown in red

demonstrated using both spectral transmittance measurements. In addition, the effect of the sample thickness has been extensively evaluated for dental materials using TP, CR, and $\%T$. Other conditions such as staining, thermocycling, and filler volume fraction were also evaluated using transmittance and TP determinations. TP associated with wavelength-specific CR was used to show changes in translucency with wavelength. TP determinations were also used to show that the translucency of translucent composites is different from that of tooth enamel. Studies on translucency of dental ceramics demonstrated differences in CR among shades of zirconia-based ceramics. Differences due to sintering conditions of these ceramics were shown using total transmission and diffuse transmittance measurements, and the effect of veneering was further demonstrated using total luminous transmittance. The curing of underlying cement was the major topic of interest in determining the translucency of these ceramics using wavelength-specific transmittance. Both CR and transmittance determinations were used to determine that CR is useful to transmission differences below 50% transmission for a wide variety of ceramic materials. TP, CR, and wavelength-specific transmittance determinations were used to show differences among shades of dental ceramic materials. TP determinations of ceramic materials were solely used to determine significant effects of the illuminant, surface texture, and surface-finishing technique. Using ceramic materials, TP values measured by the spectroradiometer and the spectrophotometer were found to be significantly different but highly correlated. A significant correlation between the translucency of ceramic materials and polymerization efficiency of underlying luting composites was found using TP determinations. TP determinations were used to demonstrate the significant effect of bleaching on human enamel. Data recommended for use as reference in the development of esthetic restorative materials and clinical shade matching were presented using both CR and TP determinations.

In summary, colorimetric and optical evaluation of dental tissues and dental materials using established and standardized methods are very important for continuing development of materials and techniques used in esthetic dentistry, assisting to improve the successful rate of esthetic dentistry procedures, where color appearance and perception are crucial, and, therefore, benefiting patients and the dental profession.

## Further Readings

1. Commission Internationale de l'Eclairage. CIE Technical Report: Colorimetry. CIE Pub No. 15.3. Vienna, Austria: CIE Central Bureau; 2004.
2. CIE. CIE Publication 11 A. Official recommendations, Committee E-1.3.1 - Colorimetry. Vienna, Austria. A: 35; 1964.
3. MacAdam DL. Visual sensitivities to color differences in daylight. J Opt Soc Am. 1942;32(5):247–74.
4. Berns RS. Billmeyer and Saltzman's - principles of color technology. New York: Wiley; 2000.
5. Schanda J. Colorimetry. Understanding the CIE system. Hoboken: Wiley; 2007.
6. Luo MR, Rigg B. Bfd (1-C) color-difference Formula.1. Development of the formula. J Soc Dyers Colourists. 1987;103(2):86–94.

7. CIE. Technical report: industrial color-difference evaluation. Vienna: International Commission on Illumination; 1995.
8. Luo MR, Cui G, Rigg B. The development of the CIE 2000 color difference formula: CIEDE2000. Color Res Appl. 2001;26(5):340–50.
9. Pérez MM, Saleh A, Yebra A, Pulgar R. Study of the variation between CIELAB ΔE∗ and CIEDE2000 color-differences of resin composites. Dent Mater J. 2007;26(1):21–8.
10. Lee YK. Comparison of CIELAB ΔE∗ and CIEDE2000 color differences after polymerization and thermo-cycling of resin composites. Dent Mater. 2005;21(7):678–82.
11. Kim SH, Lee YK, Lim BS. Influence of porcine liver esterase on the color of dental resin composites by CIEDE2000 system. J Biomed Mater Res B Appl Biomater. 2005;72(2):276–83.
12. Paravina RD, Kimura M, Powers JM. Evaluation of polymerization-dependent changes in color and translucency of resin composites using two formulae. Odontology. 2005;93(1):46–51.
13. Xu BT, Zhang B, Kang Y, et al. Applicability of CIELAB/CIEDE2000 formula in visual color assessments of metal ceramic restorations. J Dent. 2012;40(Suppl 1):e3–9.
14. Gómez-Polo C, Portillo Muñoz A, Lorenzo-Luengo MC, et al. Comparison of two color-difference formulas using the bland-Altman approach based on natural tooth color space. J Prosthet Dent. 2016;115(4):482–8.
15. Gómez-Polo C, Portillo Muñoz A, Lorenzo-Luengo MC, et al. Comparison of the CIELab and CIEDE2000 color difference formulas. J Prosthet Dent. 2016;115(1):65–70.
16. Pecho OE, Pérez MM, Ghinea R, Della Bona A. Lightness, chroma and hue differences on visual shade matching. Dent Mater. 2016;32(11):1362–73.
17. Pecho OE, Ghinea R, do Amaral EA, Cardona JC, Della Bona A, Pérez MM. Relevant optical properties for direct restorative materials. Dent Mater. 2016;32(5):e105–12.
18. Pecho OE, Ghinea R, Perez MM, Della Bona A. Influence of gender on visual shade matching in dentistry. J Esthet Restor Dent. 2017;29(2):E15–23.
19. CIE Publication. Colorimetry CIE pub no 15.2. Vienna, Austria: CIE Central Bureau; 1986. p. 36–7 [Chap. 5.3].
20. Gelarch RW, Zhou X, McClanahan SF. Comparative response of whitening strips to a low peroxide and potassium nitrate bleaching gel. Am J Dent. 2002;15:19A–23A.
21. Luo W, Westland S, Ellwood R, Pretty I, Cheung V. Development of a whiteness index for dentistry. J Dent. 2009;37:e21–6.
22. Pérez MM, Ghinea R, Rivas MJ, et al. Development of a customized whiteness index for dentistry based on CIELAB color space. Dent Mater. 2016;32(3):461–7.
23. Pérez MM, Ghinea R, Pecho OE, Pulgar R, Della Bona A. Recent advances in color and whiteness evaluation in dentistry. Curr Dent. 2019;1(1):23–9.
24. Pérez MM, Herrera LJ, Carrillo F, Pecho OE, Dudea D, Gasparik C, Ghinea R, Della Bona A. Whiteness difference thresholds in dentistry. Dent Mater. 2019;35(2):292–7.
25. Paffenbarger GC, Judd DB, Dental silicate cements, in: Optical Specification of Light-scattering Materials: RP 1026. J Res Nat Bur Standards. 1937;19:314–16. Pl.
26. Johnston WM. Color measurement in dentistry. J Dent. 2009;37(Suppl 1):e2–6.
27. Johnston WM, Ma T, Kienle BH. Translucency parameter of colorants for maxillofacial prostheses. 1995;8:79–86.
28. Salas M, Lucena C, Herrera LJ, Yebra A, Della Bona A, Pérez MM. Translucency thresholds for dental materials. Dent Mater. 2018;34(8):1168–74.
29. Lee YK. Opalescence of human teeth and dental esthetic restorative materials. Dent Mater J. 2016;35(6):845–54.
30. Lee YK. Influence of scattering/absorption characteristics on the color of resin composites. Dent Mater. 2007;23:124–31.
31. Schmeling M, Maia HP, Baratieri LN. Opalescence of bleached teeth. J Dent. 2012;40(Suppl 1):e35–9.
32. Lee YK. Fluorescence properties of human teeth and dental calculus for clinical applications. J Biomed Opt. 2015;20(4):040901.
33. Spitzer D, Bosch JJ. The total luminescence of bovine and human dental enamel. Calcif Tissue Res. 1976;20(1):201–8.

34. Matsumoto H, Kitamura S, Araki T. Applications of fluorescence microscopy to studies of dental hard tissue. Front Med Biol Eng. 2001;10(4):269–84.
35. Song SH, et al. Opalescence and fluorescence properties of indirect and direct resin materials. Acta Odontol Scand. 2008;66(4):236–42.
36. Kubelka P. New contributions to the optics of intensely light-scattering materials. Part II: non-homogeneous layers. J Opt Soc Am. 1954;44:330–5.
37. Yeh CL, Miyagawa Y, Powers JM. Optical properties of composites of selected shades. J Dent Res. 1982;61:797–801.
38. Mikhail SS, Azer SS, Johnston WM. Accuracy of Kubelka-Munk reflectance theory for dental resin composite material. Dent Mater. 2012;28:729–35.
39. Brinkworth BJ. Interpretation of the Kubelka-Munk. Coefficients in reflection theory. Appl Opt. 1972;11:1434–5.
40. Gate LF. Comparison of the photon diffusion model and Kubelka-Munk equation with the exact solution of the radiative transport equation. Appl Opt. 1974;13(2):236–8.
41. Star WM, Marijnissen JP, van Gemert MJ. Light dosimetry in optical phantoms and in tissues: I. multiple flux and transport theory. Phys Med Biol. 1988;33(4):437–54.
42. Thennadil SN. Relationship between the Kubelka-Munk scattering and radiative transfer coefficients. J Opt Soc Am A Opt Image Sci Vis. 2008;25(7):1480–5.
43. Van de Hulst HC. A new look at multiple scattering. Tech. Rep., Goddard Institute for Space Studies, NASA TM-I03044; 1963.
44. Prahl SA, van Gemert MJC, Welch AJ. Determining the optical properties of turbid media by using the adding–doubling method. Appl Opt. 1993;32(4):559–68.
45. Joiner A, Luo W. Tooth colour and whiteness: a review. J Dent. 2017;67(Suppl1):S3–10.
46. Tuncdemir AR, Polat S, Ozturk C, Tuncdemir MT, Gungor AY. Color differences between maxillar and mandibular incisors. Eur J Gen Dent. 2012;1:170–3.
47. Zhao Y, Zhu J. In vivo color measurement of 410 maxillary anterior teeth. Chin J Dent Res. 1998;3:49–51.
48. Esan TA, Olusile AO, Akeredolu PA. Factors influencing tooth shade selection for completely edentulous patients. J Contemp Dent Pract. 2006;7:80–7.
49. Gomez-Polo C, Montero J, Gomez-Polo M, Vasquez de Parga JAM, Celemin-Vinuela A. Natural tooth color estimation based on age and gender. J Prosthodont. 2015;26(2):107–14.
50. Gomez-Polo C, Gomez Polo M, Montero J, Vazquez De Parga JAM, Vinuela AC. Correlation of natural tooth colour with aging in the Spanish population. Int Dent J. 2015;65:227–34.
51. Xiao J, Zhou XD, Zhu WC, Zhang B, Li JY, Xu X. The prevalence of tooth discolouration and the self-satisfaction with tooth colour in a Chinese urban population. J Oral Rehabil. 2007;34:351–60.
52. Odioso L, Gibb RD, Gerlach RW. Impact of demographic, behavioural, and dental care utilization parameters on tooth color and personal satisfaction. Compend Contin Educ Dent. 2000;21:S35–41.
53. Sharma V, Punia V, Khandelwal M, Punia S, Lakshmana R. A study of relationship between skin color and tooth shade value in population of Udaipur, Rajasthan. Int J Dent Clin. 2010;2:26–9.
54. Haralur SB, Dibas AM, Almelhi NA, Al-Qahtani DA. The tooth and skin colour interrelationship across the different ethnic groups. Int J Dent. 2014;2014:146028.
55. Guan YH, Lath DL, Lilley TH, Willmot DR, Marlow I, Brook AH. The measurement of tooth whiteness by image analysis and spectrophotometry: a comparison. J Oral Rehabil. 2005;32:7–15.
56. Lath DL, Wildgoose DG, Guan YH, Lilley TH, Smith RN, Brook AH. A digital image analysis system for the assessment of tooth whiteness compared to visual shade matching. J Clin Dent. 2007;18:17–20.
57. Joiner A, Philpotts CJ, Alonso C, Ashcroft AT, Sygrove NJ. A novel optical approach to achieving tooth whitening. J Dent. 2008;36:S8–14.
58. Luo W, Westland S, Brunton P, Ellwood R, Pretty IA, Mohan N. Comparison of the ability of different colour indices to assess changes in tooth whiteness. J Dent. 2007;35:109–16.

59. Tao D, Smith RN, Zhang Q, Sun JN, Philpotts CJ, Ricketts SR, Naeeni M, Joiner A. Tooth whitening evaluation of blue covarine containing. J Dent. 2017;67S:S20–4.
60. Fernandez-Oliveras A, Rubiño M, Perez MM. Scattering and absorption properties of biomaterials for dental restorative applications. J Eur Opt Soc. 2013;8:13056.
61. Ragain JC, Johnston WM. Accuracy of Kubelka–Munk reflectance theory applied to human dentin and enamel. J Dent Res. 2001;80:449–52.
62. Pecho OE, Ghinea R, Ionescu AM, Cardona JC, Della Bona A, Pérez MM. Optical behavior of dental zirconia and dentin analyzed by Kubelka-Munk theory. Dent Mater. 2015;31(1):60–7.
63. Pop-Ciutrila IS, Ghinea R, Colosi HA, Dudea D. Dentin translucency and color evaluation in human incisors, canines, and molars. J Prosthet Dent. 2016;115(4):475–81.
64. Johnston WM. Review of translucency determinations and applications to dental materials. J Esthet Res Dent. 2014;26(4):217–23.

# Teaching and Training Color Determination in Dentistry

2

Oscar Emilio Pecho Yataco and Alvaro Della Bona

## Contents



## 2.1 Teaching and Training Color Science in Dentistry

For a long time, education and training in color science have been performed in many areas of arts and sciences with a variety of industrial applications. Although shade matching between natural teeth and restorations is of great importance in esthetic dentistry, education and training of color in dentistry are still not widely present in dental schools worldwide [1]. The high esthetic demand on restorative dentistry requires serious training in color science apply to Dentistry. This involves knowledge on the basics of color science and optical properties, color notation systems, dental shade matching and shade determination, and color perception and communication.

Over the years, multiple surveys on color education have been conducted at predoctoral and postdoctoral levels [2–4]; Paravina et al. 2010. All these studies were performed sending surveys to program directors or faculty members involved in teaching and training on color-related classes. As for any other survey, the response rate was below desired: 49% [4], 91% [3], 64% [2], and 63% (Paravina et al. 2010).

O. E. Pecho Yataco · A. Della Bona (✉)
Dental School, Postgraduate Program in Dentistry, University of Passo Fundo, Passo Fundo, RS, Brazil
e-mail: dbona@upf.br



A. Della Bona (ed.), *Color and Appearance in Dentistry*,
https://doi.org/10.1007/978-3-030-42626-2_2

Paravina et al. (2010) evaluated the status of teaching of color in dental schools around the world ($N = 205$) at predoctoral (Pre-D) and postdoctoral (Post-D) levels. Although the study (Paravina et al. 2010) response rate was 63%, one should be aware that in the year 2000 there were 550 dental schools in 73 countries [5], and the number of dental schools in these countries increased by 42.6% over a period of 10 years, from 1990 to 2000. Therefore, it is fair to assume there would be about 770 dental schools in the year 2010; thus, the following results represent about 25% of the dental schools in the world, probably the most active dental schools worldwide. Yet, it is an excellent study (Paravina et al. 2010) and a great reference for dental color education. Without further ado, the study showed that a dental class on "color" or "color in dentistry" was present in 80% of Pre-D programs and 82% of Post-D programs. Information on color was given in prosthodontics (68% in Pre-D and 86% in Post-D), restorative dentistry (50% in Pre-D and 21% in Post-D), and in operative dentistry classes (33% in Pre-D and 23% in Post-D). The number of hours dedicated to teaching of color-related topics was 4.0 ± 2.4 and 5.5 ± 2.9 for Pre-D and Post-D programs, respectively. Yet, these numbers were different compared to other studies performed in 1968 (2.3 h) [4] and in 1988 (5.9 h for Pre-D and 8.4 h for Post-D) [2].

A total of 64% of Pre-D programs and 58% of Post-D programs reported that their institutions have a dental or non-dental individual with expertise in color science working as faculty or associated with their staff (Paravina et al. 2010). These values were higher than those previously found, 4% in 1968 [4] and 23% for Pre-D and 24% for Post-D programs in 1988 [2]. Two books were considered by 25–30% of interviewees as references for teaching color in dentistry [6, 7]. The most frequently color concepts taught on dental classes were as follows: color dimensions and metamerism, color temperature and ceiling lights, camera selection, color communication using digital photography and written instructions, translucency, color on composite resins and dental ceramics, and methods of tooth whitening. The use of instrumental shade matching has become part of the teaching of color in dental education in many programs; however, all the factors that influence the visual shade-matching method have received substantial attention of dental educators. Color dimensions (value, chroma, and hue) are used as the most popular concepts for dental shade matching, with Vitapan Classical and Vitapan 3D-Master being the most popular shade guides (Paravina et al. 2010).

Sheets et al. [8] evaluated several concepts of esthetic dentistry in dental education. Two perspectives of education were evaluated: the intended education, provided by advanced education in prosthodontics (AEP) program chairs, and the perceived education, provided by AEP residents (junior residents: first- and second-year residents, and senior residents: third- and fourth-year residents). Surveys were sent to all US and Canadian AEP program chairs ($N = 52$) and residents ($N = 393$), with a response rate of 59.6% and 27.3%, respectively. The surveys consisted of five multiple-choice questions addressed the level of training on bleaching/whitening, shade matching, selecting porcelain systems to match translucency, transfer of information to the laboratory, and surface staining or characterization. Response options about level of education for all these questions were as follows: not taught,

by lecture only, preclinical (non-patient) care, and clinical (patient) care. AEP program chairs listed the clinical (patient) care level as their ideal level of education (83–93% depending on topic) to be taught for their graduate students. For residents, the primary response was also the clinical (patient) care level, but in a lower percentage (46–79%). Thus, a difference between the intended education and the perceived education was found. When AEP program chairs were asked what topics the residents were most interested in learning about, the responses were as follows: shade matching (57.7%), transfer of information to the laboratory (57.7%), matching inherent translucency (42.3%), surface staining or characterization (42.3%), and bleaching/whitening (15.4%). The residents were most interested in learning about matching inherent translucency (76.6%), surface staining or characterization (70.2%), shade matching (63.8%), transfer of information to the laboratory (59.6%), and bleaching/whitening (37.2%) [8]. The confidence level on all esthetic topics was greater for senior residents than for junior residents. This fact suggests that confidence is improving with experience.

## 2.2 Applying Methodologies to Dental Students and Dentists

The influence of color education and training, the so-called experience, on the ability to shade match in dentistry has been studied by many authors [9–12]. These studies showed that the ability to shade match in dentistry can be improved. Thus, a training session in a clinical setting should be considered in dental education for undergraduate and postgraduate students.

According to the International Organization for Standardization [13], color discrimination competency in Dentistry should be evaluated using matching pairs of shade tabs from two same dental shade guides. Vita Classical shade guide (VITA Zahnfabrik, Bad Säckingen, Germany) (Fig. 3.6) is an example of appropriate dental shade guide for this color discrimination test. Parameters for visual assessments should be as follows: object (e.g., shade tab) under D65 illuminant inside a viewing booth, 0°/45° optical geometry, and observer at a distance between 25 cm and 33 cm (Figs. 2.1 and 3.14). Shade tabs, with original markings covered, should be placed on the floor of the viewing booth and mixed (Figs. 2.1 and 6.5). From the results of this color discrimination test, an observer can be considered: poor (up to 60%), average (up to 75%), and superior (up to 85%) color discrimination competent [13].

This test for the evaluation of color discrimination competency in Dentistry could be performed in an initial session and after color education. A recent study [12] was performed with visual assessments of 88 dental students from Brazil and Portugal. The observers shade matched a pair of tabs from Vita Classical and VITAPAN 3D-Master shade guides (Figs. 3.6 and 3.8). The test was performed over a neutral gray background and under controlled light (D65 illuminant and 90% color rendering index). After 7–10 days of the first color matching phase, all observers watched a 50-min video lecture on color education (color attributes, importance of color matching, color-selection techniques using visual assessment,

**Fig. 2.1** The color discrimination competency test uses matching pairs of shade tabs from two same dental shade guides (Vita Classical shade guide, VITA Zahnfabrik, Bad Säckingen, Germany). Shade tabs are under D65 illuminant inside a viewing booth, with 0°/45° optical geometry, and observer at a distance between 25 cm and 33 cm

spectrophotometers, and Vita Classical and VITAPAN 3D-Master shade guides) and repeated the visual shade-matching exercise. Correct shade-matching percentage improved after color education using Vita Classical (from 64.06% ± 22.46% to 76.64 ± 20.93%) and VITAPAN 3D-Master (from 63.59% ± 21.27% to 71.59 ± 19.79%) shade guides. Thus, education and training in color science seems to improve the shade-matching ability of dental students, which shows the importance of color science education in dentistry.

## 2.3 Teaching and Learning Methods

An education and training method including lectures and exercises on color science and appearance was proposed by Paravina and Powers [7]. The topics include color science, shade guide demonstration (exercise I), other appearance parameters, color and gloss measuring instruments, surface roughness, color matching, communication and reproduction, tooth bleaching, color corrections of dental restorations, color training, shade guides (exercise II), and research on color of esthetic materials. Exercises I and II were performed by matching the 16 shade tabs from two Vita Classical shade guides under color-corrected light source with a correlated color temperature of 5300 K, a color-rendering index of 98, and illuminance of 1500 lux, with the use of 0°/45° optical geometry and a neutral gray background. Correct shade-matching percentage improved after color education from 69.4% to 82.5% [7].

There are different free online education and training programs, which can be used to improve the knowledge about color science in dentistry. A research group led by Dr. Holger Jakstat from University of Leipzig, Germany, supported by VITA Zahnfabrik, designed a dental shade selection training system in 2002, which was later improved in 2007 [9]. The learning process starts with the Toothguide Trainer

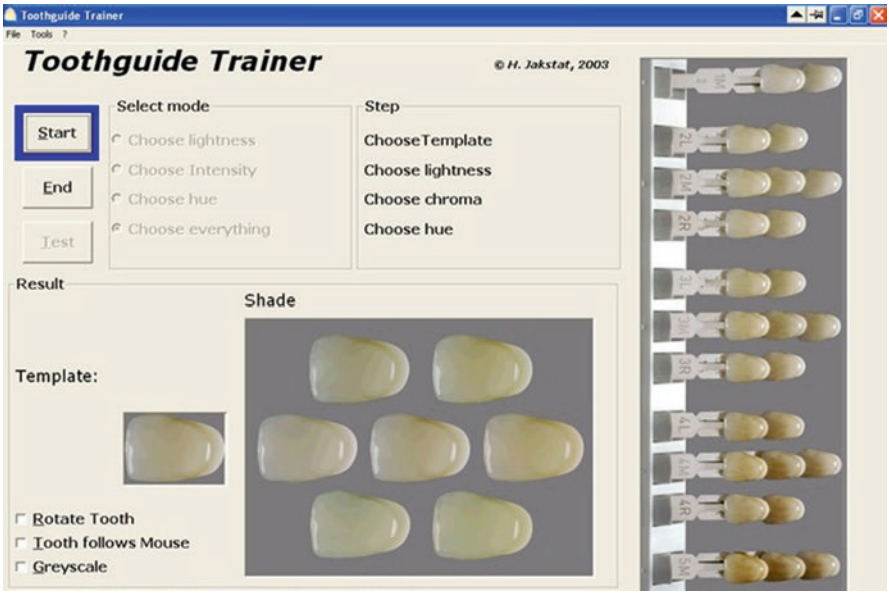


**Fig. 2.2** Original version of Toothguide Trainer (TT) program

Web (TT), which is a computer-based tool (http://www.toothguide.de/default.aspx) (Fig. 2.2). A shade tab from 3D-Master shade guide is shown on a computer monitor and the observer has to choose the perfect matching using color dimensions (value, chroma, and hue). If the selection is not correct, this procedure will be repeated until the observer reaches a specific level of performance. Following, the Toothguide Training Box (TTB) (Vita Zahnfabrik, Bad Sackingen, Germany) can be used (Fig. 2.3). The TTB was designed to be a sort of shade-matching educational game. It presents a random shade tab from the 3D-Master shade guide under artificial daylight conditions and the observer has to match it using a group of shade tabs presented by the TTB, which also indicates if the observer's selection is correct or not. The observer has to play until a specific level of performance is reached [9].

The Dental Color Matcher (DCM) is a free online education and training program for esthetic dentistry (http://www.scadent.org/news/free-color-training) aiming to improve color matching results of dental students. The program comprises of several training exercises, educational quizzes, survey, and a lecture. Precisely, the program starts with a color vision screening, which is a short version (eight plates) of the color blindness test based on Ishihara's pseudoisochromatic plates (Chap. 6). Second, a shade-matching exercise is used to select the closest match of four target teeth using Vita Linearguide 3D-Master shade guide (Fig. 3.10). Then, a traditional lecture on color science and dental shade matching is given in .pdf or video format. Furthermore, the student will be asked to match pairs of corresponding shade tabs, which are arranged in sets of light and dark sets. From this exercise onwards, the

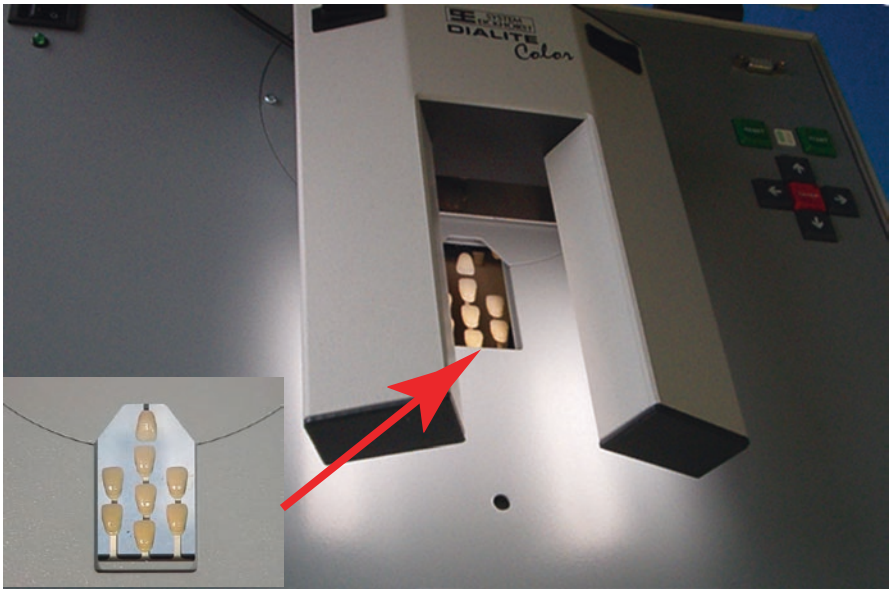


**Fig. 2.3** Original version of Toothguide Training Box (TTB). It was set up in a suitcase that could be sent to any dental school around the world

student can experiment shade matching using different backgrounds (white, different grays, and black). A gray-colored screen may be used for eye relaxation. At the end of each exercise, the student can check for matching errors. Next, there are 14 additional shade-matching exercises always using the Vita Linearguide 3D-Master shade guide. A 12-question quiz on color science applied to Dentistry with instant feedback and final checking of the answers is also part of the program. Then, the observer (student) can repeat the first shade-matching exercise (in random order) of the program to verify if there was any improvement on tooth color determination. Finally, there is a survey to collect the student opinion about the program. The program allows the student to request continuing education (CE) credits and print a conclusion certificate for the program. Therefore, it is a complete dental color education and training program. Ristic et al. [11] reported that dental students who completed the DCM program between the first and second shade-matching sessions showed significant improvement in overall shade-matching scores in the second session.

Shade matching and color reproduction is a common procedure performed in dentistry. Since, it has been reported that experience influences on shade matching, dental schools should add courses on color science in their curricula. Nevertheless, all dental students should experience, at least, one of the color discrimination tests such as Ishihara test (Fig. 6.2), Farnsworth–Munsell 100 Hue test (Figs. 6.3 and 6.4), and test for color discrimination competency in Dentistry (Fig. 6.5).

## 2.4 Scientific Communication

Traditionally, dental color research uses CIELAB color difference metric ( $\Delta E^*_{ab}$ ) to evaluate color differences between two different objects or in two different moments of a treatment performed on same object (e.g., tooth). $\Delta E^*_{ab}$ uses the Euclidean distance to measure distance within a space, that means that CIELAB color space considers equal importance for all factors [14]. Previous studies on perceptibility and acceptability thresholds of color difference (Chap. 3) suggested different weight on sensitivity to lightness ($L^*$), green-red axis ($a^*$), and blue-yellow axis ($b^*$) with the CIELAB color space [15, 16]. Therefore, additional studies [17–19] suggested the use of CIEDE2000 metrics to provide better correlation between the computed color differences with the perceived color differences. Essentially, the performance of color difference metrics depends on the agreement with the visual experience [19].

Conventionally, color research uses traditional descriptive and analytical statistics. However, the analysis of color differences findings using visual thresholds greatly supplements the interpretation of research and clinical outcomes. To perceive a color difference and whether that color difference is acceptable is of great importance. Thus, color differences should be evaluated through comparisons with 50:50% perceptibility (PT) and 50:50% acceptability (AT) thresholds. In this regard, the current PT and AT values are 1.14 and 2.65 units for CIELAB, and 0.76 and 1.76 units for CIEDE2000(1:1:1), respectively. These visual thresholds were obtained using TSK fuzzy approximation [13, 18].

## Further Readings

1. Paravina RD, O'Neill PN, Swift EJ Jr, Nathanson D, Goodacre CJ. Teaching of color in predoctoral and postdoctoral dental education in 2009. J Dent. 2010;38(Suppl 2):e34–40.
2. Goodking RJ, Loupe MJ. Teaching of color in predoctoral and postdoctoral dental education in 1988. J Prosthet Dent. 1992;67:713–7.
3. O'Keefe KL, Strickler ER, Kerrin HK. Color and shade matching: the weak link in esthetic dentistry. Compendium. 1990;11:116–20.
4. Sproull RC. A Survey of color education in the dental schools of the world. United States Research Report, William Beaumont General Hospital, El Paso, Texas, November 20, 1968.
5. Zillén PA, Mindak M. World dental demographics. Int Dent J. 2000;50(4):194–234.
6. Chu SJ, Devigus A, Mieleszko A. Fundamentals of color: shade matching and communication in esthetic dentistry. Hanover Park: Quintessence; 2004.
7. Paravina RD, Powers JM. Esthetic color training in dentistry. St. Louis: Elsevier; 2004.
8. Sheets JL, Yuan JC, Sukotjo C, Wee AG. Survey of advanced education in prosthodontics directors and residents on practices in esthetic dentistry. J Dent Educ. 2016;80(10):1205–11.
9. Corcodel N, Karatzogiannis E, Rammelsberg P, Hassel AJ. Evaluation of two different approaches to learning shade matching in dentistry. Acta Odontol Scand. 2012;70(1):83–8.
10. Llena C, Forner L, Ferrari M, Amengual J, Llambes G, Lozano E. Toothguide training box for dental color choice training. J Dent Educ. 2011;75(3):360–4.
11. Ristic I, Stankovic S, Paravina RD. Influence of color education and training on shade matching skills. J Esthet Restor Dent. 2016;28(5):287–94.

12. Samra APB, Moro MG, Mazur RF, Vieira S, De Souza EM, Freire A, Rached RN. Performance of dental students in shade matching: impact of training. J Esthet Restor Dent. 2017; 29(2):E24–32.
13. International Organization for Standardization. ISO/TR 28642: Dentistry–guidance on color measurement. Geneva: International Organization for Standardization; 2016.
14. Mangine H, Jakes K, Noel C. Preliminary comparison of CIE color differences. Color Res Appl. 2005;30:288–94.
15. Pecho OE, Pérez MM, Ghinea R, Della Bona A. Lightness, chroma and hue differences on visual shade matching. Dent Mater. 2016a;32:1362–73.
16. Perez MM, Ghinea R, Herrera LJ, Ionescu AM, Pomares H, Pulgar R, et al. Dental ceramics: a CIEDE2000 acceptability thresholds for lightness, chroma and hue differences. J Dent. 2011;39:e37–44.
17. Ghinea R, Perez MM, Herrera LJ, Rivas MJ, Yebra A, Paravina RD. Color difference thresholds in dental ceramics. J Dent. 2010;38:e57–64.
18. Paravina RD, Ghinea R, Herrera LJ, Della Bona A, Igiel C, Linninger M, Sakai M, Takahashi H, Tashkandi E, Perez MM. Color difference thresholds in dentistry. J Esthet Restor Dent. 2015;27(Suppl 1):S1–9.
19. Pecho OE, Ghinea R, Alessandretti R, Pérez MM, Della Bona A. Visual and instrumental shade matching using CIELAB and CIEDE2000 color difference formulas. Dent Mater. 2016b;32:82–92.

# Visual Shade Matching

3

María del Mar Pérez Gómez, Juan de la Cruz Cardona Pérez, Razvan Ionut Ghinea, Oscar Emilio Pecho Yataco, and Alvaro Della Bona

## Contents



M. del M. Pérez Gómez (✉) · J. de la C. Cardona Pérez · R. I. Ghinea
Optics Department, Faculty of Science, University of Granada, Granada, Spain
e-mail: mmperez@ugr.es; cardona@ugr.es; rghinea@ugr.es

O. E. Pecho Yataco · A. Della Bona
Dental School, Postgraduate Program in Dentistry, University of Passo Fundo, Passo Fundo, RS, Brazil
e-mail: dbona@upf.br


A. Della Bona (ed.), *Color and Appearance in Dentistry*,
https://doi.org/10.1007/978-3-030-42626-2_3

## 3.1 Physiology of the Eye and Vision

The human eye is a positive or convergent optical system that forms an inverted image of the external world on the sensitive layer of the retina, at the backside of the eyeball. In this section, a general review of the optical structure and formation of the image by the optical system of the human eye will be carried out, in addition to certain psychophysical properties that will help us to understand the conditions of illumination and observation when a dental restoration is performed.

### 3.1.1 Anatomical Structure of the Human Eye

The structure of the human eye is shown in Fig. 3.1. In the anterior part of the outer layer and following the sclera, the cornea is differentiated, which is more curved than the rest of the eyeball and through which light enters. The cornea is transparent and approximately spherical with a radius of curvature of approximately 8 mm. The sclera is a dense, white, opaque fibrous tissue that has a primarily protective function and is almost spherical with a curvature radius of approximately 12–13 mm [1].

The middle layer of the eye is the uvea in which the iris is differentiated in the anterior part, the choroid in backside, and the ciliary body in the intermediate part. The iris has an important optical function in regulating the size of its opening, the ciliary body is important for the accommodation process, and both (the ciliary body and the choroid) are involved in important vegetative processes. The innermost

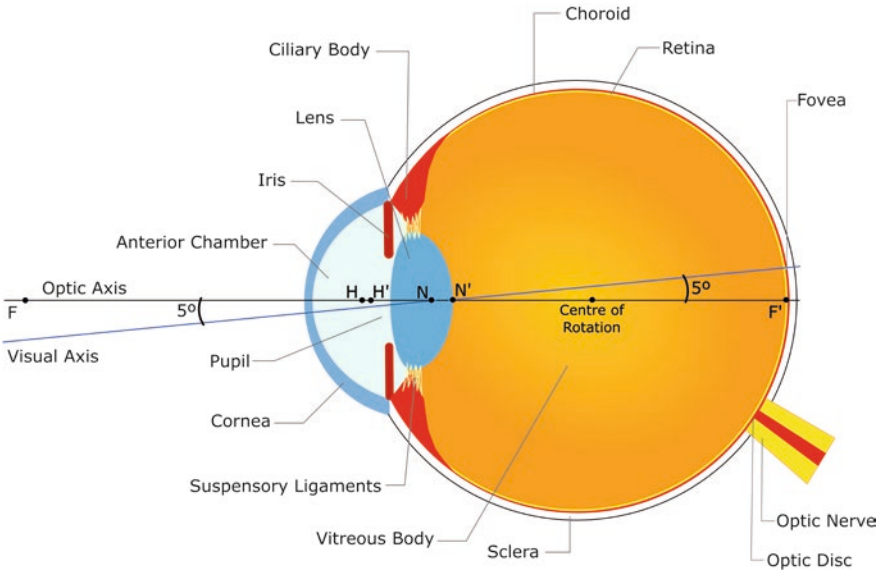


**Fig. 3.1** The human eye. Horizontal section of the right eye seen from above. Cardinal points ($F$, $F'$, $H$, $H'$, $N$, and $N'$) are those corresponding to the eye without accommodation

layer of the eye is the retina, which is an extension of the central nervous system and is connected to the brain by the optic nerve.

The interior of the eye is divided into three compartments or chambers:

1. The anterior chamber, between the cornea and the iris, contains the aqueous humor.
2. The posterior chamber, between the iris and lens, also contains the aqueous humor.
3. The vitreous chamber, between the lens and the retina (back of the eye), contains a transparent gelatinous mass called the vitreous humor.

Furthermore, the eye rotates in its orbital cavity because of the action of six extrinsic muscles.

In the eye, the principles of image formation are the same as those of a conventional optical system. Light enters the eye through the cornea, to be focused on the retina after refraction in the cornea (the most powerful refractive element) and lens. The light is refracted powerfully on the anterior corneal surface because the central spherical part has a pronounced curvature and there is a large difference between the refractive indexes of air (1.000) and the cornea (1.376–1.432) [2]. However, the refraction on the posterior surface of the cornea is very insignificant because the refractive index of the corneal stroma is practically the same as that of the aqueous humor. Light is refracted again when reaches the anterior and posterior surfaces of the lens. In this case, the refractive index of the lens is significantly greater than that of the aqueous and vitreous humors, but differences in the interfaces are not as pronounced as the one between the cornea and air and, therefore, the refractive power is lower. It follows that most ocular refraction takes place on the anterior surface of the cornea, whose refractive power (about 40–45 D) is more than double of the lens (about 20 D). However, the lens power can change when the eye needs to focus at different distances. This process is called accommodation and is due to a change in the lens shape because of the ciliary muscle.

The diameter of the incident light beam is controlled by the iris, which forms the diaphragm of the eye. The opening in the iris is called pupil. As with all optical systems, the diaphragm is a very important system component that affects a wide range of optical processes.

#### 3.1.1.1 Equivalent Power and Focal Lengths

In any centered optical system with a given equivalent power, there are three pairs of cardinal points located on the optical axis: focal points, principal or main points, and nodal points. The location of such cardinal points in the eye depends on their structure and level of accommodation. For an eye focused on infinity, the approximate location of these cardinal points is shown in Fig. 3.1. These points are defined for the paraxial zone only and are as follows:

1. Focal points ($F$ and $F'$). The light coming from the object focus emerges, after refraction in the eye, parallel to the optical axis. The rays coming from an infinite

distance that strike the eye parallel to the optical axis all pass through the image focal point $F'$.

2. Principal or Main points ($H$ and $H'$). They are conjugated points whose lateral magnification is +1. So, if an object is placed in one of these points, a right image of the same size would be formed in the other point. Therefore, the object and image are congruent.
3. Nodal points ($N$ and $N'$). They are also conjugated points on the axis for which the angular magnification is the positive unit. They have the property that any ray entering the system by the nodal point object, forming with the axis an angle $u$, leaves the system by passing through the nodal point image $N'$, forming with the axis an angle $u'$ equal to $u$. This ray is known as nodal ray, and when the point outside the axis is the point of fixation, the ray can be called visual axis. In other words, the slope of the object-space ray at $N$ is the same as the slope of the image-space ray at the $N'$. The ray is undeviated.

One of the most important properties of any optical system is its equivalent power. This is a measure of the system's ability to tilt or deflect light rays. The greater the power of the system, the greater the ability to deflect the rays. The equivalent power of an optical system is denoted by the symbol $F$. The equivalent power of the eye is related to the distances between the focal and main points by the equation:

$$\varphi = \frac{n'}{H'F'} = \frac{n}{HF}$$

where $n'$ is the refractive index in the vitreous chamber. The average power of the adult eye is approximately 60 D, but the values vary quite a lot from one eye to another. Using this power and the commonly accepted index of refraction $n'$ of the vitreous chamber (1.336), the focal distances of the eye are as follows:

$$\mathrm{HF} = -16.67\,\mathrm{mm}\ \text{and}\ \mathrm{H'F'} = +22.27\,\mathrm{mm}$$

While the equivalent power of the eye is a very important property of the eye, it is not easy to measure it directly. Its value is generally obtained from other quantities such as the radius of curvature of surfaces, separations between surfaces and eye length, and assuming refractive indexes of the ocular media.

A certain number of axes are located in the eye. Figure 3.1 shows two of these: the optical and visual axes. The optical axis is generally defined as the line joining the centers of curvature of refractive surfaces. However, the eye does not have a perfect rotation symmetry and, therefore, even if the four refracting surfaces had rotational symmetry, the four centers of curvature would not be colinear. Thus, in the case of the eye, the optical axis is defined as the line that most fits through these non-colinear points. The visual axis is defined as the line that joins the object of fixation or interest and the fovea, and it passes through the nodal points.

### 3.1.1.2 Cornea

The cornea, which is more curved than the eyeball, is a highly transparent, meniscus-shaped structure. A very thin layer of lacrimal fluid normally covers the anterior surface, but it is too thin to appreciably affect the potency and can be ignored in this context. Seen from the front, the cornea has a diameter of about 12 mm, slightly smaller vertically than horizontally. The average radius of the anterior corneal surface is approximately 7.7 mm, the values of the central part being between 7.0 and 8.6 mm. In almost 84% of all eyes, the radius is between 7.5 and 8.2 mm. The radius of curvature of the posterior surface of the cornea has an average value of 6.8 mm, less than that of the anterior surface, which determines the cornea has a concave meniscus shape where the edges are thicker than the center. The central thickness has values between 0.5 and 0.6 mm and the peripheral thickness around 0.7 mm. As for the refractive index, each layer of the cornea has its own refractive index, but since the stroma is the thickest layer, its refractive index is predominant, which is 1.36–1.38, an intermediate value between collagen (1.55) and the fundamental substance (1.34). An index of 1.336 is considered for the tear [3].

In a first approximation, the optical system of the cornea can be considered of two spherical surfaces separating three optically distinct media: air, cornea, and aqueous humor (Fig. 3.2). Generally, the mean value of the refractive index of the cornea is taken as 1.376 and that of the aqueous humor, in contact with the posterior surface of the cornea, as 1.336. The power of the two corneal surfaces is calculated from the radius of curvature, applying the power equation for spherical refractive surfaces. If the two dioptric surfaces were in the air, they would form a divergent system. However, from the ratio of the refractive indices of the separating media, a convergent system would result with a total power of +43 D, representing about

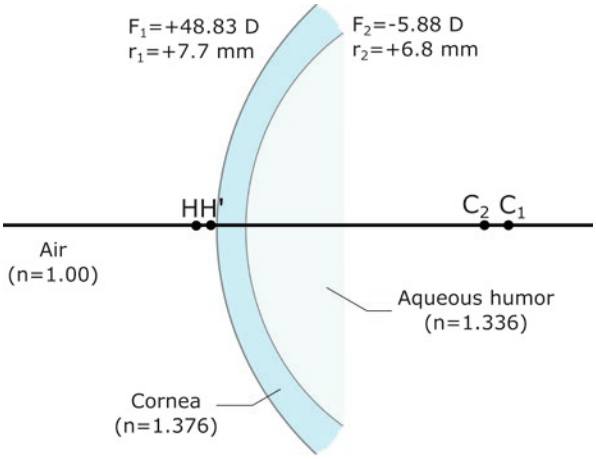


**Fig. 3.2** Dimensions of human cornea

two-thirds of the total power of the eye. The power values of the corneal surfaces only apply to the vertices of the cornea, and would apply to other parts of the corneal surfaces if they were spherical. However, neither the anterior nor the posterior surfaces are perfectly spherical, due to both toricity and asphericity. Therefore, the radius of curvature does not fully describe the shape of the cornea and its refractive properties. Thus, the location of the principal points of the cornea depends on the radius of curvature of the anterior and posterior surfaces, corneal thickness, and refractive indices. The principal (main) points ($H$ and $H'$) are located in front of the cornea (Fig. 3.2).

#### 3.1.1.3 Anterior Chamber

It is the cavity behind the cornea and in front of the iris and lens. It is filled with a colorless liquid whose water content is 98%, which is the reason for calling it as aqueous humor and, unlike any other optical media in the eye, presents a refractive index perfectly defined in all its extension, thus being a homogeneous medium. The depth of the anterior chamber, measured along the optical axis, is determined by the distance from the vertex of the posterior surface of the cornea to the anterior pole of the lens, but sometimes the corneal thickness is also included in this measure. Thus, it is between 3 and 4.5 mm, with an accepted average value of 3.6 mm. The power of the ocular optical system is slightly affected by the depth of the anterior chamber, so that if all the other elements do not change, a decrease of 1 mm in the depth of the anterior chamber will increase the total power of the eye by 1.4 D and an increase in depth will proportionally decrease dioptric power of the ocular.

#### 3.1.1.4 Iris and Pupil

The free edge of the iris is located almost tangentially to the first surface of the lens, its function is to regulate the amount of light that passes into the retina through the pupil. This is a circular central opening that varies in diameter depending on the level of illumination, from 2 to 3 mm with bright light to about 8 mm in dark conditions. Even considering situations of identical illumination, there are important individual variations in pupillary diameter. Thus, around the age of 25 the diameter can be between 3 and 6 mm in the eye adapted to the light. The pupil size decreases with increasing age. Typical diameters for the light-adapted eye are 4.8 mm at 10 years, 4.0 mm at 45 years, and 3.4 mm at 80 years. For the eye in total darkness the most frequent diameters are 7.6 mm at 10 years, 6.2 mm at 45 years, and 5.2 mm at 80 years old.

#### 3.1.1.5 Lens

Contained in an elastic capsule, it is a biconvex lens of variable dioptric power that can focus at different distances because of the mechanism of accommodation and whose main characteristic is its physical and optical heterogeneity (Fig. 3.3). The anterior surface is in contact with the posterior surface of the iris and is bathed by the aqueous humor, while the posterior surface is in contact with the vitreous humor, which refractive index can be considered same as for the aqueous humor (1.336).

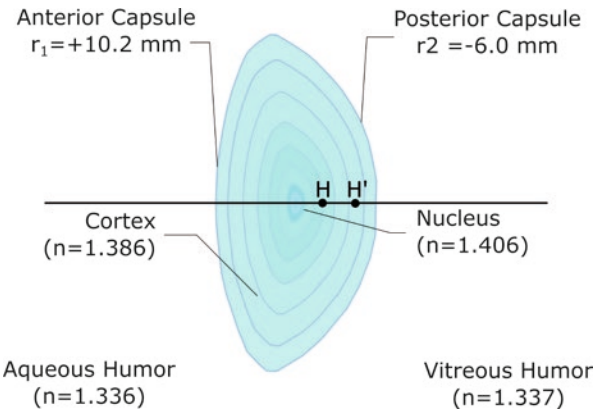


**Fig. 3.3** Cross-section of the lens estimating the position of its main points (H and H′)

The lens has a very complex layered structure with a non-uniform index gradient. Throughout life the lens continues to grow in thickness by forming new layers of fibers on the outer surface. As a normal result of this aging process the lens loses flexibility and transparency, getting yellowish with age, which can influence color judgments. The lens capsule plays an important role in the accommodation process. The suspensory ligaments of the Zinn's zonula, which extend from the periphery of the elastic capsule surrounding the lens to the ciliary body, support the lens and control the curvature of its surfaces through variations in the tension of the zonula produced by the action of the ciliary muscle. This process causes a change in the equivalent power of the lens and therefore in the power of the eye, allowing the eye to focus on objects at different distances. The frontal or equatorial diameter of the lens is approximately 8.5–10 mm. The central thickness, which is the distance between the poles or vertices of the two surfaces, has an average value in the adult eye without accommodation around 3.7 mm, which increases with age. During accommodation, the central thickness increases and the vertex of the anterior surface moves forward reducing the depth of the anterior chamber. In addition, this depth reduces with age. The values of the radius of curvature of the surfaces of the lens must be considered with caution because (1) they change with accommodation, (2) they are highly dependent on age, and (3) any measure of the lens in vivo depends on knowledge of the values of all the optical parameters that precede the surface in question. This is a more pronounced problem with the posterior surface due to the uncertainty of the distribution of the refractive index in a given lens. The curvature of the anterior surface at rest is flatter than the posterior surface. Average values of 11 mm for the radius of anterior curvature and 6.5 mm for the posterior radius have been reported. The shape of both surfaces presents a certain asphericity, so the curvature is flattened towards the periphery. The distribution of the refractive index of the lens varies according to the location, since it is an optically heterogeneous medium due to its structure in layers and the compression exerted on the innermost layers. In the central biconvex zone (called nucleus) the

refractive index is almost constant with a value of 1.41, which is greater than the peripheral cortical zone that surrounds it (1.38), where the variations in the index are greater. This progressive increase of the optical density towards the interior notably increases the convergent power of the lens and produces a progressive and continuous refraction of the rays. It can also improve image quality by reducing spherical aberration. This structure of the lens and the comparatively greater power of its nucleus are of great biological importance since they allow for greater refractive power, a reduction in optical errors such as spherical and chromatic aberrations, a reduction in the dispersion of light within the eye, and the accommodation is exercised with a margin about double that would correspond to the lens if it did not have these characteristics.

During accommodation, when the eye needs to shift focus from distant to near objects, the ciliary muscle contracts by decreasing the tension in the suspensory ligaments that attach to the lens. The relaxation of the zonules allows both lens surfaces, and especially the anterior lens, to take on a more curved shape, thickening the lens in the center and moving the front surface slightly forward. These changes result in an increase in the equivalent power of the eye. In a relaxed eye focused on infinity, the equivalent power of the lens is approximately 19 D. In an eye accommodating a point 10 cm from the cornea, the power of the lens is approximately 30 D. For the relaxed eye, the accommodation level is zero, but the power of the eye is approximately 60 D. Although the level of accommodation and the increase in lens power are not the same, they are closely related variables.

#### 3.1.1.6 Retina

The retina extends over the inner surface of the back of the eyeball to almost the ciliary body, internally it is in contact with the vitreous body and externally with the choroid. Its structure is very complex both anatomically and functionally as it is an extension of the central nervous system where the process of analysis of luminous information begins. The retina contains two types of photoreceptors, rods and cones, which constitute two distinct systems operating at different levels of luminance. The cones are responsible for daytime vision and the rods function with the weak light that is present in twilight and darkness. The central part of the retina, named luteal macula, is distinguished by the presence of a non-photolabile yellow carotenoid pigment and by having a greater density of cones than the peripheral retina. This macular zone has a diameter of 5.5 mm, with a center depression and circular fovea of 1.5 mm in diameter (5° subtended in the nodal point image) with a central area of greater sensitivity for the perception of details, the foveola, populated only by very fine cones. When the two eyes direct their gaze towards an object, their image is placed on each of the fovea. The area of the retina where the optic nerve enters is called the optic disc or optic papilla. There are no cones or sticks in it and it therefore represents a blind spot in the subject's visual field. From an optical point of view, the retina is the screen on which the image is formed. It can be considered as part of a concave spherical surface with a radius of curvature around −12 mm. This curvature approximates the ideal optical conditions for greater peripheral vision efficiency.

### 3.1.2 Field of Vision

On the temporal side, where there are no anatomical obstacles, the field of vision extends beyond 90° of the optical axis. The nose, eyebrow, and cheek limit the monocular field of vision in other directions, so that its shape is irregular, being the limit of 60° on the nasal side. The papilla or optic disc of the retina, which lacks photo receptors, has a "blind spot" in the monocular visual field. The optical disc measures about 2 mm vertically by 1.5 mm horizontally, subtends an angle of about 7° by 5° at the image nodal point. This is also the angle subtended by the blind region in space. The center of the optical disc is approximately 15° nasally from the fovea and 1.5° upward. Consequently, the blind spot is located at 15° temporarily and 1.5° downwards in relation to the point of fixation.

The use of both eyes provides a better perception of the outside world than a single eye and due to the lateral displacement between them the three-dimensional perception of the world is possible, which includes the perception of depth known as stereopsis.

### 3.1.3 Accommodation

It is the ability of the eye to focus at different distances. In the emmetropic eye parallel rays from an object in the infinite are focused on the retina; if the object is placed closer, the image will form in the conjugated focus located behind the retina, and in the retina will form a large circle of diffusion that will only allow to see a blurred image. Thus, accommodation is the mechanism by which the convergence power of the eye increases to clearly see the object, moving from the primary focus to the retina. In the young eye, the refractive power is modified by changing the curvature of the lens. The exact nature of the accommodation mechanism is still discussed, but there is a fundamental agreement, which is an increase in the curvature of the lens that mainly affects the anterior surface.

In a relaxed state, the radius of curvature of the anterior surface of the lens is 11 mm, while during accommodation it may decrease to 5 or 6 mm; this variation in shape increases the converging power of the eye, so that the focus can be shifted as needed. When accommodating a young eye, there is a shortening of the focal length corresponding to an increase in the power of the eye from 60 to 70 D. In the near vision approach, the ciliary muscle contracts, the fibers of the zonula relax, and the lens capsule is distended, so that the lens adopts a spheroidal shape, thereby increasing its refractive power. In the distant vision approach, the ciliary muscle is relaxed, the zonula fibers contract, and the elliptical-shaped flattened lens decreases its refractive power.

To sum up, modifications that occur in the eye during accommodation are as follows:

(a) The pupil contracts when looking at a nearby object. Its function is to act as a diaphragm that suppresses the relative increase of light entering the eye from nearby objects and, therefore, decreases diffusion circles. It also reduces aberrations by blocking the outer portions of the lens. This pupillary contraction triggered by accommodation is slower than that produced by light.

(b) Decreasing the depth of the anterior chamber by the center. The pupillary edge moves forward approximately 0.4 mm for an accommodation of 7 D. However, because of its peripheral part, the anterior chamber suffers an increase in depth.
(c) Changes in the lens. In its anterior surface, it undergoes a change in location and shape. As for the shape, its radius of curvature decreases during accommodation. This increase in curvature is not uniform and mainly affects the central region, where a conoid deformation occurs. In the posterior surface, the lens undergoes fewer changes. The variation in the position of the posterior edge is minimal, around 0.01 mm. The front (equatorial) diameter of the lens decreases during accommodation by 0.4–0.5 mm. The total index increases due to a displacement of the lenticular fibers. Gullstrand called this mechanism the intracapsular accommodation mechanism. The ripples at the edge of the lens are lost during near vision and reappear in distant vision. It is attributed to the relaxation of the zones and to the slight displacement of the lens by the action of gravity and to the small rotation around a vertical axis.
(d) Modifications in the ciliary muscle, in the zonula, and in the ciliary processes. The ciliary muscle acts on the lens through the fibers of the zonula. The contraction of the ciliary muscle produces a displacement of the ciliary processes, which are close to the antero-posterior axis of the eye, but without coming into contact with the lens and, as a consequence, the fibers of the zonula relax. The ability of the ciliary muscle to contract is little affected by age, so presbyopia is not due to a loss of muscle power but to processes that take place in the lens.

There are two phenomena related to accommodation that, although they do not necessarily accompany it in all cases or in the same amount, generally act in accordance with it. This associated action has been called synkinesia (from the Greek: with movement). Therefore, it is necessary for several phenomena to come into play simultaneously in order for the next vision to be clear:

1. Accommodation, which allows the image to be focused on the retina, due to the contraction of the ciliary muscle.
2. Convergence, which allows the eyes to turn inwards, through the internal rectus muscles, so that their visual axes are directed towards the near object. The closer the object is, the greater the convergence and, at the same time, the greater the accommodation.
3. Miosis, produced by the contraction of the pupillary sphincter, has several functions: it reduces optical aberrations due to changes in the curvature of the lens during accommodation by eliminating the peripheral areas of the lens; and above all, it suppresses the relative increase of light entering the eye from nearby objects. It also increases the depth of focus and reduces diffusion circles.

These three phenomena are physiologically linked to each other since they depend on the same innervation: the third cranial pair; but they are independent, although when a close object is focused they are requested simultaneously by the same central impulse.

### 3.1.4 Depth of Focus and Depth of Field

The emmetropic eye is able to see clearly without the need to accommodate objects located between infinity and 6 m. At distances of less than 6 m, in order to see the objects clearly, the mechanism of accommodation has to be put into play. The distant objects can be seen clearly because the retina has a certain thickness and the object can suffer displacements of a certain intensity, without the image experiencing an appreciable blurring. This ability to see two objects at different distances at the same time without any change in accommodation or pupillary aperture is called depth of focus. Therefore, depth of focus is the distance in the retina over which an optical image can move without altering clarity. The depth of focus ranges from +0.04 D to +0.47 D. The depth of the area of sharp vision in the visual field, in which an object appears in focus, is known as depth of field, and its existence reduces the need for exact accommodation; in fact, the accommodation mechanism is usually exerted only as needed for clear vision. In addition, the cones respond both to a point of light and to a circle of light that fills their opening. This amplitude of response allows the image in the retina to be a little sub-focused or over-focused, without altering the quality of the message transmitted centrally through the optic nerve.

The smaller the pupil size, the greater the depth of field. This is also critical when we want to value the dental structure in all its dimensions without blurring, to perceive all shades. The depth of focus of the eye decreases with accommodation and becomes less the closer the object is. This decrease is partly compensated by pupillary contraction. A small pupil overcomes minor refractive errors because it increases the depth of field of the eye and the depth of focus. With the small pupil narrower light beams enter and smaller diffusion circles are produced that are limited to a few cones in the pitting, consequently, the poorly focused retina image improves. Therefore, we can understand why reading is easier when illumination increases and the pupil contracts by increasing the depth of field and the need for precise accommodation is reduced. Same happens when we have to observe teeth in detail at short distances.

Since retinal images are never truly accurate, the visual system is constantly processing somewhat blurred images. Thus, this tolerance to blurring considerably expands the apparent depth of field, so that the eye can be ±0.25 D out of focus without stimulating an accommodative change.

### 3.1.5 Evaluation of the Amount of Light

The first important characteristic of the retina that we want to highlight is its heterogeneity. It is made up of a multitude of nerve cells to which cones and rods respond to light and, therefore, called photoreceptors. Three types of cones (*L*, *M*, and *S*) have been found, according to the area of the visible spectrum that present their maximum sensitivity. Thus, although their spectral absorption curves extend to practically all the visible spectrum, *L*, *M*, and *S* cones present their maximum sensitivity, respectively, in long, medium, and short wavelengths (Fig. 3.5).

In the retina we first distinguish the fovea, where visual acuity is maximum and the image of the point of fixation is formed. We know that it is slightly displaced with respect to the optical axis and subtracts an angle from the nodal point image of the eye of 5°.

The density of cones in the fovea is maximum (above 57,000 cones/mm$^2$, reaching 35,000 cones in 0.25 mm$^2$ in the foveola) to decay rapidly towards the periphery (about 5000 cones/mm$^2$ at 10° eccentricity). The rods have zero density in the central pivot and maximum density at 15–20° eccentricity (160,000 rods/mm$^2$).

In the central pivot, the cones have a diameter between 1 and 2 microns with a 2–26.6 microns separation between their centers. In addition, each ganglion cell is connected to a single cone. As we move away from the fovea, the number of photoreceptors (cones and rods) that form a single sensory unit increases, leading, for example, to 100 rods connecting 17 bipolar cells around a single ganglion cell. In primate retinas have been showed $6.5 \times 10^6$ cones, $120 \times 10^6$ rods, and only $10^6$ ganglion cells [4].

It is often assumed that the retina is symmetrical with respect to the pitting, but in detail there are differences. In addition, there is the so-called blind spot, which involves the exit of the optic nerve, with no photoreceptor cells (scotoma). It is situated at about 15° towards the temporal side and 2°–3° downwards, with an approximate extension of 6°.

#### 3.1.5.1 Luminous Efficiency Curve

The eye is a selective detector that does not respond equally to radiations of different wavelengths. For example, it does not respond to radiation below 380 nm and above 760 nm. For lights between these wavelengths, the same amount of radiant flux can generate a different response: different color, different clarity.

So, let us consider "clarity," trying to extract it from the concept of color, in which this attribute is included. In fact, there are two attributes of visual perception that is important to define:

1. Luminosity (using for direct lights, light sources): attribute of the visual perception according to which an object and/or a field seems to exhibit more or less amount of light.
2. Clarity (used for both opaque and transparent objects): Attribute of visual perception known as the luminosity of a field judged in proportion to the luminosity of a similarly illuminated field that appears as white or perfectly transparent.

Thus, a tooth will be qualified as clear if it presents a high clarity, assuming a comparison with a clear object, whose ideal would be an absolute white tooth, of same material, placed next to it. Such classification on clarity would stand even if illumination becomes more intense. Luminosity is used almost exclusively for light sources, thus a lamp can be more or less luminous. In this way we evaluate the perception associated with the amount of light. So, both attributes are related to the amount of light exhibited or seemed to exhibit by an object and/or a field.

If two equally juxtaposed fields of equal radiance and quasi-monochromatic lights of equal wavelength will exhibit equal luminosity, the division line between them would disappear. However, if one of them has a superior radiance, it will appear more luminous. Yet, if radiance is same, but the two fields have different wavelength, these fields will not show as same, and although different in color, they will also appear different in luminosity.

For example, if the radiance is high, a light of 600 nm (red) is more luminous than one of 430 nm (blue), although they have the same radiance, the visual system does not give equal response. It would be more sensitive at 600 nm than at 430 nm. This is what is known as selective receiver. This is necessary to measure the spectral sensitivity of our vision, meaning, something that indicates the sensitivity for wavelengths, which enables us to make a visual evaluation of the monochromatic radiations, and then of a compound radiation, as the sum of the visual evaluations of the different monochromatic lights that compose it.

These approaches lead us to measure what is known as the luminous efficiency curve (Fig. 3.4). Imagine a circular field with half of it occupied by a quasi-monochromatic radiation of wavelength ($\lambda_1$) and in the other half by a $\lambda_2$. Supposing the level of light is sufficient, then in central vision the main responsible for the vision are the cones. We act on one of the half-fields in such a way that we vary its radiance until it appears equally luminous, although of a different color. So, the radiance of the first wavelength will not be equal to the value of the radiance of the second wavelength. In this way, we can compare the efficiency of one wavelength with that of the rest of the visible spectrum. Normalized to the radiance of the wavelength in which we have a greater luminous efficiency, we will be able to represent all the values in a curve of luminous efficiency (Fig. 3.4). The monochromatic light

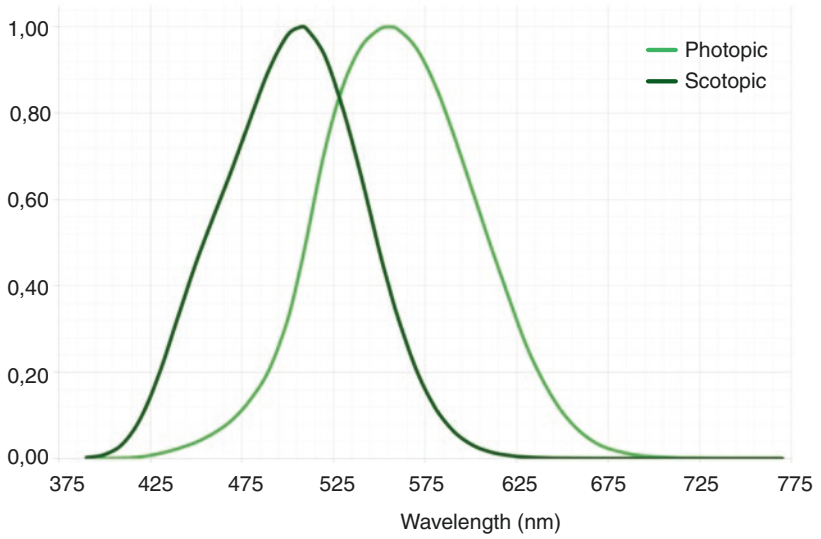


**Fig. 3.4** Scotopic and photopic luminous efficiency curves

at wavelength of 555 nm is the one that needs less radiance for equalization, and it is the most efficient. The visual system, with respect to luminosity, is more sensitive in the medium wavelengths of the visible spectrum, and its sensitivity decays towards the extremes.

#### 3.1.5.2 Scopic Vision

When lighting conditions are very low, it is known that the sensitivity of the visual system changes. According to the luminance presented by the lights or objects observed, the vision is classified in:

1. Photopic vision: when the luminances are higher than 10 cd/m$^2$.
2. Scotopic vision: luminances are lower than $10^{-3}$ cd/m$^2$.
3. Mesopic vision: between the two (photopic and scotopic vision).

The cones are directly responsible for the photopic vision, which is how we perceive color and where unforced observation is always central. Although the rods take part of the photopic vision, it is estimated that they saturate above 125 cd/m$^2$ and stop giving response.

In scotopic vision, the acting photoreceptors are rods, the cones remain inactive. It is said that in scotopic vision a central scotoma is present, since the central retina is not excited. As a consequence, the fixation point moves and centers at 1°–2° of the edge of the fovea. In mesopic vision the level of illumination is intermediate and the indefiniteness for visual judgment is important. This is the reason to recommend reaching photopic levels of luminance when a clinical judgment of color is made, so that the fovea is active and the cones work.

However, some factors can cause us to lose light as it propagates through the eye media, either within the eye or because of pupil size. Light can be lost in the eye before excitation of the photoreceptors, although most of them are included in the measures of transmittance. The reasons for that are as follows:

(a) Absorption in the ocular means (e.g., cornea, lens, humors);
(b) Reflections on the interfaces (e.g., air-cornea);
(c) Absorption in retina layers prior to photoreceptors;
(d) Scattering in the ocular media.

To calculate the value of retinal illumination it should be considered these losses and the transmittance of the ocular media, which is selective and changes its value with the wavelength. In addition, the spectral transmittance of the lens varies with age, especially due to the yellowing of the lens.

With respect to the size of the pupil, retinal illumination is directly proportional to it. The pupil varies in diameter (from 2 to 8 mm) getting smaller as the luminance of the observed object gets greater, meaning, its diameter ranges from 5 to 8 mm in darkness and from 2 to 3 mm in low glare. It is one of the reasons for controlling illumination conditions for color assessments, trying to surpass the threshold of illumination in retina above 125 cd/m$^2$.

Other interesting aspects with respect to pupil size are as follows:

(a) The opening speed of the iris observed at sudden changes in luminance levels is different from the closing speed when the change is inverse.
(b) The possibility of opening and closing the iris towards its extreme values is reduced with age. The eye tends to show small variation in pupil size due to loss of contraction capacity.

## 3.2 Color Perception

### 3.2.1 Color Vision

Color perception mainly depends on the ambient light conditions. For scotopic vision (vision under low-light levels), only rods are used. Rods have a maximum sensitivity at a wavelength of 507 nm. This is the reason for not distinguishing color at night.

For photopic vision (vision under well-lit conditions), the human eye uses three types of cones (*S*, *M*, *L*) with different spectral sensitivity (Fig. 3.5). The three detector types allow us to have trichromatic vision. Light with wavelength between 380 and 780 nm (0.38–0.78 μm) can be processed by retina, which actually determines the

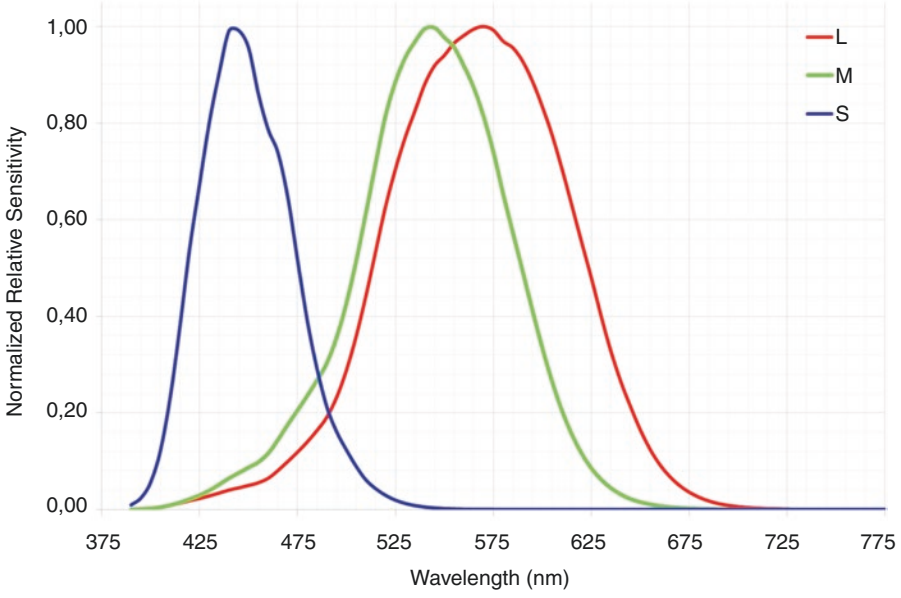


**Fig. 3.5** Dependence of normalized relative sensitivity of *S*, *M*, *L* cones on the wavelength. Data taken from [5]

visible spectrum. From the mean value of sensitivity curves of all cones (Fig. 3.5), we obtain a maximum sensitivity at a wavelength of 555 nm under photopic conditions.

For vision, the signals of *S*, *M*, and *L* cones are combined in the brain, resulting in a visual stimulus interpreted as a color. An unknown number of women may perceive millions of colors invisible to the rest of human beings. It is suggested that they have four, instead of three different types of cones which expand the perceivable spectral range. Hence, the color at which an object appears to us is not an inherent property of the object itself, but rather depends on our visual impression. The wavelength dependent visual stimulus is characterized by three parameters:

**Hue** It determines the degree to which a visual stimulus can be described as red, green, blue (primary hues). It largely depends on the predominant wavelength of light reflected or sent from an object is perceived by the eye and brain.

**Saturation or Chroma** It characterizes the purity of color. If all light seen by the eye has the same wavelength, the color appears fully saturated. The more wavelengths are added, the paler (less saturated) the color appears.

**Brightness** It determines the intensity level at which the visual impression is perceived. It is the subjective interpretation of luminance.

White, gray, and black stimuli cannot be described as color, as they have no hue and saturation and are completely determined by the brightness. In contrast to the ears that are able to distinguish several acoustic frequencies playing at once, the eyes and the brain cannot determine which wavelengths of light are simultaneously present in the observed color. For example, if we look at a monochromatic laser beam that solely consists of light with a wavelength of 590 nm, the eye perceives a yellow color. The same impression can be obtained when we spatially overlap two laser beams with wavelengths of 540 and 680 nm and proper intensity. In this case, we do not realize the beam consists of green and red lights. This, in fact, is the basis for the concept of primary hues (red, yellow, blue). With these hues, we can "mix" any other color of the visible spectrum and get another, for example, cyan is a combination of blue and green.

### 3.2.2 Subjectivity of Color Vision Determination in Dentistry

The perception of tooth color is a complex phenomenon and can be influenced by a number of factors, including the type of incident light, the reflection and absorption of light by the tooth structure, the adaptation state (mainly, eye accommodation) of the observer, and the context in which the tooth is viewed. Different light sources significantly reduced the accuracy of visual shade selection and the ability of dental students to conduct shade matching improved under certain lighting conditions [6].

Reflection and absorption of light by the tooth structure can be influenced by several factors including the following: specular transmission of light through the

tooth structure; specular reflection and diffuse light reflection at the tooth surface; absorption and scattering of light within the dental tissues; amount of enamel mineral content; enamel thickness; dentine color, and the presence of extrinsic and intrinsic stains.

Considering the human observer, this book (mainly this chapter and Chaps. 1 and 6) shows that experience, age, eye fatigue, and physiological variables, such as color blindness, can impact color perception and color matching.

The perceived tooth shade may change with the context the tooth is viewed, meaning, the surrounding features of the oral environment, for example, influence the perceived shade of a tooth. Further, brightness of the tooth can change depending on the brightness of the background, and the perceived hue of the tooth can change depending on the color of the background (Chaps. 2, 5, and 6).

Despite the reported limitations of visual shade matching of teeth, the use of shade guides is a quick and cost-effective method for selecting tooth color. In addition, tooth color discriminatory ability can be improved with training and it is often reported that investigators undergo a number of color calibration exercises about color discrimination [7, 8].

The appearance of teeth was found to be more important to women than men and significantly more important to younger people than older, as showed a survey on dental esthetics attitudes involving 250 subjects [9]. In addition, it was found the notion of having very white teeth as being beautiful, significantly decreased with increasing age of the subject, meaning, younger subjects express a greater preference for white teeth than older subjects. It was speculated that differential expectations among the age groups may affect color satisfaction and that individuals may seek to have whiter teeth within their peer group rather the whitest teeth possible [10]. The esthetic expectations are greatly associated to fashion and people culture.

## 3.3 Description of Available Dental Shade Guides and Shades Matching Procedures

Subjective visual shade matching in dentistry is performed by comparing (and matching) the dental structures or dental materials with available shade tabs from a given dental shade guide. There are several dental shade guides available (Ivoclar Vivadent Chromascop, Dentsply Esthet-X, Blue Line, etc.) and many dentists fabricated their own (custom guides). However, the most commonly used shade guides in dentistry are from the VITA family of shade guides: VITA Classical and VITA system 3D-Master (Toothguide, Linearguide, and Bleachedguide) (Figs. 3.6, 3.8, 3.10, and 3.11).

### 3.3.1 VITA Classical and Lumin Vacuum Shade Guides

VITA classical (Lumin Vacuum) shade guide system has been the standard and the most popular dental shade matching system for more than 60 years. It includes 16 shade samples (tabs) and optionally three VITA bleached shades from the Vita


**Fig. 3.6** VITA Lumin Vacuum shade guide

3D-Master shade system. It is one-step shade matching by direct comparison of a tooth to one of the A–D shade tabs (Fig. 3.6).

Among the disadvantages of this shade guide is the empirical arrangement of shades and the uneven coverage of the available shades of the natural tooth color space: there is a greater number of shade tabs covering the central area of the tooth color space than the tabs covering the shades in the dark and light regions. This distribution of shade tabs was reported to cause difficulties for adequate shade matching or leading to poor matches between natural tooth and the selected shade tab (Fig. 3.7).

### 3.3.2 VITA System 3D-Master

This shade guide system (Toothguide, Linearguide, and Bleachedguide) includes a higher number of shades: 26 and three additional bleached shades (Figs. 3.8, 3.9, and 3.10). The main difference to VITA Classical is that the shade tabs are systematically arranged, based on value, chroma, and hue, to uniformly cover the dental chromatic color space. This shade tab arrangement (Figs. 3.8 and 3.9) along with the three-step shade matching procedure has the intention to improve the color matching process. Yet, it has been reported to be a more time consuming process [11]. Intending to overcome this adversity, Vita introduced the VITA Linearguide 3D-Master containing the same 29 shades from the 3D-Master system but in a linear design. It consists of 1 Valueguide with six shade samples (Value or Lightness levels 0–5) with intermediate Hue (M) and Chroma (2) levels, and 5 Chroma/Hueguides containing the 29 shade samples. As for the Toothguide, in the Linearguide the first step is selecting value (Valueguide) then determine chroma and hue using the corresponding Chroma/Hueguide (Fig. 3.10).

The VITA Bleachedguide 3D-Master (Fig. 3.11) was especially developed to tooth whitening treatments. It brings 15 of the 29 shade tabs from the 3D-Master

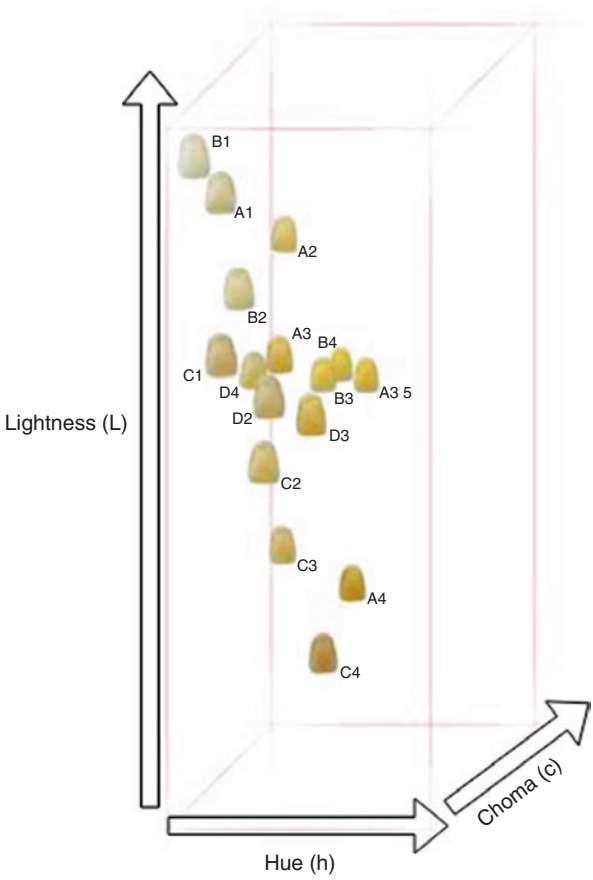


**Fig. 3.7** Chromatic distribution of the 16 shade tabs from VITA Classical (Lumin Vacuum) shade guide. Lightness (*L*) goes from darker (bottom) to brighter (top) shades. Hue (*h*) goes from more yellow (left) to more red (right), and chroma (*c*) goes from paler to more intensive shades

system, which includes the bleached shade tabs (0), and the remaining 14 shades are interpolated. One of the main characteristics of this shade guide is the uniform arrangement of the tabs in terms of saturation, whiteness index, and value. It is also recommended and approved for evaluation of home whitening products by the American Dental Association (ADA).

All VITA shade tabs are manually layered, ceramic specimens and are designed to represent the nature of human teeth, including features of cervical, incisal, central, and lateral areas. However, it is important to highlight that only the central area of the tab represents the shade. In this sense, when performing a visual match with any of the VITA shade guide systems, the dental professional has to compare the central area to the patient's tooth with the shade tab while trying to mask out the other areas.

There are several factors that have to be considered or taken into account when visual shade matching is being carried out. For example, the most important shade matching has to be done prior to tooth preparation, since the dental structures are prone to dehydration during preparation and they might change their chromatic

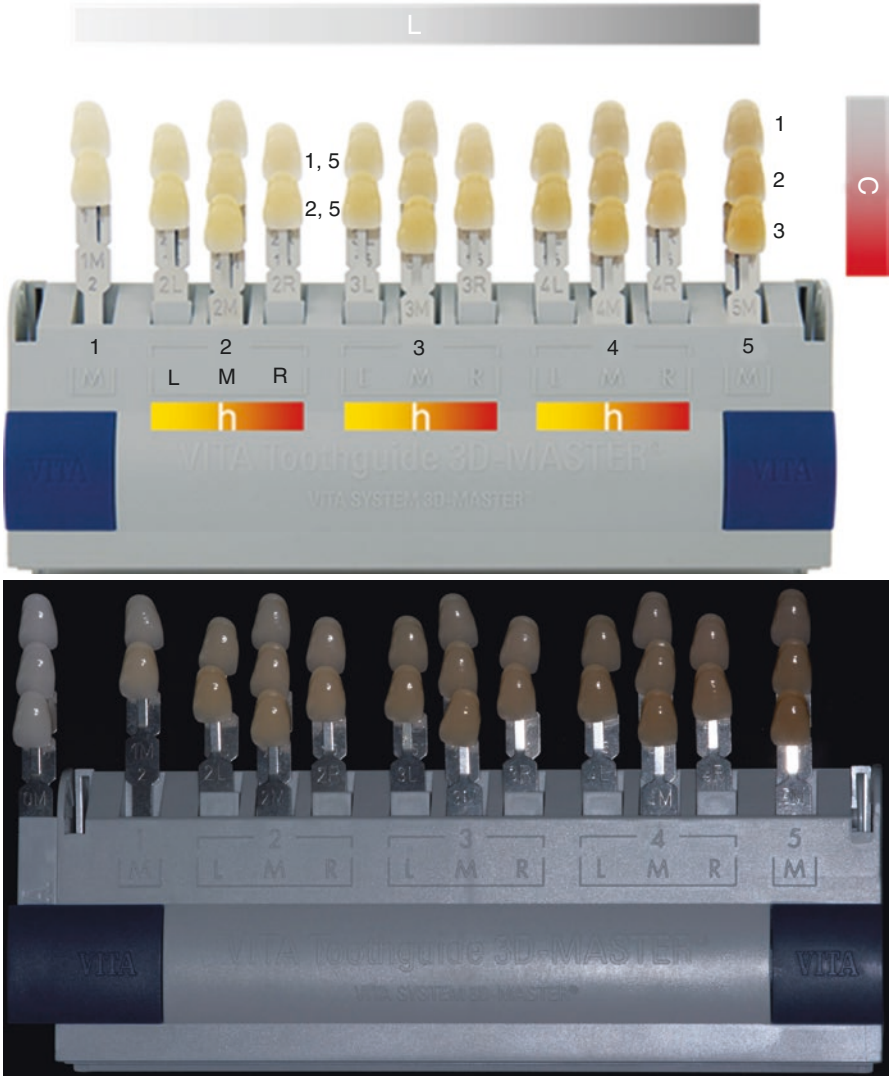


**Fig. 3.8** Schematic representation (top) and the VITA Toothguide 3D-Master (bottom) including the bleached shades (left). The system is organized considering value or lightness (*L*), chroma (*C*), and hue (*h*); where *L* varies from 1 to 5 (bright to dark) and 0 being bleached shades, *C* varies from 1 to 3 (pale to intense), and *h* ranges from yellowish (L), medium (M) to reddish (R)

appearance (Chap. 6). However, shade of prepared tooth structure may be registered and communicated to the dental laboratory technician to assist his/her job on fabricating the indirect restoration (Chap. 6). The use of a standardized lighting is highly recommended (a CCT of approximately 6.500 K would be the best option) (Chaps. 5 and 6). In addition, cleaning the surface area to be matched is essential

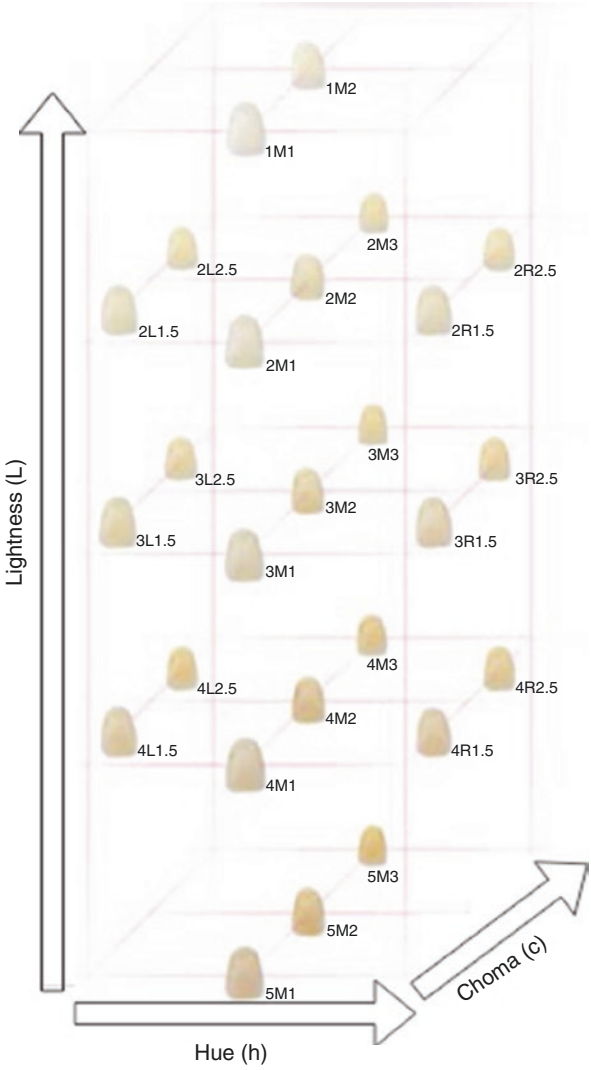


**Fig. 3.9** Chromatic distribution of the 26 shade tabs of the VITA 3D-Master system. Lightness (*L*) goes from darker (shades #5) to brighter (shades #1); hue (*h*) goes from more yellow (*L* shades) to more red (R shades); and chroma (*c*) goes from paler (shade final digit #1) to more intensive (shade final digit #3) shades. This shade guide has a better and more symmetrical distribution than VITA Classical shown in Fig. 3.7

and special care has to be taken with the surrounding areas of the tooth, as any eccentric (too bright or too dark) color might influence the outcome of the shade matching (Chaps. 5 and 6).

A recommended distance between the eye and the shade tab for the shade matching procedure should be about 30–40 cm. The shade tab must be hold parallel to the patients' tooth and as close to the gingiva as possible. The dental practitioner has to focus his/her attention on the central area of the shade tab while trying to mask out other portions of the tab. If different shades are required for cervical, central, and incisal areas, the shade matching procedure has to be repeated and done separately for each of these areas.

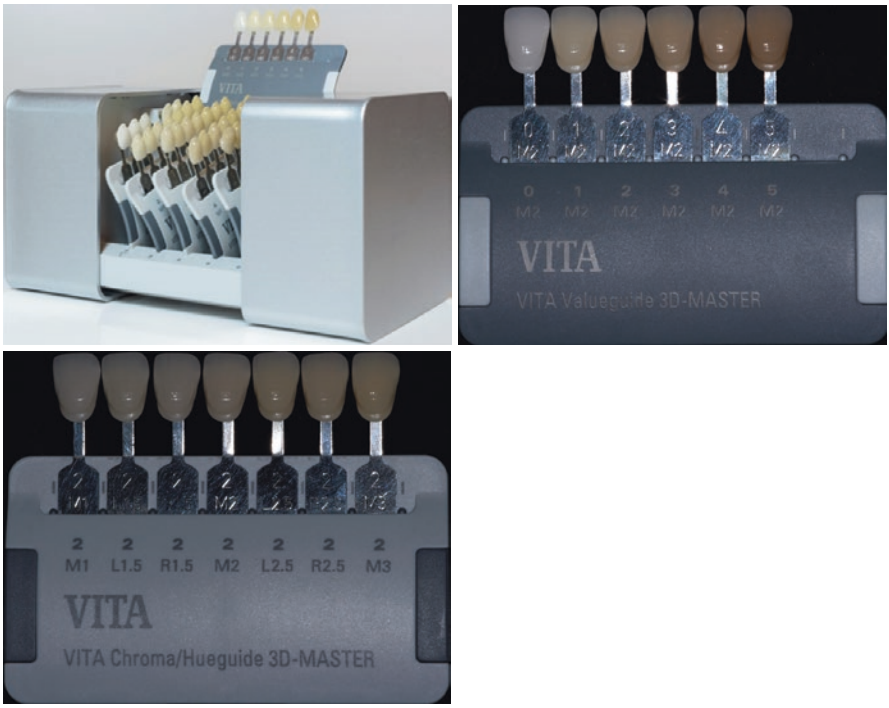


**Fig. 3.10** VITA Linearguide 3D-Master. Using the same shade samples from 3D-Master system, it comes in an acrylic box (top image) containing one VITA Valueguide 3D-Master (bottom left) and five VITA Chroma/Hueguides 3D-Master (bottom right) where tabs are organized according to the lightness levels (0/1, 2, 3, 4, and 5) and including the chromas 1–3 (pale to intense) and hues (yellowish (*L*), medium (*M*), and reddish (*R*))


**Fig. 3.11** VITA Bleachedguide 3D-Master shade guide

It is also important to make a decision in a short period of time (normally less than 10 s) since dehydration of the tooth might occur as well as other phenomena, as eye fatigue, for example. If a satisfactory match is not achieved in this period of time, it is recommended to rest and look to a gray area for about 20 s to wash away any eye fatigue or visual chromatic adaptations.

Bottom line, one should not forget that shade matching does not exclusively depend on the color, since there are other factors, such as translucency, fluorescence, or opalescence of the dental structures that can alter the visual perception of the dental structure to be matched.

## 3.4 Perceptibility and Acceptability Thresholds

Perceptibility difference threshold represents the lower perceptual limit, and it is widely applicable, mainly, to develop new color notation systems and their color difference metrics, to study discernible colors by the human visual system, and to understand the mechanisms of color vision. However, in many practical situations, differences above the threshold (supra-threshold) are used, passing from perceptibility thresholds or *just noticeable differences* to higher differences, named *acceptable differences* or *tolerances*. The industrial interest on these differences is justified, on the one hand, by the high cost required to maintain the industrial production below the limits of the visual threshold (PT- perceptible threshold) and, on the other hand, by the need of maintaining the differences under an admissible limit. The complete absence of control (monitoring) should involve a lack of similarity in the production outcome, with negative implications on the overall quality of the product.

### 3.4.1 Color Perceptibility and Acceptability Thresholds (PT and AT) Apply to Dentistry

Dental materials need to match and reproduce the color appearance of natural teeth and other soft tissues, such as gingiva, oral mucosa, and skin (in maxillofacial prosthodontics) to achieve the desired esthetic outcome in an efficient manner. Visual judgment is the most frequently used method to evaluate color in dentistry. Therefore, knowledge on perceptual limits of color in the color space related to dentistry is of critical importance for understanding color differences in clinical dentistry and dental research. In color science, a color difference ($\Delta E$) formula is designed to give a quantitative representation of the perceived color difference ($\Delta V$) between a pair of colored specimens under a given set of experimental conditions (Chap. 1). Thus, the quality of color match between a dental restoration and adjacent natural tooth to a large extent correlates with the magnitude and direction of color difference.

**Table 3.1** Overview of thresholds research applied to Dentistry and the studies main findings (adapted from [12])

| Study | Main findings |
|---|---|
| *Teeth* | |
| Ruyter et al. [13] | 50:50% AT: $\Delta E_{ab} = 3.3$ |
| Johnston and Kao [14] | Match/mismatch: $\Delta E_{ab} = 3.7/6.8$ |
| Douglas and Brewer [15] | 50:50% PT/AT: $\Delta E_{ab} = 0.4/1.7$ |
| Ragain and Johnston [16] | 50:50% AT: $\Delta E_{ab} = 2.7$ |
| Ragain and Johnston [17] | 50:50% AT: $\Delta E_{CMC} = 2.3$ |
| Douglas et al. [18] | 50:50% PT/AT: $\Delta E_{ab} = 2.6/5.5$ |
| Lindsey and Wee [19] | 50:50% AT: $\Delta L_{ab} = 1.0$, $\Delta a_{ab} = 1.0$; $\Delta b_{ab} = 2.6$ |
| Wee et al. [20] | $\Delta E_{00}$, $\Delta E_{CMC}$ outperformed $\Delta E_{ab}$ |
| Silva et al. [21] | 100% AT: $\Delta E_{ab} = 2.7$ |
| Ishikawa-Nagai et al. [22] | 100% PT: $\Delta E_{ab} = 1.6$ |
| Ghinea et al. [23] | 50:50% PT/AT: $\Delta E_{ab} = 1.7/3.5$ |
| del Mar Pérez et al. [24] | 50:50% AT: $\Delta E_{00} = 1.9$ |
| Alghazali et al. [25] | 50:50% PT/AT: $\Delta E_{ab} = 1.9/4.2$ |
| Dietschi et al. [26] | 50:50% PT/AT: $\Delta E_{ab} = 1.1/3.3$ |
| Paravina et al. [27] | 50:50% PT/AT: $\Delta E_{ab} = 1.2/2.7$; $\Delta E_{00} = 0.8/1.8$ |
| Thoma et al. [28] | 100% PT: $\Delta E_{ab} = 1.9$ |
| *Gingiva* | |
| Sailer et al. [29] | 100% PT: $\Delta E_{ab} = 3.1$ |
| Ren et al. [30] | 50:50% PT/AT: $\Delta E_{ab} = 2.1/4.6$; $\Delta E_{00} = 1.7/4.1$ |
| Pérez et al. [31] | 50:50% PT/AT: $\Delta E_{ab} = 1.7/3.7$; $\Delta E_{00} = 1.1/2.8$ |

Visual thresholds are of paramount importance as quality control tool and guide for evaluation and selection of dental materials, evaluation and interpretation of clinical outcome, in vivo and in vitro dental research, and standardization in dentistry. A variety of visual color threshold values have been reported in numerous studies (Table 3.1) related to teeth and gingiva [12].

Most studies used CIELAB color difference formula. The first study [23] to determine PT and AT in Dentistry using CIEDE2000 colors difference formula and the Takagi–Sugeno–Kang (TSK) fuzzy approximation only appeared in 2010. An observer's panel performed independent assessments of perceptibility and acceptability judgments on 105 pairs of ceramic discs. Color differences for each pair of discs were calculated using CIELAB and CIEDE2000 color differences formulas. From the resultant fitting curves the 50:50% thresholds were calculated resulting in an AT of 2.23 (CIEDE2000(1:1:1)) and 3.48 (CIELAB) and a PT of 1.25 (CIEDE2000(1:1:1) and 1.74 (CIELAB). The authors concluded that CIEDE2000 formula provided a better fit than CIELAB formula to evaluate color difference thresholds of dental ceramics, recommending its use in dental research and in vivo instrumental color analysis. In addition, the study showed a significant difference between PT and AT for dental ceramics and that TSK fuzzy approximation is a reliable alternative approach for the color threshold calculation procedure.

Subsequently, a multicenter study [27] was designed to determine 50:50% PT and 50:50% AT of dental ceramic under simulated clinical settings. Each research center recruited 25 observers, divided into five groups of observers: dentists, dental students, dental auxiliaries, dental technicians, and laypersons. Visual color comparison conditions and fitting procedure were the same as previous studies [23, 24]. The determined general (taking all groups of observers into account) CIELAB50:50% PT was $\Delta E^*_{ab}$ = 1.2, whereas 50:50% AT was $\Delta E^*_{ab}$ = 2.7. These results were included as reference values within ISO/TR 28642:2016 and can be applied to all issues related to quality of tooth color matching in dentistry, such as color compatibility among dental materials, color compatibility between dental materials and human tissues, coverage error assessment of dental shade guides, color stability during fabrication and at placement, color stability after aging and staining or masking potential of opaque dental materials. Yet, the thresholds values using CIEDE2000 ($\Delta E_{00}$) were PT = 0.8 and AT = 1.8. These values can serve as a quality control tool to guide the selection of esthetic dental materials, evaluate clinical performance, and interpret visual and instrumental findings in clinical dentistry, dental research, and subsequent standardization (Fig. 3.12).

Additionally, a study [24] involving 30 observers and 58 tooth-colored ceramic discs reported CIEDE2000 acceptability thresholds (AT) for individual axis of lightness ($\Delta L'$), chroma ($\Delta C'$), and hue ($\Delta H'$). The 50:50% AT were 2.92, 2.52, and 1.90, respectively.

There are very few papers on visual thresholds for gingiva and/or gingiva-colored materials. A study [29] reported on 100% visual threshold, which is a threshold level considered not clinically relevant. Another study [30] reported on PT of 1.7 and 2.1, and AT of 4.1 and 4.6 for CIEDE2000 and CIELAB color difference formulas, respectively, but such values are considerably higher than the corresponding thresholds for tooth colors. Another study [31] determined 50:50% perceptibility thresholds (PT) and 50:50% AT for computer-simulated samples of human gingiva using CIEDE2000 and CIELAB formulas. The PT and AT for CIEDE2000 were 1.1 and 2.8, respectively, and the corresponding CIELAB values were 1.7 and 3.7. Visual thresholds of human gingiva were not dependent upon lightness of adjacent teeth.

### 3.4.2 Whiteness Perceptibility and Acceptability Thresholds in Dentistry

There have been few attempts to reach whiteness perceptibility and acceptability thresholds in Dentistry. The perceptual thresholds for $\Delta L^*$(1.14), $\Delta a^*$(3.24), and $\Delta b^*$(1.11) in tooth whiteness conducted a psychophysical experiment based on visual assessments of digital images of teeth on a calibrated display [32].

A study [33] determined the visual whiteness thresholds using the whiteness index for dentistry based on CIELAB color space ($WI_D$). A total of 60 observers

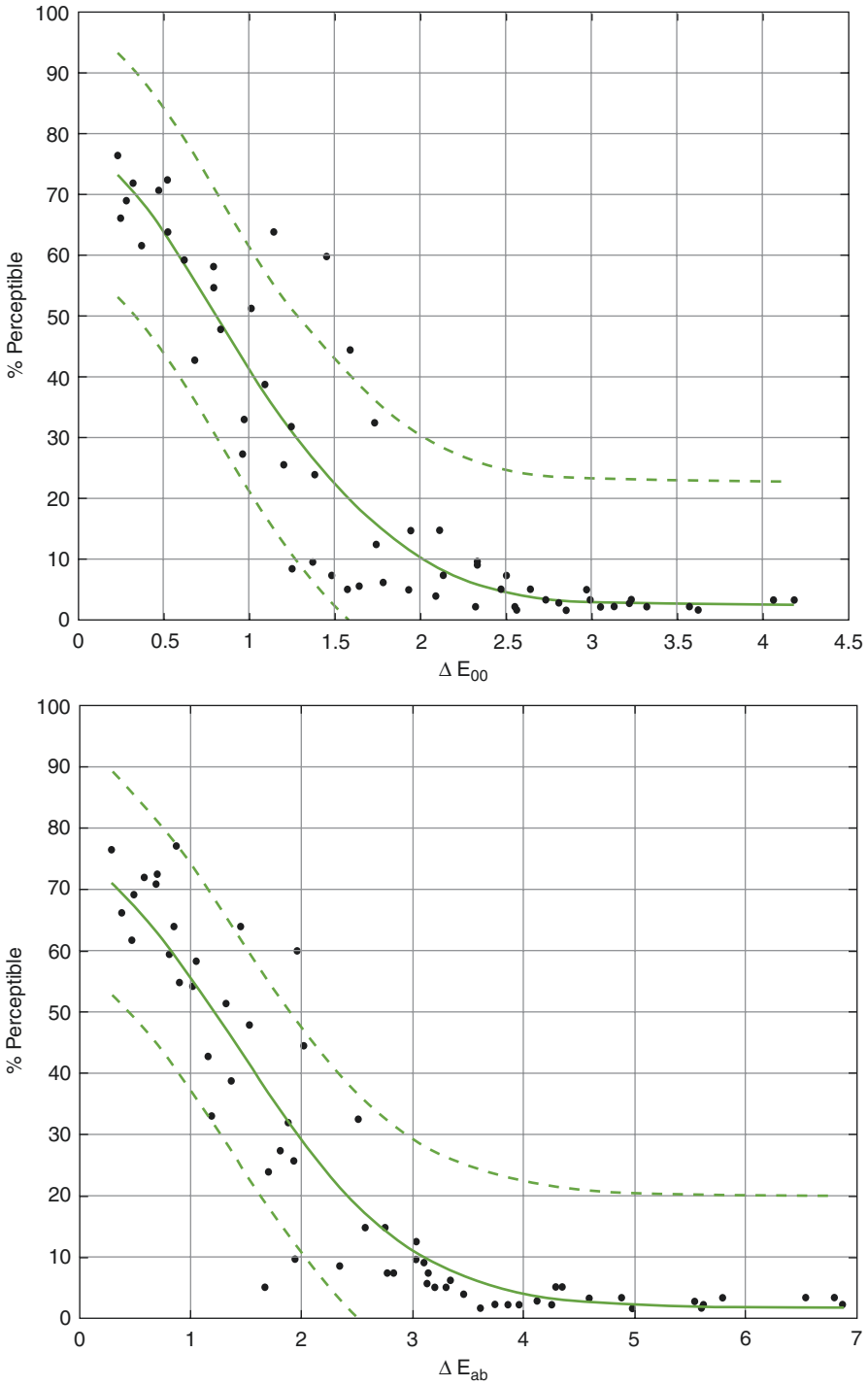


**Fig. 3.12** Fitting process and estimation of color thresholds from a multicenter study [27]

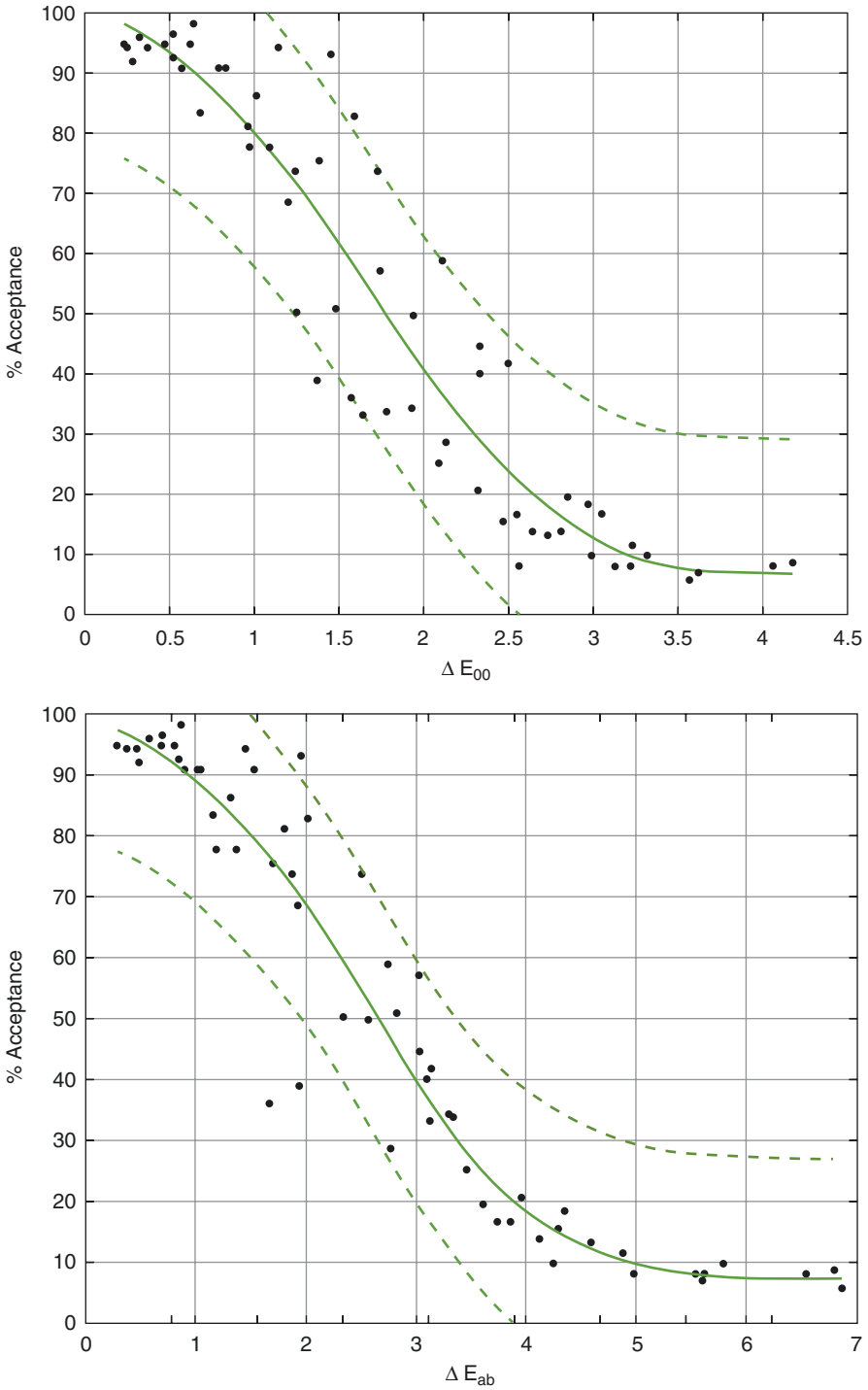


**Fig. 3.12** (continued)

(dentists and laypersons) from three research sites participated/performed in a psychophysical experiment based on visual assessments of simulated images of teeth on a calibrated display. Images of simulated upper central incisors (SUCI) were consecutively displayed in pairs (60) and the whiteness of each SUCI pair was compared. $WI_D$ was used to calculate the visual thresholds (WPT- perceptibility threshold; and WAT- acceptability threshold) with 95% confidence intervals (CI) and TSK fuzzy approximation model was used as fitting procedure. WPT and WAT were 0.72 (CI: 0.0–2.69; $r^2 = 0.52$) and 2.62 (CI: 0.2–7+; $r^2 = 0.57$) $WI_D$ units, respectively (Fig. 3.13). Significant differences ($p < 0.05$) were found between WPT and WAT, and between dentist (WPT = 0.46$WI_D$ units; WAT = 2.20 $WI_D$ units) and layperson (WPT = 0.94 $WI_D$ units; WAT = 2.95 $WI_D$ units). These values can serve as reference values for research and manufacturing of dental materials, and for clinical practice situations such as assessing the effectiveness of bleaching treatments.

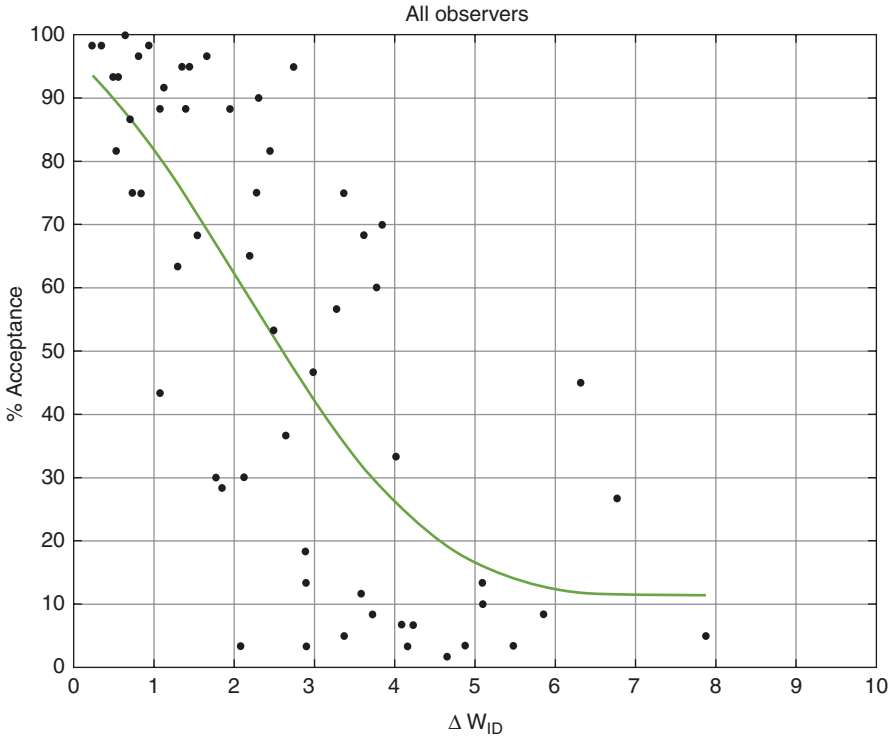


**Fig. 3.13** Acceptance (left curve) and perceptibility (right curve) percentages versus whiteness differences ($\Delta WI_D$) for all observers [33]

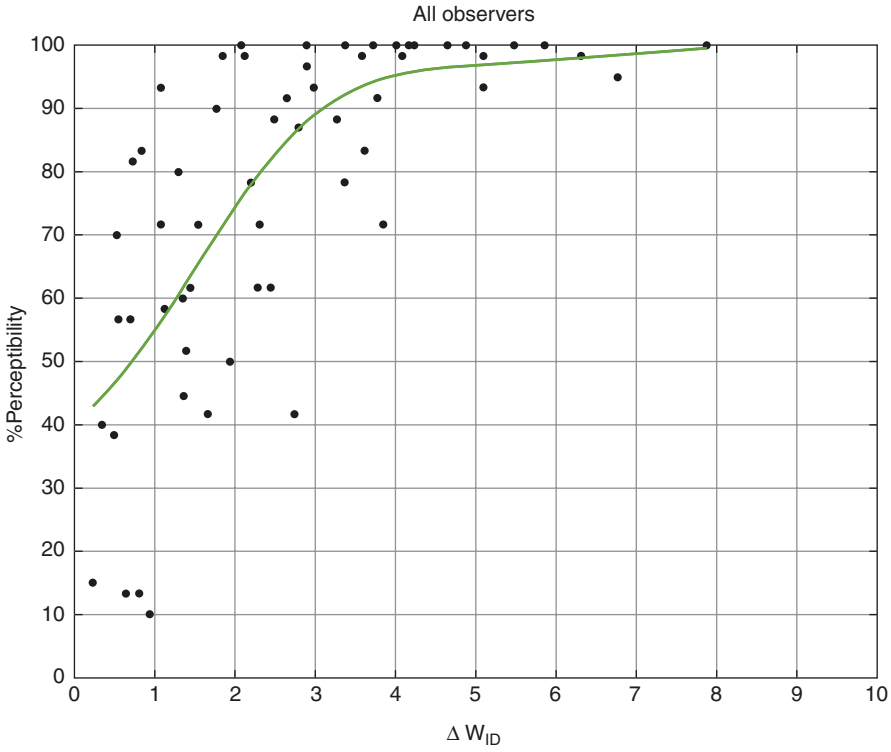


**Fig. 3.13** (continued)

### 3.4.3 Translucency Perceptibility and Acceptability Thresholds in Dentistry

In dentistry, there were few attempts to reach a translucency perceptibility and acceptability thresholds. A translucency perception threshold calculated using CR (contrast ratio) determinations on dental porcelains was reported as overall mean translucency perceptibility threshold of 0.07 and 50% of this population perceived a 0.06 CR (6%) difference in translucency. Using regression equations between TP (translucency parameter) and CR, the authors reported visual perceptibility thresholds for translucency difference in TP of 2 [34].

Another study [35] determined the translucency acceptability and perceptibility thresholds for dental resin composites using CIEDE2000 and CIELAB color difference formulas. A30-observer panel performed perceptibility and acceptability judgments on 50 pairs of resin composites discs (Fig. 3.14). Disc pair differences for the translucency parameter (ΔTP) were calculated using both

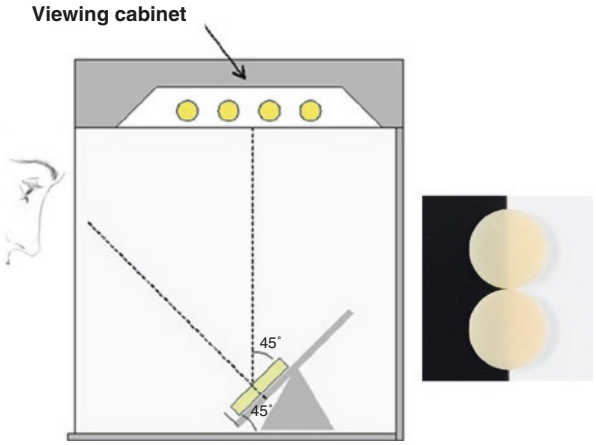


**Fig. 3.14** Schematic representation of the visual set-up including the viewing booth, observation distance of 30 cm, and optical geometry (left). A specimen pair ready for visual assessment is also shown (right) [35]

color difference formulas ($\Delta TP_{00}$ ranged from 0.11 to 7.98, and $\Delta TP_{ab}$ ranged from 0.01 to 12.79). From the resultant fitting curves, the 95% confidence intervals were estimated and the 50:50% translucency perceptibility and acceptability thresholds (TPT and TAT) were calculated. CIEDE2000 50:50% TPT was 0.62 and TAT was 2.62 (Fig. 3.15). Corresponding CIELAB values were 1.33 and 4.43, respectively. Translucency perceptibility and acceptability thresholds were significantly different using both color difference formulas ($p = 0.01$ for TPT and $p = 0.005$ for TAT). CIEDE2000 color difference formula provided a better data fit than CIELAB formula. Thus, the authors stated that the visual translucency difference thresholds determined with CIEDE2000 color difference formula can serve as reference values in the selection of resin composites and evaluation of its clinical performance.

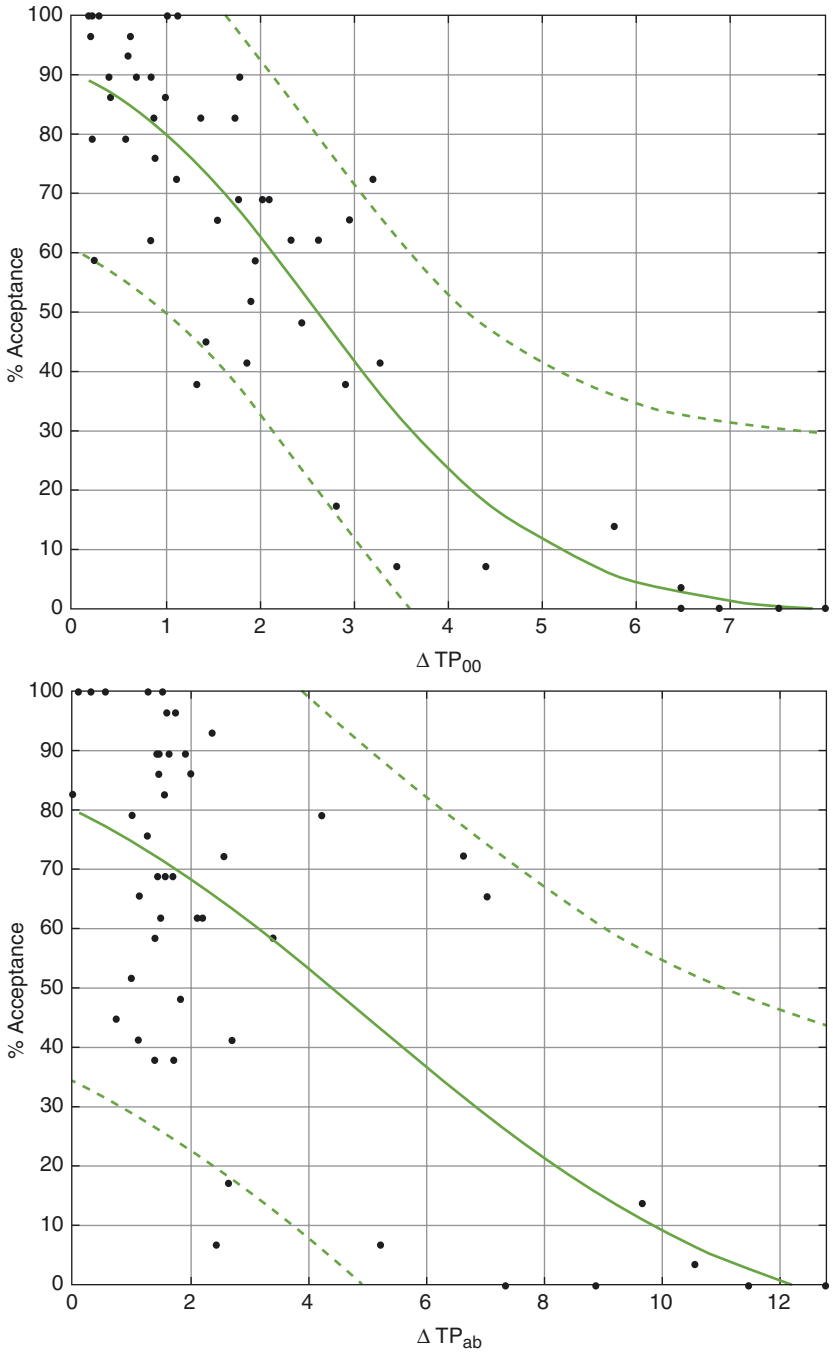


**Fig. 3.15** Acceptable percentages versus translucency differences ($\Delta TP_{00}$ and $\Delta TP_{ab}$) between experimental pairs. Curves denote the 50:50% acceptability translucency threshold (center curve) and its corresponding confidence curves (upper and lower lines) using CIEDE2000 and CIELAB color difference formulas [35]

## Further Readings


1. Kaschke M, Donnerhacke KH, Rill MS. Optical devices in ophthalmology and optometry: technology, design principles and clinical applications. Weinheim: Wiley; 2013.
2. Patel S, Tutchenko L. The refractive index of the human cornea: a review. Cont Lens Anterior Eye. 2019;42(5):575–80.
3. Sridhar MS. Anatomy of cornea and ocular surface. Indian J Ophthalmol. 2018;66(2):190.
4. Goldstein EB. Sensation and perception. 7th ed. Belmont: Wadsworth; 2007.
5. Gross H, Blechinger F, Achtner B. Handbook of optical systems – survey of optical instruments, vol. 4. Weinheim: Wiley-VCH Verlag GmbH; 2008.
6. Curd FM, Jasinevicius TR, Graves A, Cox V, Sadan A. Comparison of the shade matching ability of dental students using two light sources. J Prosthet Dent. 2006;96:391–6.
7. Joiner A, Luo W. Tooth colour and whiteness: a review. J Dent. 2017;67(Suppl 1):S3–10.
8. Joiner A. The bleaching of teeth: a review of the literature. J Dent. 2006;34:412–9.
9. Vallittu PK, Vallittu ASJ, Lassila VP. Dental aesthetics- a survey of attitudes in different groups of patients. J Dent. 1996;24:335–8.
10. Odioso LL, Gibb RD, Gerlach RW. Impact of demographic, behavioral, and dental care utilization parameters on tooth color and personal satisfaction. Comp Contin Educ Dent. 2000;21:S35–41.
11. Della Bona A, Barrett AA, Rosa V, Pinzetta C. Visual and instrumental agreement in dental shade selection: three distinct observer populations and shade matching protocols. Dent Mater. 2009;25(2):276–81.
12. Paravina RD, Pérez MM, Ghinea R. Acceptability and perceptibility thresholds in dentistry: a comprehensive review of clinical and research applications. J Esthet Restor Dent. 2019;31(2):103–12.
13. Ruyter IE, Nilner K, Moller B. Color stability of dental composite resin materials for crown and bridge veneers. Dent Mater. 1987;3:246–51.
14. Johnston WM, Kao EC. Assessment of appearance match by visual observation and clinical colorimetry. J Dent Res. 1989;68:819–22.
15. Douglas RD, Brewer JD. Acceptability of shade differences in metal ceramic crowns. J Prosthet Dent. 1998;79:254–60.
16. Ragain JC, Johnston WM. Color acceptance of direct dental restorative materials by human observers. Color Res Appl. 2000;25:278–85.
17. Ragain JC, Johnston WM. Minimum color differences for discriminating mismatch between composite and tooth color. J Esthet Restor Dent. 2001;13:41–8.
18. Douglas RD, Steinhauer TJ, Wee AG. Intraoral determination of the tolerance of dentists for perceptibility and acceptability of shade mismatch. J Prosthet Dent. 2007;97:200–8.
19. Lindsey DT, Wee AG. Perceptibility and acceptability of CIELAB color differences in computer-simulated teeth. J Dent. 2007;35:593–9.
20. Wee AG, Lindsey DT, Shroyer KM, Johnston WM. Use of a porcelain color discrimination test to evaluate color difference formulas. J Prosthet Dent. 2007;98(2):101–9.
21. Silva JD, Park SE, Weber HP, Ishikawa-Nagai S. Clinical performance of a newly developed spectrophotometric system on tooth color reproduction. J Prosthet Dent. 2008;99(5):361–8.
22. Ishikawa-Nagai S, Yoshida A, Sakai M, Kristiansen J, da Silva JD. Clinical evaluation of perceptibility of color differences between natural teeth and all-ceramic crowns. J Dent. 2009;37(Suppl 1):e57–63.
23. Ghinea R, Pérez MM, Herrera LJ, Rivas MJ, Yebra A, Paravina RD. Color difference thresholds in dental ceramics. J Dent. 2010;38(Suppl 2):e57–64.
24. Pérez MM, Ghinea R, Herrera LJ, Ionescu AM, Pomares H, Pulgar R, Paravina RD. Dental ceramics: a CIEDE2000 acceptability thresholds for lightness, chroma and hue differences. J Dent. 2011;39(Suppl 3):e37–44.
25. Alghazali N, Burnside G, Moallem M, Smith P, Preston A, Jarad FD. Assessment of perceptibility and acceptability of color difference of denture teeth. J Dent. 2012;40(Suppl 1):e10–7.

26. Dietschi D, Abdelaziz M, Krejci I, Di Bella E, Ardu S. A novel evaluation method for optical integration of class IV composite restorations. Aust Dent J. 2012;57(4):446–52.
27. Paravina RD, Ghinea R, Herrera LJ, Della Bona A, Igiel C, Linninger M, Sakai M, Takahashi H, Tashkandi E, Perez MM. Color difference thresholds in dentistry. J Esthet Restor Dent. 2015;27(Suppl 1):S1–9.
28. Thoma DS, Ioannidis A, Fehmer V, Michelotti G, Jung RE, Sailer I. Threshold values for the perception of color changes in human teeth. Int J Periodontics Restorative Dent. 2016;36(6):777–83.
29. Sailer I, Fehmer V, Ioannidis A, Hämmerle CH, Thoma DS. Threshold value for the perception of color changes of human gingiva. Int J Periodontics Restorative Dent. 2014;34(6):757–62.
30. Ren J, Lin H, Huang Q, Zheng G. Determining color difference thresholds in denture base acrylic resin. J Prosthet Dent. 2015;114(5):702–8.
31. Pérez MM, Ghinea R, Herrera LJ, Carrillo F, Ionescu AM, Paravina RD. Color difference thresholds for computer-simulated human gingiva. J Esthet Restor Dent. 2018;30(2):E24–30.
32. Westland S, Luo W, Li Y, Pan Q, Joiner A. Investigation of the perceptual thresholds of tooth whiteness. J Dent. 2017;67(Suppl):S11–4.
33. Pérez MM, Herrera LJ, Carrillo F, Pecho OE, Ghinea R, Gasparik C, Dudea D, Della Bona A. Whiteness difference thresholds in dentistry. Dent Mat. 2019;35(2):292–7.
34. Lee YK. Criteria for clinical translucency evaluation of direct esthetic restorative materials. Restor Dent Endod. 2016;41:159–66.
35. Salas M, Lucena C, Herrera LJ, Yebra A, Pecho EO, Della Bona A, Pérez MM. Translucency thresholds for dental materials. Dent Mat. 2018;34(8):1168–74.

# Instrumental Shade Matching

# 4

Razvan Ionut Ghinea, María del Mar Pérez Gómez, Luis Javier Herrera Maldonado, Oscar Emilio Pecho Yataco, and Alvaro Della Bona

## Contents



R. I. Ghinea · M. del M. Pérez Gómez
Optics Department, Faculty of Science, University of Granada, Granada, Spain
e-mail: rghinea@ugr.es; mmperez@ugr.es

L. J. Herrera Maldonado
Department of Architecture and Computer Technology, School of Informatics Engineering and Telecommunication, University of Granada, Granada, Spain
e-mail: jherrera@ugr.es

O. E. Pecho Yataco · A. Della Bona (✉)
Dental School, Postgraduate Program in Dentistry, University of Passo Fundo, Passo Fundo, RS, Brazil
e-mail: dbona@upf.br


A. Della Bona (ed.), *Color and Appearance in Dentistry*,
https://doi.org/10.1007/978-3-030-42626-2_4

## 4.1 Science and Technology of Instruments to Measure Color, Color Coordinates, and Optical Properties

Instrumental shade matching was introduced to Dentistry as an attempt to reduce the subjectivity of visual shade matching that is mostly due to inherent problems related to visual chromatic associations, including lighting conditions, surface characteristics of the sample, optical properties, and translucency, which were mostly discussed in Chap. 3. Thus, the development of instruments to objectively measure color of dental structures and dental materials, and also have the capacity to provide a match with a shade tab of a dental chromatic guide is an expected and desired benefit to the dental profession. Yet, measuring color of dental structures is a challenging task mostly because of the inherent characteristics of the human teeth (e.g., curved surfaces, relatively small, layered structure with distinctive optical properties, and translucency) and their colorimetric features, with multidirectional color transitions (gingivo-incisal/occlusal, mesial-distal, and buccal-lingual).

Digital imaging systems, colorimeters, and spectrophotometers are the most popular instruments for objective color measurements in Dentistry (Table 4.1). These measuring devices have been developed primarily to fit the needs of the dental clinician, providing information related to the corresponding shade tab, tooth translucency, or information associated with color determination, communication, reproduction, and verification [1]. In terms of color matching, shade verification (quality control), communication, and reproduction of color in dentistry, the use of these instruments can help overcoming some shortcomings of the visual method by bringing accuracy in stable readings and reducing the chair side time. Yet, these instruments have their pros and cons, for example, colorimeters show good measurement repeatability but they are exposed to systematic errors caused by edge-loss effects from sample surface, and spectrophotometers precisely measure color from reflectance or transmittance data but they offer some difficulties for clinical tooth color evaluation [1]. In this sense, the recent incorporation of spectroradiometers for color measurements in dental research provided accurate and highly repeatable non-contact measurements [2].

Radiometry is the science of measuring electromagnetic radiation in terms of its power, polarization, spectral content, and other parameters relevant to a particular source or detector configuration. A radiometer is an instrument that measures

**Table 4.1** Most popular instruments used for measuring color in dentistry

| Instrument, manufacturer | Type | Measuring area |
|---|---|---|
| Vita Easyshade, VITA | Spectrophotometer | 5-mm diameter |
| SpectroShade Micro II, MHT | Imaging spectrophotometer | Complete tooth |
| CrystalEye, Olympus | Imaging spectrophotometer | Complete tooth |
| Shade-X, X-Rite | Spectrophotometer | 3-mm diameter |
| ShadeVision, X-Rite | Imaging colorimeter | Complete tooth |
| TRIOS, 3Shape | Intraoral scanner | Variable measurement circle, complete tooth |

optical radiation. There are a variety of radiometric quantities that can be used to specify the properties of a sample. Of particular interest in color appearance measurements are the irradiance and, especially, the radiance. Radiance differs from irradiance, since it is a measure of the power emitted from a source (or reflected from a surface), rather than incident upon a surface, per unit area per unit solid angle. Spectral radiance includes a wavelength dependency.

Radiance is preserved through optical systems (neglecting absorption) and is independent of distance. That is, radiance leaving from A to B is same radiance arriving at B. So, radiance has a highly desirable property and the human visual system responds commensurably to radiance, making it a key measurement in color appearance specification. Furthermore, radiance does not fall off with the square of distance from the surface, since the decrease in power incident on the pupil is directly canceled by a proportional decrease in the solid angle subtended by the pupil with respect to the surface in question [3]. In addition, spectroradiometers are a non-contact technique that can match the geometry of visual assessments, which turned to be one of the main reasons for spectroradiometric measurements become first choice for spectral measurements in dental color studies [4].

However, there are important assumptions to make on performing adequate spectroradiometric measurements, such as:

- the radiance leaving a point on a surface is due only to radiance arriving at this point (although radiance may change directions at a point on a surface, we assume that it does not skip from point to point);
- radiation leaving a surface at a given wavelength (efflux) is due to incident radiation at that wavelength (influx);
- the surface does not generate light internally, treating light sources separately.

There are many uses of radiometry in industrial applications to monitor manufacturing processes, and in scientific and technical activities that utilize the sensing of optical radiation to deduce information about a wide range of physical, chemical, and biological processes. So far in dentistry, spectroradiometric color measurements are used exclusively for research purposes.

Several factors need to be considered when selecting a color-measuring instrument. If no spectral data is required, and all the stimuli requiring measurements are composed of the same components, then colorimeters, spectrometers, or imaging systems can be used. It has to be taken into account that this type of devices are usually designed for one CIE Standard Illuminant and Observer combination (most often CIE D65 Illuminant and CIE 2° Standard Observer, discussed in Chap. 3). However, the majority of measurements require spectral data, as is the case for most applications in dentistry. One of the main advantages in obtaining complete spectral data is that it provides information on the consistency of the material and can detect potential problems of metamerism, allowing to calculate colorimetric data for the actual spectral power distribution of each source expected to illuminate the specimen [5].


**Fig. 4.1** Spectrophotometer VITA Easyshade V (art and digital compositing from picture)

One of the most popular instruments for measuring color in Dentistry is the VITA Easyshade (Table 4.1). This small and portable spectrophotometer, designed to be used in the dental practice, has been in development for several years and the manufacturer has been introducing new versions of the instruments, with improved and new features, every 2–3 years (Fig. 4.1). The device allows rapid digital shade matching of natural teeth and ceramic restorations with no influence from the environment, and it supports dentists and dental technicians in tooth shade matching and communication, shade reproduction, and verification of final shade of ceramic dental restoration. In this sense, it has six different shade-matching modes applied to Dentistry, as follows:

- *Basic shade matching*: For selection of suitable composite or for bleaching documentation.
- *Average shade matching*: Especially recommended in case of multi-chromatic teeth. For selection of composite, CAD/CAM materials, veneering material, or prosthetic teeth.
- *Tooth area shade matching*: Measuring three areas of interest: cervical, middle, and incisal (occlusal) thirds.
- *Control of ceramic restorations*: Shade matching during and after the restoration preparation process, quality control and quality management in the dental laboratory.
- *Crown shade matching*: Shade matching of existing crowns in vivo and in vitro.
- *Training mode*: To practice the handling of the instrument on a VITA shade guide, using CL for VITA classical A1-D4 or 3D for VITA SYSTEM 3D-MASTER.

Another popular portable equipment is the SpectroShade Micro II digital shade-matching device that uses a digital camera along with a LED spectrophotometer (Fig. 4.2). Due to the illuminating/measuring configuration, the measured spectral data are not influenced by any external lighting or any other environmental conditions. In addition to the capability of capturing the tooth image and registering the colorimetric information, it can measure and save spectral data and


**Fig. 4.2** The imaging spectrophotometer SpectroShade Micro II Dental Color Complete Tooth Analysis System (art and digital compositing from picture)

transfer it to a computer. Thus, the SpectroShade analyzes the color of the tooth and indicates the closest available chromatic standard from its vast colorimetric database applied to Dentistry. It calculates the color difference between the analyzed dental structure and the selected color tab in terms of brightness, chroma, and hue. As the spectrophotometer is associated with an imaging system, the device can analyze the color of an entire tooth and provide a comprehensive color map of it. The technical specifications include an light output from 410 nm to 680 nm; an image output with calibrated data from 400 nm to 720 nm, and steps of 10 nm; 2 × 45°, polarized, telecentric, monochromatic illumination; 0°, polarized, telecentric measurements; approximately 18 × 14 mm on 640 × 480 points (resolution) of reading area; and CCD Black and White sensor (for spectrum data readings).

## 4.2 Reliability of Dental Color-Measuring Devices

One of the most important issues to consider when using a dental color measuring device is the reliability. The dental clinician (in this case, the operator) has to recognize if the device measures color precisely and according to a reference system (a gold standard) and if it is CIE (International Comission on Illumination) compliant.

In this sense, a study measured the $L^*C^*h°$ color coordinates of ceramic samples matching the shades from VITA Linearguide 3D-Master using four dental color-measuring devices (VITA Easyshade, VITA Easyshade Compact, DeguDent Shadepilot, and X-Rite ShadeVision) and compared to the values obtained by a spectrophotometric reference system [6]. The dental color-measuring devices showed excellent repeatability, although some of them showed important differences in color coordinate values with the spectrophotometric reference system. It is interesting to highlight that the Shadepilot and the ShadeVision showed higher precision than the two VITA Easyshade devices included in the study [6].

In a similar study, the readings from four color-measuring devices (Vita Easyshade Advance; DeguDent Shadepilot; X-Rite ShadeVision; and CrystalEye Olympus) were compared with a CIE-compliant reference system by recording the $L^*C^*h°$ color coordinates of ceramic samples matching the tooth colors of the Vita Linearguide 3D-Master, under standardized test conditions [7]. All devices offered high intraclass correlation coefficients (0.9771–0.9999) for the $L^*C^*h°$ color coordinates. Excluding the $L^*$ and h° coordinate measurements performed with Vita Easyshade Advance, all color-measuring devices exhibited deviations from the reference system that were greater than those expected by chance. Authors concluded that all dental color-measuring devices evaluated offered excellent reproducibility, but showed significant deviations from the CIE-compliant reference system regarding the $L^*C^*h°$ color coordinates [7].

## 4.3 Reproducibility and Inter-Device Agreement for Dental Color Measurement Devices

The ability of a dental color-measuring device to produce constant values is a decisive factor in the reproduction of tooth-colored restorations. From start to end of a laboratory or clinical procedure involving dental color, it is necessary to obtain reliable data about the targeted color values and to ensure that the device can repeat measurements with consistency. Such process, meaning, consistently choosing an accurate shade match, is more difficult than it seems.

The short-term inter-device agreement between eight equivalent dental color-measuring devices (VITA Easyshade Advance) was evaluated [8]. Statistical analysis involved calculating the intraclass correlation coefficients (ICCs) and color differences ($\Delta E^*$) for corresponding measurements taken by the devices. All devices showed high ICCs for all the color coordinates ($L$ = 0.996, $a$ = 0.993, $b$ = 0.999) while the color difference ($\Delta E^*$) between measurements of the same sample performed with different devices ranged from 0.62 to 1.67 units. Such high inter-device

agreement of the VITA Easyshade Advance means that dental professionals can use this device independently and interchangeably, without compromising the consistency and quality of color measurements.

The intra- and inter-device repeatability of three color-measuring devices (VITA Easyshade compact, DeguDent Shadepilot, and X-Rite ShadeVision) in different tooth regions and under clinical conditions was assessed using ICCs [9]. CIELAB total color difference ($\Delta E$) between measurements was used to evaluate the clinical acceptability of repeatability values. The evaluated devices showed high repeatability for color readings and small color differences for all tooth regions. In contrast, inter-device repeatability was low for all tooth regions. Authors concluded that a high intra-device repeatability of color coordinates can be easily achieved for all tooth regions when the same color-measuring device was used. However, because of low inter-device repeatability, results using different color-measuring devices are not comparable.

The accuracy and precision of five commercially available dental color-measuring devices (ShadeScan, Easyshade, Ikam, IdentaColor II, and ShadeEye) in both standardized and clinical environments were evaluated [10]. According to the results of this study, the Easyshade was the most precise and accurate, while ShadeEye was the least precise and the IdentaColor II was the least accurate in vitro. Clinically (in vivo), Easyshade and Ikam systems were the most precise, while the least precise was ShadeScan. For in vivo accuracy, IdentaColor II was considered inaccurate.

An in vivo study [11] on individual repeatability of three color measuring devices (Vita Easyshade, X-Rite ShadeVision, and SpectroShade Micro) recorded three shade measurements (cervical, body, and incisal) for each of the upper maxillary anterior teeth in 20 participants. The SpectroShade Micro showed the most repeatable measurements, exhibiting better repeatability and agreement of Vita shades than the other systems.

## 4.4 Agreement Between Visual and Instrumental Shade Matching

A study [12] comparing visual and instrumental methods for shade matching evaluated the performance of three dental color-measuring devices (Shadepilot, CrystalEye, and ShadeVision). It was shown that the ShadePilot provided an agreement of 56.3% with the visual shade determination, while CrystalEye reached only 49.0% and ShadeVision 51.3%. None of these results can be considered satisfactory under clinical circumstances. The total color difference between the visually and instrumentally selected shade tabs and natural teeth was, in most cases, higher than the acceptability threshold, independently of the color measuring device used.

Another study [13] evaluated the reliability and reproducibility of two digital shade selection devices (ShadePilot and ShadeVision), and correlated the results with visual shade assessment. Instrumental shade determination was done for 40 subjects under clinical conditions using the two devices and compared with visual shade judgements performed by three human examiners. The same shade was

obtained by all three human examiners in 22.5% of the cases, by all colorimetric readings in 35% of the cases, and by all spectrophotometry readings in 55% of the cases. It was suggested that spectrophotometric shade determination is more reproducible than visual shade matching. Similarly, another study [14] compared shade-matching results using the SpectroShade spectrophotometer on three different commercially available shade guides (Vita Lumin Vacuum, Chromascop, and Vita 3D Master) with visual shade matching of two operators with more than 10 years experience. In 47% of the cases, the spectrophotometer provided more accurate results than visual selection. Instrumental shade determination was also better than visual shade assessment for porcelain-fused-to-metal (PFM) restorations [15].

The accuracy and consistency of a dental spectrophotometer (VITA Easyshade) was compared to visual shade matching of three experienced clinicians using Vita 3D Master shade guide system for the maxillary anterior teeth of 16 participants in three separate moments (once a month) [16]. Exact matches were found in 41% of the cases with the spectrophotometer and in 21% of the cases for the visual matching. It was concluded that the instrument performance was at least comparable to, if not better than, the dentists [16]. Similarly, shade-matching quality between a color-measuring device and visual shade assessment of dental students was evaluated [17]. The shade-matching device was significantly better than the conventional visual method (36.3% vs 80.4%). Neither experience nor gender influenced shade-matching quality.

More recently, the repeatability of an intraoral scanner (3Shape TRIOS) was compared to the classical visual shade matching in dental patients [18]. Thirty observers (15 men and 15 women) were asked to select the shade of the middle third portion of right maxillary central incisor (according to VITA Toothguide 3D-MASTER) from ten patients on three different occasions under different ambient lighting conditions (twice under fluorescent lighting and once under natural lighting). For the instrumental method, it was used the same teeth scanned by the 3Shape TRIOS intraoral scanner and same sequence of settings used for the visual method. The intraoral scanner showed a statistically significant higher repeatability (86.66%) compared to the visual method (75.22%) suggesting that the intraoral scanner can serve as a reference for dental health professionals and laboratory technicians. Yet, the instrument accuracy was not investigated, which may lead to systematic errors and shade mismatches [18].

## 4.5 Objective Values and Their Adequate Interpretation

Once the color of a sample is objectively measured, the CIE $L^*a^*b^*$ colorimetric coordinates obtained can be used in many different ways. For instance, one of the most direct applications is the assessment of color similarity (or color compatibility) between different samples (e.g., natural dental tissue and a dental restorative material) through a one-to-one comparison of the colorimetric coordinates. Color compatibility can also include comparisons among different dental materials or

**Table 4.2** Clinical and research interpretation of color differences for dental applications (adapted from [22])

| Threshold-related value | Interpretation | $\Delta E_{00}$ | $\Delta E_{ab}$ |
|---|---|---|---|
| ≤PT | 5—Excellent match | ≤0.8 | ≤1.2 |
| >PT, ≤AT | 4—Acceptable match | >0.8, ≤1.8 | >1.2, ≤2.7 |
| >AT, ≤2 × AT | 3—Moderately unacceptable | >1.8, ≤3.6 | >2.7, ≤5.4 |
| >2 × AT, ≤3 × AT | 2—Clearly unacceptable | >3.6, ≤5.4 | >5.4, ≤8.1 |
| >3 × AT | 1—Extremely unacceptable | >5.4 | >8.1 |

between a target tooth and the corresponding restoration or shade tab. Another interesting topic, where the application of objective color measurements can be very helpful, is the assessment of color stability of different dental materials (composites, ceramics, etc.) during fabrication, controlling color shifts from blending and/or layering of materials, at clinical placement, and in follow-up visits of the patient [19–21]. However, in most cases, a direct comparison of chromatic coordinates is not easy or simple to make and the outcome is not clearly understood. Nevertheless, color differences ($\Delta E$) are important because they reduce the comparison dimensions to a single value, which can be easily analyzed and clinically interpreted, especially through the corresponding threshold values (perceptibility (PT) and acceptability (AT)). There is a large variety of studies in dental research that reported significant differences on CIEL*$a^*b^*$ color coordinate values or even statistical significant $\Delta E$ values, however these values may not be clinical relevant, which is the main reason for using perceptibility and acceptability thresholds (PT and AT), which are thoroughly described in Chap. 3.

Recently, a consistent and systematic model for the clinical and research application and interpretation of color difference findings (when using both CIELAB and CIEDE2000 total color difference formulas) related to visual thresholds was introduced [22]. It consists of a 1–5 grading system derived from research findings on perceptibility and acceptability thresholds (PT and AT) and their values [23]. In the proposed grading system, grades 5 and 4 are evidence based and correspond to excellent match (≤PT) and acceptable match (>PT, ≤AT). Grades 3 to 1 correspond to three mismatch types: grade 3 (>AT, ≤2 × AT)—moderately unacceptable; grade 2 (>2 × AT, ≤3 × AT)—clearly unacceptable; and grade 1 (> 3 × AT)—extremely unacceptable (Table 4.2).

## 4.6 Color Stability of Dental Materials

Relevant studies have investigated the color stability of esthetic restorative materials, mostly resin-based composites. A study [24] evaluated the color stability of four indirect restorative resin-based composites (all A2 shade according to VITA Classical shade guide) after accelerated aging (ISO 7491) in a weathering device. Direct comparisons of the CIEL*$a^*b^*$ coordinates (before and after aging) as well as the CIELAB total color difference ($\Delta E^*_{ab}$) were measured. No significant differences

were found in $\Delta L^*$, $\Delta a^*$, $\Delta b^*$ among materials. The registered color changes after aging were all within clinically acceptable range.

The color stability of CAD/CAM fabricated inlays from three different materials (resin nanoceramic, feldspathic ceramic, and leucite-reinforced ceramic) was evaluated after accelerated artificial aging using individual variations of the CIE$L^*a^*b^*$ color coordinates and the CIELAB total color difference [25]. The resin nanoceramic showed an extremely unacceptable match ($\Delta E$ = 9.3 units; grade 1 from Table 4.2) after aging, and both feldspathic and leucite ceramics showed an acceptable match ($\Delta E$ = 2.1 and 2.5 units, respectively).

Total color differences were used to evaluate the influence of 1-week water storage on color stability of 13 resin-based composites (A2 shade) indicated to restore anterior teeth and to evaluate the interchangeability of different composite brands of equal color shade [26]. Most composites showed significant $L^*a^*b^*$ differences between pre- and post-water storage values. However, in most cases, the color difference values were below PT (grade 5 according to Table 4.2). In few cases, grades 4 and 3 color differences were registered. The data highlight the discrepancy that exists between a clinically oriented result analysis and traditional statistical evaluation, which does not take into consideration visual perception threshold.

Furthermore, considerable color mismatches between various resin-based composite brands (A2 shade) were observed when the color differences were calculated. More than 79% of composite pairs were moderately unacceptable color matches for, otherwise claimed to be, same color (A2) [26]. These considerable color differences would be clinically synonym of highly visible color mismatch and unsatisfactory esthetic result. Furthermore, differences in inherent color among lots of one brand of resin-based composite with same shade designation were found to be above the acceptability threshold [27].

Staining susceptibility correlated to the induced color shift for any esthetic restorative material is of paramount importance. Color changes for direct, indirect, and CAD/CAM resin-based composites after immersion in cola, tea, coffee, red wine, and distilled water (control) at 37°C for 7 days were reported using CIELAB total color difference—$\Delta E^*_{ab}$ [28]. For all materials, exposure to red wine, tea, and coffee generally resulted in grade 3 or lower color mismatches. Conditioning in cola and distilled water generally resulted in minimal color changes. Differences in stain susceptibility were observed between materials. CAD/CAM composites seemed to stain less when exposed to red wine, compared to direct and indirect composites.

Color variations among three brands of *A*2 shade resin-based composites relative to VITA Classical *A*2 shade tab over a period of 21 days in dry storage and immersed in artificial saliva were reported using CIEDE2000 color difference formula [29]. Color of all composites progressively and significantly changed as a function of time up to 14 days of storage, then color stabilized and no significant variations were registered until day 21. Color differences at day 14 were moderately unacceptable.

The CIEDE2000 total color difference formula was also used to quantify the effect of coffee staining on color of a hybrid ceramic, a resin nanoceramic, a lithium disilicate glass-ceramic, and a nanohybrid resin-based composite with different thicknesses [30]. The nanohybrid resin-based composite showed the highest color change ($\Delta E_{00}$ = 4.3 units; clearly unacceptable—grade 2), followed by the resin nanoceramic ($\Delta E_{00}$ = 3.7 units; clearly unacceptable—grade 2). The hybrid ceramic showed an acceptable color difference after staining ($\Delta E_{00}$ = 1.4 units) while thermocycling in coffee caused no perceivable color change for the lithium disilicate glass-ceramic at any thickness ($\Delta E_{00}$ = 0.4 units).

## 4.7 Objective Shade Matching

The ability to reproduce the exact shade of natural teeth using esthetic restorative materials is one of the most challenging tasks in clinical dentistry [19]. Visual shade matching using commercially available shade guides is the most common method to select shade in dentistry. Recent progress on technology and materials offers the potential to improve shade-matching skills of dental practitioners. In this sense, selecting the proper shade of the restorative material using an objective approach based on the minimum color difference between the target tooth and the shade guide elements seems to be a straightforward approach. Unfortunately, this direct application of color difference metrics to clinical dentistry has to be supported by additional scientific evidence before it can be brought to clinical practice. Despite recent developments in industrial color difference evaluation, color matching in dentistry still largely relies on visual perception. Regardless of all possible problems associated with the subjective assignment of shade in dentistry, color matching decisions exclusively based on color differences performed by instrumental devices remain a desideratum far from being met. Even with the improvements of CIEDE2000 color difference formula, the level of agreement between instrumental and visual color matching decisions remains lower than desired. Color research has yet to find an acceptable level of performance of color difference equations by improving existing metrics or suggesting new ones.

The discrepancies among the minimum color difference between the target tooth, the shade guide elements, and the visual judgements have already been highlighted [31]. Visual shade matching using two dental shade guides (VITA Classical and VITA 3D Master) of four extracted teeth performed by 100 dental students was compared to instrumental shade matching based on measurements from a spectroradiometer and a dental spectrophotometer, and three different total color difference metrics (CIELAB, CIEDE2000(1:1:1), and CIEDE2000(2:1:1)). None of the color difference formulas showed 100% efficiency (Fig. 4.3). Yet, the use of CIEDE2000 (2:1:1) jointly with the Vita Classical shade guide mostly resembled the dental students visual perception. It was recommended that instrumental shade determination should be accompanied by experienced human visual determination.

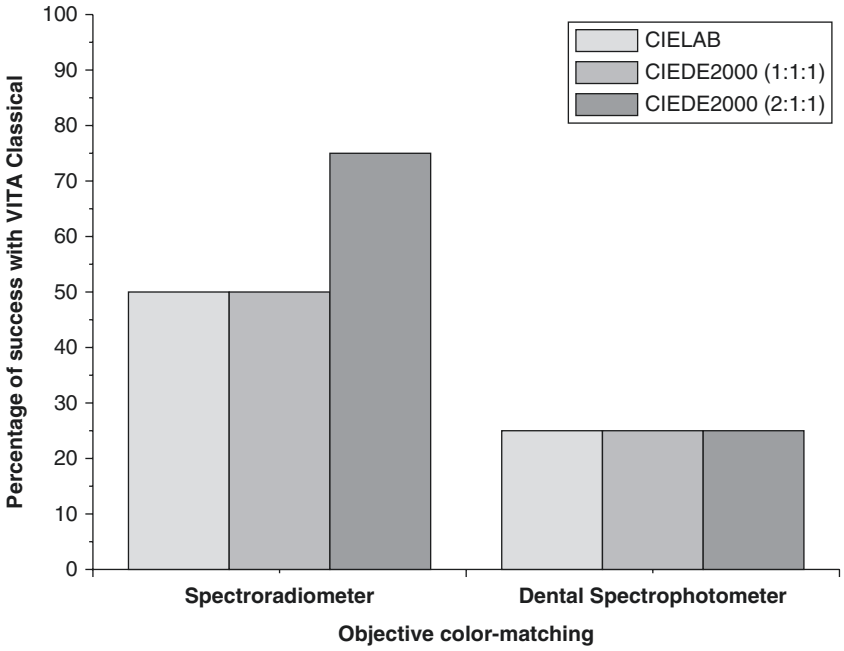


**Fig. 4.3** Level of agreement between instrumental and visual shade matching by dental students using Vita Classical shade guide (adapted from [31])

## 4.8 Clinical Relevance and Application of Whiteness Indices: Monitoring Bleaching Process and Efficiency

Tooth whitening is probably the most popular cosmetic procedure in dentistry. Tooth whitening efficacy can be monitored and documented using visual and/or instrumental method (for further reading, please see *ADA guidelines: Definition of different thresholds for clinical success of tooth whitening products based on the tooth whitening technique*). However, the visual method is still the most popular method in assessing bleaching procedure efficacy due to limited number of dental clinics that have color-measuring devices. The visual method requires usage of dedicated dental shade guides (e.g., VITA Bleachedguide—Fig. 3.11) where the whiteness shift is expressed in shade guide units (SGU). One SGU means the tooth become one shade tab lighter upon bleaching. Consequently, whitening efficacy is calculated as the difference between the shade tab number before whitening and the shade tab number after whitening.

Apart from the measurement of color, measuring whiteness is of key importance to research and manufacture of dental materials as well as to clinical practice. Applications include monitoring of tooth whitening and evaluating the effectiveness of whitening agents. Spectrally, a white material maintains constant and high (tending to unity) reflectance across the whole range of the visible spectrum. In terms of

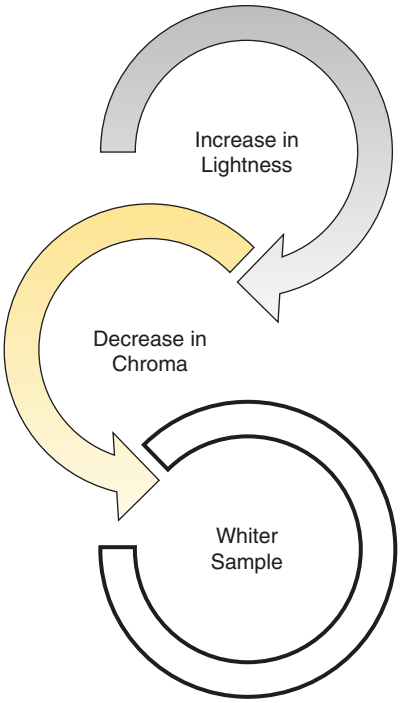


**Fig. 4.4** Description of chromatic changes that usually occur during a whitening process

the CIELAB color space, this type of spectral behavior means a very high lightness and a very low chroma (ideally tends to zero). This implies that when a sample undergoes a whitening process, its chromatic variation is expected to be towards a higher lightness and lower chroma (Fig. 4.4).

As presented in Chap. 1, common measures for visual perception of whiteness/brightness are whiteness indices, e.g., WIO (Whiteness Index Optimized), $WI_D$ (Whiteness Index for Dentistry). In this regard, it seems that $WI_D$ is more consistently distributed for VITA Bleachedguide tabs than for VITA Classical shade tables [32].

Another important consideration involves the overlapping of shades that reduces the quality of color distribution, i.e., color uniformity. It was demonstrated that the shade overlapping for VITA Bleachedguide is 23% while for the VITA Classical the corresponding shade overlap increments up to 71% [32]. This implies that 1 SGU for VITA Bleachedguide would correspond to CIEDE2000 total color difference value of $\Delta E' = 0.7$ units, while a VITA Classical shade change of 1 SGU would correspond to $\Delta E' = 0.88$ [22, 32]. This result provides additional evidence of uniformity for VITA Bleachedguide when compared with the VITA Classical.

A recent study [33] established the thresholds for differences in whiteness in dentistry. It used $WI_D$ index to calculate the visual thresholds (WPT perceptibility threshold and WAT acceptability threshold), which resulted in WPT = 0.72 units and WAT = 2.62 units. Furthermore, another study [22] suggested a classification to

**Table 4.3** Interpretation of differences in tooth whiteness based on whiteness index thresholds (*WPT* whiteness perceptibility threshold; *WAT* whiteness acceptability threshold) (adapted from [22])

| Threshold | Classification and interpretation | $\Delta WI_D$ |
|---|---|---|
| ≤WPT | Not effective | ≤0.7 |
| ≤WAT | Moderately effective | >0.7 ≤2.6 |
| ≤2x WAT | Good effectiveness | >2.6 ≤5.2 |
| ≤3x WAT | Very good effectiveness | >5.2 ≤7.8 |
| >3x WAT | Excellent effectiveness | >7.8 |

assist the interpretation of clinical dental bleaching treatments based on WAT and WPT values (Table 4.3).

Teeth whiteness can be affected by intrinsic and extrinsic factors. Extrinsically, substances such as tobacco, coffee, dark tea, wine, or carbonated drinks can affect teeth whiteness and the bleaching treatment outcome when consuming them during treatment [34–42].

$WI_D$ index has been used to evaluate the whiteness of dental materials, such as dental ceramics and resin-based composite [43, 44]. The color stability and whiteness of two resin-based composites (Z250 and Z350 with A2 and A3 shades) were subjected to two dental bleaching procedures (at-home and in-office bleaching) and to artificial accelerated chromatic aging (450 KJ/m$^2$ and 900 KJ/m$^2$). Aging produced unacceptable color matches, while bleaching treatments produced, in most cases, imperceptible color changes of the composites (Fig. 4.5) [43].

Furthermore, it was shown that the whiteness index $WI_D$ in conjunction with its acceptability and perceptibility thresholds is a suitable tool to monitor teeth whitening treatments [45] (Fig. 4.6).

This means that the Whiteness Index for Dentistry can be directly applied into clinical practice to quantify variations in whiteness that are being produced during teeth bleaching. Implicitly, this also means that the bleaching process can now be easily and, most importantly, objectively monitored and this undoubtedly benefits clinical decision making. In this sense, a bleaching agent is efficient when it produces whiteness variations higher than the whiteness perceptibility threshold (WPT). On the other hand, if the whiteness variation exceeds the acceptability threshold (WAT), the efficiency of the whitening agent is expected to be satisfactory for the patient. In a clinical decision-making tree, the optimal application time of a bleaching agent or the most adequate moment to cease the treatment (bearing in mind other clinical criteria) may be when the whiteness variation (between consecutive measures) is lower than or equal to the whiteness perceptibility threshold (≤WPT).

A simulated example of such a clinical decision-making tree is given in Fig. 4.7: 1 week after at-home bleaching the whiteness variation is higher than three times the WAT (excellent effectiveness according to Table 4.1); during the second week of treatment the whiteness variations are lower than two times the WAT (good

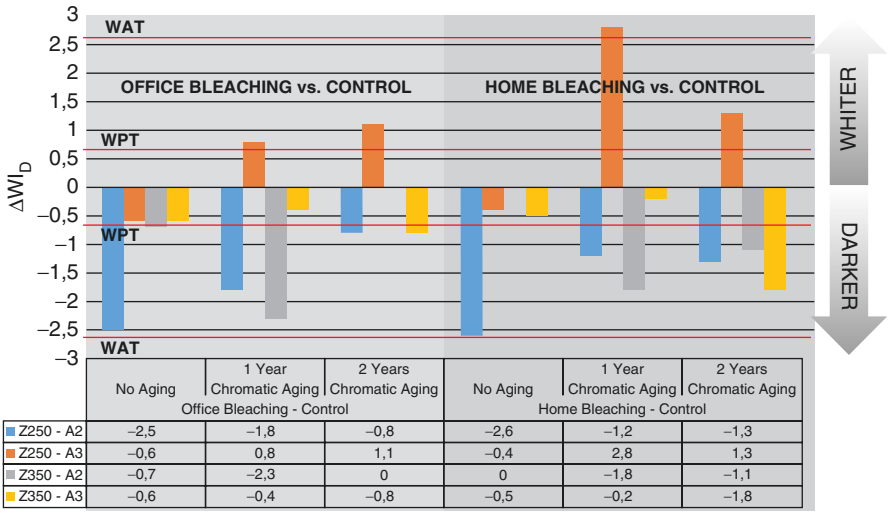


| | Office Bleaching - Control | | | Home Bleaching - Control | | |
|---|---|---|---|---|---|---|
| | No Aging | 1 Year Chromatic Aging | 2 Years Chromatic Aging | No Aging | 1 Year Chromatic Aging | 2 Years Chromatic Aging |
| Z250 - A2 | –2,5 | –1,8 | –0,8 | –2,6 | –1,2 | –1,3 |
| Z250 - A3 | –0,6 | 0,8 | 1,1 | –0,4 | 2,8 | 1,3 |
| Z350 - A2 | –0,7 | –2,3 | 0 | 0 | –1,8 | –1,1 |
| Z350 - A3 | –0,6 | –0,4 | –0,8 | –0,5 | –0,2 | –1,8 |

**Fig. 4.5** Whiteness index ($WI_D$) variations for specific resin-based composites after at-home and in-office bleaching and chromatic artificial aging. Horizontal lines are the whiteness perceptibility threshold (WPT) and the whiteness acceptability threshold (WAT) (adapted from [43])

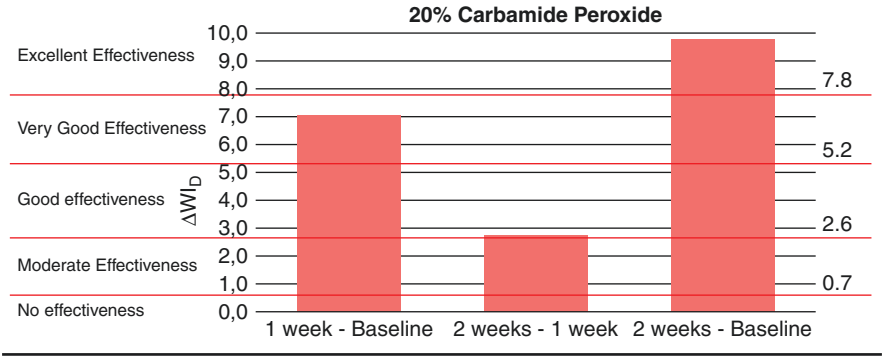


**Fig. 4.6** Variations of the whiteness index ($WI_D$) among 2 weeks of bleaching treatment with 20% carbamide peroxide (adapted from [45])

effectiveness), and in the third week of treatment the whiteness variations are lower than the WPT, which translates into a lack of effectiveness and, therefore, it would be prudent to discontinue the bleaching treatment. The amount of sessions and extent of the bleaching treatment can be, therefore, related to the thresholds values. Yet, there are other factors to consider, such as the perception and desire of the patients according to their esthetic standards.


**Fig. 4.7** Simulated example of bleaching treatment monitoring and clinical decision-making tree based on whiteness index ($WI_D$) variations. *WPT* whiteness perceptibility threshold, *WAT* whiteness acceptability threshold

## Further Readings


1. Chu SJ, Trushkowsky RD, Paravina RD. Dental color matching instruments and systems. Review of clinical and research aspects. J Dent. 2010;38(S2):e2–e16.
2. Ghinea R, Pérez MM, Herrera LJ, Rivas MJ, Yebra A, Paravina RD. Color difference thresholds in dental ceramics. J Dent. 2010;38(Suppl 2):e57–64.
3. Fairchild MD. Color Appearance Models - Second Edition. England, John Wiley & Sons Ltd. 2005. ISBN 0-470-01216-1.
4. Pérez MM, Saleh A, Pulgar R, Paravina RD. Light polymerization-dependent changes in color and translucency of resin composites. Am J Dent. 2009;22(2):97–101.
5. Ghinea R. Evaluation of the CIEDE2000 (KL:KC:KH) color difference metrics and development of color prediction algorithms: Application to dental materials. PhD Thesis, 2013 Editorial de la Universidad de Granada; ISBN: 978-84-9028-762-0.
6. Lehmann KM, Igiel C, Schmidtmann I, Scheller H. Four color-measuring devices compared with a spectrophotometric reference system. J Dent. 2010;38(Suppl. 2):e65–70.
7. Lehmann KM, Devigus A, Igiel C, Weyhrauch M, Schmidtmann I, Wentaschek S, Scheller H. Are dental color measuring devices CIE compliant? Eur J Esthet Dent. 2012;7(3):324–33.
8. Weyhrauch M, Igiel C, Pabst AM, Wentaschek S, Scheller H, Lehmann KM. Interdevice agreement of eight equivalent dental color measurement devices. Clin Oral Investig. 2015;19(9):2309–18.
9. Lehmann KM, Devigus A, Igiel C, Wentaschek S, Azar MS, Scheller H. Repeatability of color-measuring devices. Eur J Esthet Dent. 2011;6(4):428–35.
10. Dozic A, Kleverlaan CJ, El-Zohairy A, Feilzer AJ, Khashayar G. Performance of five commercially available tooth color-measuring devices. J Prosthodont. 2007;16(2):93–100.
11. Khurana R, Tredwin CJ, Weisbloom M, Moles DR. A clinical evaluation of the individual repeatability of three commercially available colour measuring devices. Br Dent J. 2007;203(12):675–80.
12. Igiel C, Weyhrauch M, Wentaschek S, Scheller H, Lehmann KM. Dental color matching: a comparison between visual and instrumental methods. Dent Mater J. 2016;35(1):63–9.
13. Gehrkea P, Riekebergbr U, Facklei O, Dhomd G. Comparison of in vivo visual, spectrophotometric and colorimetric shade determination of teeth and implant-supported crowns. Int J Comput Dent. 2009;12(3):247–63.

14. Fani G, Vichi A, Davidson CL. Spectrophotometric and visual shade measurements of human teeth using three shade guides. Am J Dent. 2007;20(3):142–6.
15. Paul SJ, Peter A, Rodoni L, Pietrobon N. Conventional visual vs spectrophotometric shade taking for porcelain-fused-to-metal crowns: a clinical comparison. Int J Period Rest Dent. 2004;24(3):222–31.
16. Browning WD, Chan DC, Blalock JS, Brackett MG. A comparison of human raters and an intra-oral spectrophotometer. Oper Dent. 2009;34(3):337–43.
17. Bahannan SA. Shade matching quality among dental students using visual and instrumental methods. J Dent. 2014;42(1):48–52.
18. Reyes J, Acosta P, Ventura D. Repeatability of the human eye compared to an intraoral scanner in dental shade matching. Heliyon. 2019;5(7):e02100. Published 2019 July 23. https://doi.org/10.1016/j.heliyon.2019.e02100.
19. Della Bona A. Bonding to ceramics: scientific evidences for clinical dentistry. São Paulo: Artes Médicas; 2009. 310p.
20. Paravina RD, Kimura M, Powers JM. Evaluation of polymerization-dependent changes in color and translucency of resin composites using two formulae. Odontology. 2007;93:46–51.
21. Paravina RD, Westland S, Johnston WM, Powers JM. Color adjustment potential of resin composites. J Dent Res. 2008;87(5):499–503.
22. Paravina RD, Pérez MM, Ghinea R. Acceptability and perceptibility thresholds in dentistry: a comprehensive review of clinical and research applications. J Esthet Restor Dent. 2019;31(2):103–12.
23. Paravina RD, Ghinea R, Herrera LJ, Della Bona A, Igiel C, Linninger M, Sakai M, Takahashi H, Tashkandi E, Perez MM. Color difference thresholds in dentistry. J Esthet Restor Dent. 2015;27(Suppl 1):S1–9.
24. Papadopoulos T, Sarafianou A, Hatzikyriakos A. Colour stability of veneering composites after accelerated aging. Eur J Dent. 2010;4(2):137–42.
25. Karaokutan I, Yilmaz Savas T, Aykent F, Ozdere E. Color stability of CAD/CAM fabricated inlays after accelerated artificial aging. J Prosthodont. 2016;25(6):472–7.
26. Ardu S, Gutemberg D, Krejci I, Feilzer AJ, Di Bella E, Dietschi D. Influence of water sorption on resin composite color and color variation amongst various composite brands with identical shade code: an in vitro evaluation. J Dent. 2011;39(Suppl 1):e37–44.
27. Carney MN, Johnston WM. Appearance differences between lots and brands of similar shade designations of dental composite resins. J Esthet Restor Dent. 2017;29(2):e6–e14.
28. Quek SHQ, Yap AUJ, Rosa V, Tan KBC, Teoh KH. Effect of staining beverages on color and translucency of CAD/CAM composites. J Esthet Restor Dent. 2018;30:E9–E17.
29. Uchimura JY, Sato F, Bianchi G, Baesso ML, Santana RG, Pascotto RC. Color stability over time of three resin-based restorative materials stored dry and in artificial saliva. J Esthet Restor Dent. 2014;26(4):279–87.
30. Acar O, Yilmaz B, Altintas SH, Chandrasekaran I, Johnston WM. Color stainability of CAD/CAM and nanocomposite resin materials. J Prosthet Dent. 2016;115(1):71–5.
31. Pecho OE, Ghinea R, Alessandretti R, Pérez MM, Della Bona A. Visual and instrumental shade matching using CIELAB and CIEDE2000 color difference formulas. Dent Mater. 2016;32(1):82–92.
32. Paravina RD, Sanchez NAP, Ghinea R, Powers JM. Colorimetric (CIEDE2000) comparison between two shade guides used for visual evaluation of tooth whitening efficacy. Srp Arh Celok Lek. 2019;147(3–4):142–7.
33. Pérez MM, Herrera LJ, Carrillo F, Pecho OE, Dudea D, Gasparik C, Ghinea R, Della Bona A. Whiteness difference thresholds in dentistry. Dent Mater. 2019;35(2):292–7.
34. Farawati FAL, Hsu SM, O'Neill E, Neal D, Clark A, Esquivel-Upshaw J. Effect of carbamide peroxide bleaching on enamel characteristics and susceptibility to further discoloration. J Prosthet Dent. 2019;121(2):340–6.
35. Geus JL, Rezende M, Margraf LS, Bortoluzzi MC, Fernández E, Loguercio AD, Reis A, Kossatz S. Evaluation of genotoxicity and efficacy of at-home bleaching in smokers: a single-blind controlled clinical trial. Oper Dent. 2015;40(2):e47–55.

36. Karadas M, Seven N. The effect of different drinks on tooth color after home bleaching. Eur J Dent. 2014;8(2):249–53.
37. Meireles SS, Heckmann SS, Leida FL, dos Santos IS, Della Bona A, Demarco FF. Efficacy and safety of 10% and 16% carbamide peroxide tooth-whitening gels: a randomized clinical trial. Oper Dent. 2008;33(6):606–12.
38. Meireles SS, Demarco FF, dos Santos IS, Dumith Sde C, Della Bona A. Validation and reliability of visual assessment with a shade guide for tooth-color classification. Oper Dent. 2008;33(2):121–6.
39. Meireles SS, Heckmann SS, Santos IS, Della Bona A, Demarco FF. A double blind randomized clinical trial of at-home tooth bleaching using two carbamide peroxide concentrations: 6-month follow-up. J Dent. 2008;36(11):878–84.
40. Meireles SS, dos Santos IS, Della Bona A, Demarco FF. A double-blind randomized controlled clinical trial of 10 percent versus 16 percent carbamide peroxide tooth-bleaching agents: one-year follow-up. J Am Dent Assoc. 2009;140(9):1109–17.
41. Meireles SS, Fontes ST, Coimbra LA, Della Bona A, Demarco FF. Effectiveness of different carbamide peroxide concentrations used for tooth bleaching: an in vitro study. J Appl Oral Sci. 2012;20(2):186–91.
42. Meireles SS, Goettems ML, Dantas RV, Della Bona A, Santos IS, Demarco FF. Changes in oral health related quality of life after dental bleaching in a double-blind randomized clinical trial. J Dent. 2014;42(2):114–21.
43. Della Bona A, Pecho OE, Ghinea R, Cardona JC, Paravina RD, Perez MM. Influence of bleaching and aging procedures on color and whiteness of dental composites. Oper Dent. 2019;44(6):648–58.
44. Mada et al. Evaluation of chromatic changes of a nanocomposite resin using the new whitness index. Clujul Med. 2018;91(2):222–28.
45. Megias S, Ghinea R, Perez MM. $WI_D$ Index: A new tool for evaluation of dental bleaching process. Master Thesis - MOCOA, University of Granada; 2019.

# Color Management and Communication in Dentistry

5

Oscar Emilio Pecho Yataco, Razvan Ionut Ghinea, and Alvaro Della Bona

## Contents



## 5.1 Digital Photography and Ambient Setup for Dental Photography

There are two essential features for a useful dental picture. The correct color rendition, which includes correct exposure, and sufficient resolution to record hard and soft tissue features.

Color rendition is crucial to obtain a precise dental color image that is perceived by the human eye. Thus, color rendition should be as close as possible to what is observed during the shade matching performance. If different light sources or illuminants are eliminating, the image should faithfully reproduce the color of hard and soft tissues. A correct color rendition of teeth can reveal numerous aspects and

O. E. Pecho Yataco · A. Della Bona (✉)
Dental School, Postgraduate Program in Dentistry, University of Passo Fundo, Passo Fundo, RS, Brazil
e-mail: dbona@upf.br

R. I. Ghinea
Optics Department, Faculty of Science, University of Granada, Granada, Spain
e-mail: rghinea@ugr.es



A. Della Bona (ed.), *Color and Appearance in Dentistry*,
https://doi.org/10.1007/978-3-030-42626-2_5

features such as erosion and abrasion, enamel translucency, decay, cervical dentine exposure, and sclerosis. Correct color reproduction is an essential communication tool for shade matching [1].

Images with sufficient resolution are very important for examination, diagnosis, treatment planning, and assessing treatment outcomes. A good and accurate dental picture should record the following features, whenever they are present [1]:

- Tooth shade transition from cervical to incisal edge.
- Enamel surface texture and particular features, such as stains, chips, hypoplasia, cracks, fractures, and perikymata, in addition to incisal and interproximal translucency.
- Non-carious lesions (abrasion, erosion, abfraction, and attrition).
- Cervical dentine exposure.
- Secondary caries.
- Restorative material wear.

It could be necessary to take several pictures and probably use different camera settings, diverse light and exposure directions, and even different light sources to be able to capture and show the abovementioned features.

### 5.1.1 Visual Shade Matching Environment

The quality and intensity of the light reaching the dental structure to be matched is a critical factor to obtain adequate pictures for shade matching, and consequently successful restorations. Lighting in dental environments (dental clinic and laboratory) should be spectrally balanced in the visible range (380–780 nm) and should have a color temperature of approximately 6500 K (natural day light) and a color rendering index of >90 [2].

### 5.1.2 Electronic Flash

There are, basically, two types of electronic flash: compact flash (mounted onto the camera) and studio flash (Fig. 5.1). Both flashes are used as illuminants for dental photography. The light output of electronic flashes is corrected to "photographic daylight" with a color temperature of 5500 K [3]. The advantage of electronic flash is that the light output is predictable, instantaneous, and universally attachable to any type of camera.

Ring flashes create a uniform burst of light, useful for posterior teeth or areas of difficult access. The major disadvantage of ring flashes is the uniform light output that creates shadow-less, flat, soft, and less expressive images. Thus, the use of ring flashes is not recommended for anterior teeth, since the uniform burst of light obliterates fine detail, translucency, and subtle color transitions within individual teeth [3] (Figs. 5.2 and 5.4).

**Fig. 5.1** Professional setup in a dental office: digital camera (Canon EOS 6D Mark II), studio flashes, and GODOX S-type soft boxes

**Fig. 5.2** Schematic image of a ring flash with light reflections generated from curved surfaces such as the buccal surface of upper anterior teeth

Uni-directional flashes create shadows and highlights, increasing contrast and detail, giving a kind of 3D appearance to a 2D image of teeth. The usual directional lighting used in dental photography is two bi-lateral flashes mounted on a bracket arm (twin flash setup). The bracket allows positioning the flashes as desired, depending on the shape of the arch form and tooth alignment of the patient [3]. This setup is an ideal choice for photographing anterior teeth, capturing nuances of characterization and color, texture, and translucency, which are critical for esthetic anterior restorations [3] (Figs. 5.3, 5.5, 5.6, and 5.7).

### 5.1.3 Photographic Tools Used in Dental Shade Matching

The use of photography is a popular way to assist and record dental shade matching. This procedure will need adequate illumination often reached by electronic flashes, such as a ring flash setup (Fig. 5.4), a bi-lateral flash, or a twin flash setup (Figs. 5.5, 5.6, and 5.7). Image quality can be maximized by using professional flash pocket bouncers (Fig. 5.6). A gray background may be useful to keep the focus on the shade matching procedure (Fig. 5.7). The use of external flashes and soft boxes

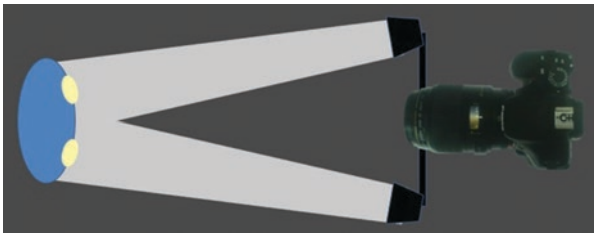

**Fig. 5.3** Schematic image of a twin flash on a bracket arm with light reflections generated from curved surfaces such as the buccal surface of upper anterior teeth

**Fig. 5.4** Shade matching procedure using a B1 shade tab (VITA Classical shade guide). Picture was taken using a Canon EOS 7D Mark II camera with a Canon EF 100 mm f/2.8 macro USM lens and a ring flash setup (picture taken by Matheus Basegio)

**Fig. 5.5** Shade matching procedure using a B1 shade tab (VITA Classical shade guide). Picture was taken using a Canon EOS 7D Mark II camera with a Canon EF 100 mm f/2.8 macro USM lens and a twin flash bracket setup (picture taken by Matheus Basegio)

**Fig. 5.6** Shade matching procedure using a B1 shade tab (VITA Classical shade guide). Picture was taken using a Canon EOS 7D Mark II camera with a Canon EF 100 mm f/2.8 macro USM lens, a twin flash bracket setup, and two professional flash pocket bouncers (picture taken by Matheus Basegio)


**Fig. 5.7** Shade matching procedure using a B1 shade tab (VITA Classical shade guide) on a gray background. Picture was taken using a Canon EOS 7D Mark II camera with a Canon EF 100 mm f/2.8 macro USM lens, a twin flash bracket setup, and two professional flash pocket bouncers (picture taken by Matheus Basegio)


**Fig. 5.8** Shade matching procedure using a B1 shade tab (VITA Classical shade guide). Picture was taken using a Canon EOS 7D Mark II camera with a Canon EF 100 mm f/2.8 macro USM lens, two external flash setup, and two soft boxes (picture taken by Matheus Basegio)

allows for a 3D-like picture (Figs. 5.1, 5.8, 5.9, 5.10, and 5.11), improving deepness and giving some perspective to the image, but increasing the challenge to obtain a perfect shade from the middle third of teeth. This type of image is useful for surface texture. In challenging shade matching cases, it may be useful take pictures with more than one shade tab near the target dental structure or tooth (Fig. 5.9) and using a black background (Fig. 5.10).

The influence of background (white, gray, and black) on color difference perception in dentistry was evaluated using 100 observers from five types of population (DS—dental students; D—dentists; A—auxiliaries; T—technicians; and L—laypersons), balanced by gender. The perceptibility and acceptability thresholds (PT and AT; Chap. 3) for each type of population and background were calculated using CIELAB and CIEDE2000 color difference formulas (Chap. 1). Regardless of the metric used, PT values showed no differences among the different backgrounds for all groups. Dental lab technicians (T), who constantly deal with color perception, presented the lowest AT values, which were similar for the three background colors, regardless of the color difference metric used. This finding suggests that experience plays an important role on color perception. When data from all observers (total data) were considered, the lowest and the highest

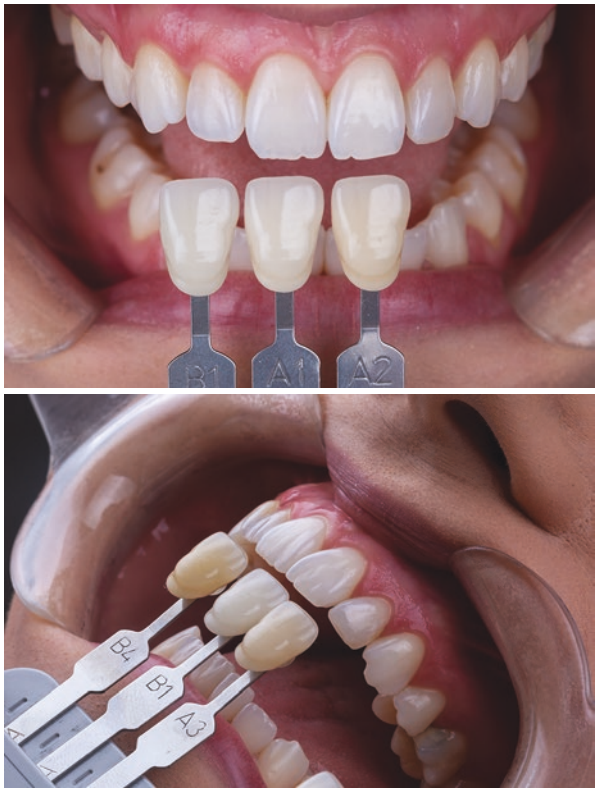


**Fig. 5.9** Shade matching procedure. Top image—Traditional front view using B1, A1, and A2 shade tabs (VITA Classical shade guide). Bottom image—45° lateral-backwards inclination using B4, B1, and A3 shade tabs (VITA Classical shade guide); this patient position may offer a better view of teeth volume and surface features. Pictures were taken using a Canon EOS 7D Mark II camera with a Canon EF 100 mm f/2.8 macro USM lens, two external flash setup, and two soft boxes (pictures taken by Matheus Basegio)

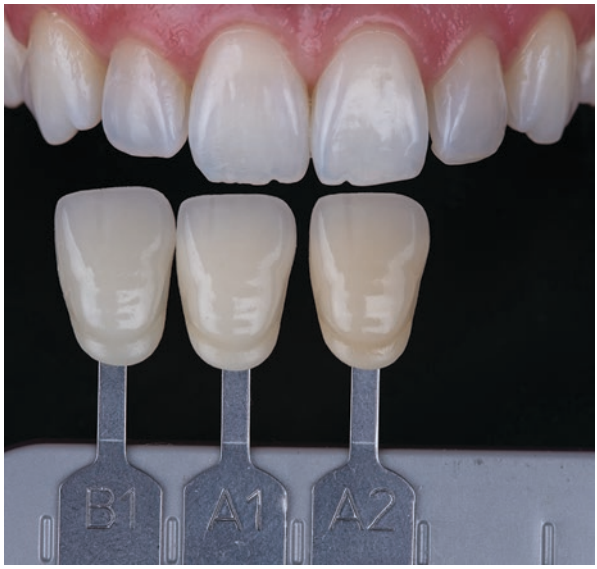


**Fig. 5.10** Same shade matching procedure as in Fig. 5.9 (top image), here using a black background, which is suggested to improve color perception on challenging matching procedures. Picture was taken using a Canon EOS 7D Mark II camera with a Canon EF 100 mm f/2.8 macro USM lens, two external flash setup, and two soft boxes (picture taken by Matheus Basegio)

**Fig. 5.11** The incisal edges of target tooth and shade tab should be as close as possible, aligned, and at the same plane. Picture was taken using a Canon EOS 7D Mark II camera with a Canon EF 100 mm f/2.8 macro USM lens, two external flash setup, and two soft boxes (picture taken by Matheus Basegio)

values of AT were found for black and white backgrounds, respectively, which means that the color background influenced on the color perception and suggesting that a black background can be used for challenging color differences. Figures 5.9 and 5.10 illustrate this issue.

It is important that tooth surface and shade tab surface are at same plane (depth of field) when the picture is taken. As a result, similar amount of flashlight reaches both structures and color matching is not influenced by different light incidence. Thus, on shade matching exercises, it is recommended to place the incisal edge of the shade tab as close as possible to and aligned to the incisal edge of the target tooth (Fig. 5.11). Additional information on step-by-step visual shade matching is presented in Chap. 6.

## 5.2 Imaging Assisting Shade Determination

You have learnt throughout this book that visual shade matching is the most popular method for color selection in dentistry. This subjective procedure is considered complex and dependent on several factors related to the observer, such as gender [4–6], experience [7, 8], and the presence of visual color alterations [9]. The type and quality of lighting in the dental environment is the most important factor related to illumination that can influence on visual shade matching. Dental offices could present different lighting conditions, which can significantly change according to

different variables such as type of light sources, day time, year season, and even the hemisphere where the dental office is located [10].

Nevertheless, visual shade matching can be improved using some strategies and auxiliary devices. Light-correcting devices, with and without polarization filters, can minimize the negative effect of deficient environmental lighting [11, 12]. The purpose of using polarization filters is to reduce reflected light from the light-correcting device [4]. An example of light-correcting device that uses a polarizing light is the Smile Lite MDP (Smile Line Europe GmbH, Goethestraße, Germany) (Figs. 5.12 and 5.13). Similar type of image may also be obtained using polarizing filters onto lens and flash of cellular phones (Figs. 5.14 and 5.15).

The influence of such light-correcting device with a polarization filter [4] was evaluated by 21 observers (dental students) that performed visual shade matching of the upper anterior teeth of a patient using two shade guides (VITA Classical

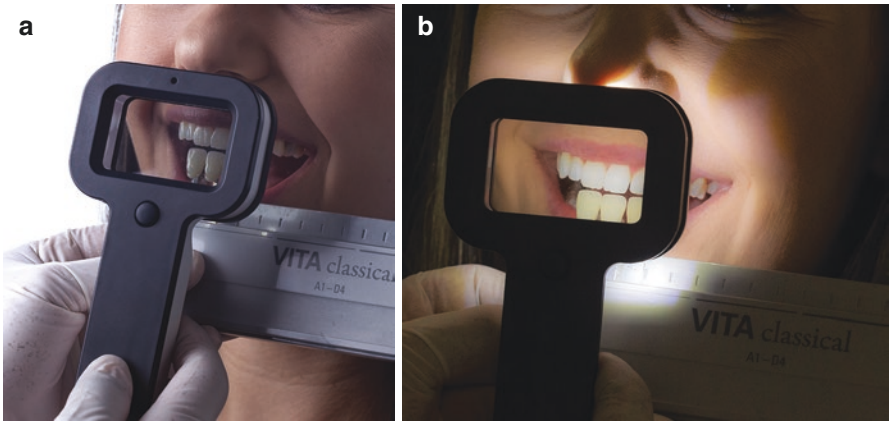


**Fig. 5.12** Shade matching procedure using Smile Lite MDP (Smile Line Europe GmbH, Goethestraße, Germany): device light turned off (**a**) and on (**b**) (pictures taken by Matheus Basegio)

**Fig. 5.13** Shade matching procedure using a B1 shade tab (VITA Classical shade guide) under polarized light of the Smile Lite MDP (Smile Line Europe GmbH, Goethestraße, Germany). Picture was taken with a Canon EOS 7D Mark II camera with a Canon EF 100 mm f/2.8 macro USM lens (Picture taken by Matheus Basegio)

**Fig. 5.14** Shade matching procedure using a B1 shade tab (VITA Classical shade guide). Picture was taken with the camera from a cellular phone (Galaxy S6 Samsung) using polarizing filters

**Fig. 5.15** Shade matching procedure using a B1, A1, and A2 shade tabs (VITA Classical shade guide) with a black background. Picture was taken with the camera from a cellular phone (Galaxy S6 Samsung) using polarizing filters

and 3D-Master). The visual shade matching was performed under three lighting conditions: daylight, daylight associated with a light-correcting device (Smile Lite, Switzerland), and daylight associated with the light-correcting device with a polarization filter attached. The light-correcting device improved the shade matching performance. However, the attached polarization filter did not improve the shade matching performance. Yet, further studies should confirm these findings.

New devices such as intraoral scanners have been developed for shade selection. A study compared visual shade matching performed by three experienced clinicians using two shade guides (VITA Classical and VITAPAN 3D-Master) with and

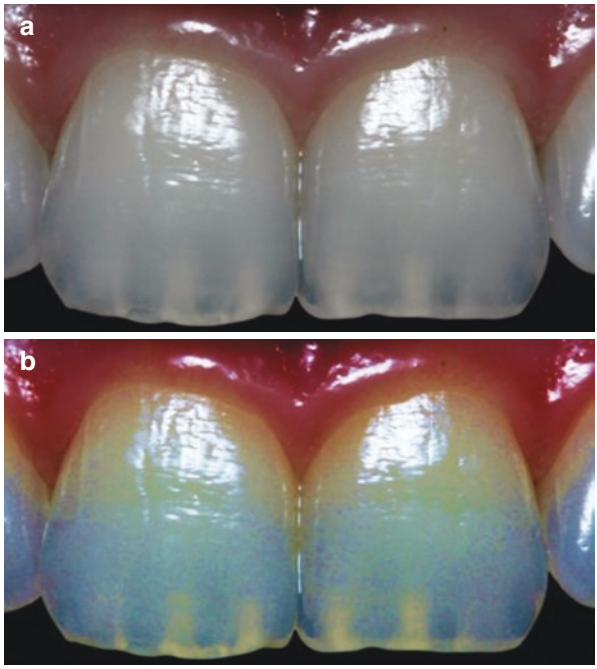


**Fig. 5.16** (**a**) Original image (100% saturation). (**b**) Edited image to 200% saturation. Original picture was taken using a Canon EOS 600D camera with a Canon EF 100 mm f/2.8 macro USM lens

without the use of a polarized light (Smile Lite MDP, Smile Line Europe GmbH, Goethestraße, Germany), an intraoral scanner (TRIOS, 3Shape A/S), and a spectrophotometer (VITA Easyshade® Advance 4.0, VITA Zahnfabrik). The intraoral scanner configured for the VITAPAN 3D-Master shade guide showed the best performance (Fleiss' kappa value of 0.87), followed by the spectrophotometer configured for the VITA Classical shade guide (Fleiss' kappa value of 0.81). The best visual shade matching method was performed using the VITA Classical shade guide associated with the light-correcting device (Fleiss' kappa value of 0.32) [13].

Computer assisted learning using precise color charts for color matching exercises should also improve visual shade matching. In addition, any color editing software is able to change the contrast and brightness of an image, which often reveal important intrinsic features of the tooth structure [14] (Fig. 5.16).

Digital dentistry associated with artificial intelligence and computer learning techniques (Chap. 7) have been introduced to assist dental professionals on shade determination, digital mock-ups for oral rehabilitation, and facial harmonization procedures, making for a great substitution of dull wax-ups demonstrations.

## 5.3 Dentist–Patient Communication

Satisfaction with esthetic dental treatments is often a challenge. As the visual perception about color and whiteness improves with experience, dental lab technicians and dentists have a greater ability to perceive minor color and whiteness differences

than laypersons [7, 8, 15, 16]. Thus, perceptibility and acceptability thresholds were developed and are very useful to assist on understanding differences on color (shade) and whiteness perception. Yet, patient expectations can vary and the dental professional should be careful on explaining color changes to patients. Any dentist–patient communication should focus on evidence-based dentistry associated with illustrative clinical examples.

Considering color differences, perceptibility (PT) and acceptability (AT) thresholds are lower for dentists (PT = 1.02 $\Delta E^*_{ab}$ units and 0.62 $\Delta E_{00}$ units, and AT = 2.57 $\Delta E^*_{ab}$ units and 1.79 $\Delta E_{00}$ units) than for laypersons (PT = 1.49 $\Delta E^*_{ab}$ units and 1.00 $\Delta E_{00}$ units, and AT = 2.89 $\Delta E^*_{ab}$ units and 2.04 $\Delta E_{00}$ units) [15, 16]. These thresholds are useful for evaluating shade matching between two restorations or between a tooth and a restoration. Such rationale was confirmed by the latest Guidance on Color Measurements published by the International Organization for Standardization (ISO/TR 28642:2016), which states that color variation should be assessed based on comparisons with 50:50% thresholds. Nevertheless, PT and AT are very useful and clinical relevant on dentist–patient communication.

Considering whiteness differences, the whiteness perceptibility (WPT) and whiteness acceptability (WAT) thresholds are also lower for dentists (WPT = 0.46 $\Delta WI_D$ units, and WAT = 2.20 $\Delta WI_D$ units) than for laypersons (WPT = 0.94 $\Delta WI_D$ units, and WAT = 2.95 $\Delta WI_D$ units) [15, 16]. These whiteness thresholds can be used to assess the effectiveness of bleaching treatments (Chap. 4). Yet, any esthetic outcome should take into account the patient perception and desire (WPT and WAT for laypersons), which depend much on patient esthetic standards.

The fact that the visual thresholds for color (PT and AT) and whiteness (WPT and WAT) differences were lower for dentists than laypersons mean that dental professionals have a more acute visual judgment, which is associated with experience, than laypersons.

Different tools can be used to evaluate the efficacy of bleaching treatments. The following clinical case (Figs. 5.17, 5.18, 5.19, 5.20, 5.21, 5.22, 5.23, 5.24, and 5.25) used two shade guides (VITA Classical® and VITA Bleachedguide 3D-Master®) and a polarized light (Smile Lite MDP) for visual shade matching, and a dental spectrophotometer (VITA Easyshade® Advance 4.0) and whiteness difference thresholds

**Fig. 5.17** Initial image of a tooth bleaching treatment (54-year-old man). Picture was taken using a Canon EOS 600D camera with a Canon EF 100 mm f/2.8 macro USM lens, two Canon speedlite 270EX II flashes attached to NOVOFLEX flash holding system, and two professional flash pocket bouncers

**Fig. 5.18** Visual shade matching (2M2 shade tab) using VITA Bleachedguide 3D-Master® shade guide (VITA Zahnfabrik) before tooth bleaching treatment. Picture was taken under polarized light (Smile Lite MDP, Smile Line Europe GmbH) using a Canon EOS 600D camera with a Canon EF 100 mm f/2.8 macro USM lens

**Fig. 5.19** Visual shade matching (A2 shade tab) using VITA Classical® shade guide (VITA Zahnfabrik) before tooth bleaching treatment. Picture was taken under polarized light (Smile Lite MDP) using a Canon EOS 600D camera with a Canon EF 100 mm f/2.8 macro USM lens

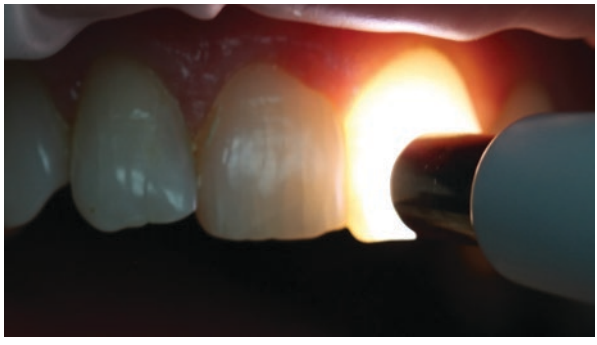

**Fig. 5.20** Objective shade matching before tooth bleaching treatment using VITA Easyshade® Advance 4.0 (VITA Zahnfabrik). Picture was taken using a Canon EOS 600D camera with a Canon EF 100 mm f/2.8 macro USM lens

for objective shade determination. Initial CIELAB coordinates for the upper right central incisor (#11) were $L^* = 86.43 \pm 0.57$; $a^* = -1.80 \pm 0.00$; $b^* = 17.50 \pm 0.52$, and its final coordinates were $L^* = 87.10 \pm 0.00$; $a^* = -2.00 \pm 0.00$; $b^* = 15.80 \pm 0.00$. Initial CIELAB coordinates for the upper left central incisor (#21) were $L^* = 86.27 \pm 0.40$; $a^* = -1.73 \pm 0.00$; $b^* = 17.27 \pm 0.35$, and its final coordinates

**Fig. 5.21** In-office bleaching using 35% hydrogen peroxide whitening gel (Whiteness HP AutoMixx, FGM Dental Products) for 15 min. Picture was taken using a Canon EOS 600D camera with a Canon EF 100 mm f/2.8 macro USM lens, two Canon speedlite 270EX II flashes attached to NOVOFLEX flash holding system, and two professional flash pocket bouncers

**Fig. 5.22** Images recorded right after removing bleaching gel from teeth. Top image—Visual shade checking using the shade tab (2M2) previously selected from VITA Bleachedguide 3D-Master® shade guide. Bottom image—Visual shade matching (shade tab 1M2) using VITA Bleachedguide 3D-Master®. According to this shade guide (Fig. 3.11), the treatment whitened the teeth in two shade guide steps or tabs (1.5M2 and 1M2). Pictures were taken under polarized light (Smile Lite MDP) using a Canon EOS 600D camera with a Canon EF 100 mm f/2.8 macro USM lens


**Fig. 5.23** Images recorded right after removing bleaching gel from teeth. Top image—Visual shade checking using the shade tab (A2) previously selected from VITA Classical® shade guide. Bottom image—Visual shade matching (shade tab A1) using VITA Classical® shade guide (Fig. 3.6). Pictures were taken under polarized light (Smile Lite MDP) using a Canon EOS 600D camera with a Canon EF 100 mm f/2.8 macro USM lens

**Fig. 5.24** Final image right after removing the bleaching isolation barrier. In this clinical case, deficient gum isolation resulted in mild burned gum (white spots on gum) by the bleaching gel, which was readily and thoroughly washed out and treated immediately with a peroxide neutralizing solution (Neutralize, FGM Dental Products). White spots disappeared in, approximately, 15 min. Picture was taken using a Canon EOS 600D camera with a Canon EF 100 mm f/2.8 macro USM lens, two Canon speedlite 270EX II flashes attached to NOVOFLEX flash holding system, and two professional flash pocket bouncers

**Fig. 5.25** Same as for previous image, however picture was taken under polarized light (Smile Lite MDP) using a Canon EOS 600D camera with a Canon EF 100 mm f/2.8 macro USM lens

were $L^* = 87.10 \pm 0.00$; $a^* = -2.00 \pm 0.00$; $b^* = 15.80 \pm 0.00$ (final values). Therefore, both teeth showed initial $WI_D$ values of $29.10 \pm 0.80$ for tooth #11 and $29.12 \pm 0.64$ for tooth #21, and the final $WI_D$ values were $31.78 \pm 0.00$ for tooth #11 and $31.78 \pm 0.00$ for tooth #21. Both teeth showed $\Delta WI_D$ values above whiteness acceptability threshold ($2.68 \pm 0.80$ for #11 and $2.66 \pm 0.64$ for #21), which means that the patient should detect the whiteness variation of the teeth [15, 16].

## 5.4 Dentist–Lab Technician Communication

Tooth color and appearance information beyond an indication of a basic single-shade designation is required when the esthetic is predominant. Visual and instrumental shade matching should be accompanied with images of the selected shade tab(s) from a commercial shade guide near the tooth to be restored or matched (Chap. 6). Shade communication and color mapping can be done by drawing, editing images (e.g., increasing contrast and decreasing brightness), and using professional software for digital dentistry. Often, the color of a single image is not enough to make an accurate judgment on shade matching. However, any image would be helpful and much better than drawing to communicate the visual appearance of translucency, specific characterizations, and color blending. Thus, digital images can be electronically sent to the laboratory technician and fluent communication between dentist and technician tend to enhance the success rate of esthetic indirect restorative dentistry [2].

## Further Readings

1. Ahmad I. Digital dental photography. Part 1: an overview. Br Dent J. 2009;206:403–7.
2. Brewer JD, Wee A, Seghi R. Advances in color matching. Dent Clin N Am. 2004;48:341–58.
3. Ahmad I. Digital dental photography. Part 5: lighting. Br Dent J. 2009;207:13–8.
4. Gasparik C, Grecu AG, Culic B, Badea ME, Dudea D. Shade-matching performance using a new light-correcting device. J Esthet Restor Dent. 2015;27(5):285–92.

5. Haddad HJ, Jakstat HA, Arnetzl G, Borbely J, Vichi A, Dumfahrt H, Renault P, Corcodel N, Pohlen B, Marada G, de Parga JA, Reshad M, Klinke TU, Hannak WB, Paravina RD. Does gender and experience influence shade matching quality? J Dent. 2009;37(Suppl 1):e40–4.
6. Pecho OE, Ghinea R, Perez MM, Della Bona A. Influence of gender on visual shade matching in dentistry. J Esthet Restor Dent. 2017;29:E15–23.
7. Della Bona A, Barrett AA, Rosa V, Pinzetta C. Visual and instrumental agreement in dental shade selection: three distinct observer populations and shade matching protocols. Dent Mater. 2009;25:276–81.
8. Paravina RD, Ghinea R, Herrera LJ, Della Bona A, Igiel C, Linninger M, Sakai M, Takahashi H, Tashkandi E, Perez MM. Color difference thresholds in dentistry. J Esthet Restor Dent. 2015;27(Suppl 1):S1–9.
9. Deebs SS. The molecular basis of variation in human color vision. Clin Genet. 2005;67:369–77.
10. Gokce HS, Piskin B, Ceyhan D, Gokce SM, Arisan V. Shade matching performance of normal and color vision-deficient dental professionals with standard daylight and tungsten illuminants. J Prosthet Dent. 2010;103(3):139–47.
11. Curd FM, Jasinevicius TR, Graves A, Cox V, Sadan A. Comparison of the shade matching ability of dental students using two light sources. J Prosthet Dent. 2006;96(6):391–6.
12. Jasinevicius TR, Curd FM, Schilling L, Sadan A. Shade-matching abilities of dental laboratory technicians using a commercial light source. J Prosthodont. 2009;18:60–3.
13. Liberato WF, Barreto IC, Costa PP, Almeida CC, Pimentel W, Tiossi R. A comparison between visual, intraoral scanner, and spectrophotometer shade matching: a clinical study. J Prosthet Dent. 2019;121:271–5.
14. Salat A, Devoto W, Manauta J. Achieving a precise color chart with common computer software for excellence in anterior composite restorations. Eur J Esthet Dent. 2011;6:280–96.
15. Pérez MM, Herrera LJ, Carrillo F, Pecho OE, Dudea D, Gasparik C, Ghinea R, Della Bona A. Whiteness difference thresholds in dentistry. Dent Mater. 2019;35:292–7.
16. Pérez MM, Ghinea R, Pecho OE, Pulgar R, Della Bona A. Recent advances in color and whiteness evaluation in dentistry. Curr Dent. 2019;1(1):23–9.

# Avoiding Complications and Pitfalls with Color in Dentistry

6

Alvaro Della Bona and Oscar Emilio Pecho Yataco

## Contents



## 6.1 Recognizing Color Blindness

The human eye works as a complex light capture system where cells, proteins, and their amino acids from the photoreceptors located at retina are major players, as described in Chap. 3. For the purpose of the present chapter, it is important to recall there are two types of photoreceptors: the cones, used for vision in daylight and for color vision, and the rods, used for vision in dim light. Thus, normal color vision in humans is trichromatic, that is, based on three classes of cones that are sensitive in the blue, green, and red regions of the visible spectrum, with maximum sensitive to light at about 440 nm, 540 nm, and 570 nm, respectively (Fig. 3.5). Each photoreceptor cell contains a single type of photopigment that is composed of a protein moiety (opsin) to which the chromophore 11-cis retinal is covalently bound. Thus, light absorbed by these photoreceptors is processed by neural circuits allowing perception of red, green, yellow, and blue colors individually or in many combinations. As previously mentioned (Chap. 1), such colors comprise the color axes ($a^*$ = red-green axis and $b^*$ = blue-yellow axis) of color space (Fig. 1.2).

A. Della Bona (✉) · O. E. Pecho Yataco
Dental School, Postgraduate Program in Dentistry, University of Passo Fundo, Passo Fundo, RS, Brazil
e-mail: dbona@upf.br



A. Della Bona (ed.), *Color and Appearance in Dentistry*,
https://doi.org/10.1007/978-3-030-42626-2_6

It has been observed that some individuals considered to have normal color vision present a slight variation in color perception, mainly in the red-green region of the spectrum, which is mostly explained by a large number of common variants of the red and green cone pigments generated by gene conversion (e.g., polymorphisms). However, there is a wide range of variation in defective color vision, with severity ranging from mild to severe color blindness. A color vision deficiency or impaired color vision is the decreased ability to see color or differences in color (color blindness). About 1% of males have no functional red cones (protanopes) or no functional green cones (deuteranopes), which are considered severe color blindness. These people have dichromatic color vision, which is based on the use of only two types of photoreceptors, blue plus green (protanopia—no red) or blue plus red (deuteranopia—no green). Males with mild color vision defects have, in addition to blue cones, either normal green plus anomalous green-like cones (protanomalous, ≈1%), or normal red plus anomalous red-like cones (deuteranomalous, ≈5%). These individuals have anomalous trichromatic color vision (Fig. 6.1). The anomalous pigments are red/green chimeras encoded by hybrid genes. The normal red and green pigment spectra overlap significantly but are well separated by wavelength of maximal absorption (λmax) of about 30 nm. The ratio of light absorbed by the red

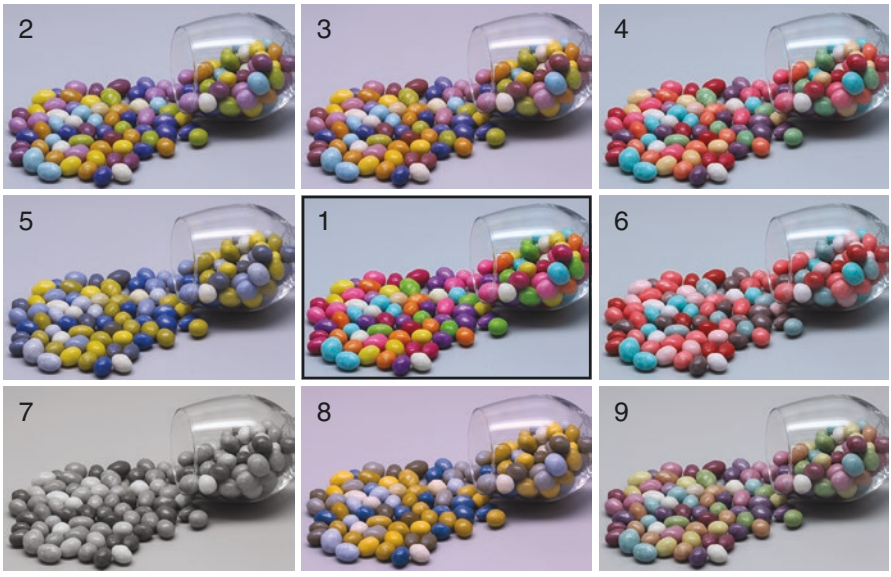


**Fig. 6.1** Appearance of a natural scene to individuals with normal color vision (1) and simulated images (2–9) perceived by various types of color vision defective individuals. (2) Anomalous trichromacy, red-weak, protanomaly. (3) Anomalous trichromacy, green-weak, deuteranomaly. (4) Anomalous trichromacy, blue-weak, tritanomaly. (5) Dichromatic view, red-blind, protanopia. (6) Dichromatic view, blue-blind, tritanopia. (7) Monochromatic view, monochromacy, achromatopsia. (8) Dichromatic view, green-blind, deuteranopia. (9) Monochromatic view, blue-cone, monochromacy. Simulation of images was performed by software from Coblis—Color Blindness Simulator (freely available at http://www.color-blindness.com/coblis-color-blindness-simulator/)

and green cones at various wavelengths is the basis for color perception. Different colors (wavelengths of light) give different ratios of absorption. Protanomalous subjects have a normal green plus a green-like pigment with spectra that differ in λmax by 2–6 nm, and deuteranomalous subjects have a normal red plus a red-like pigment that differ in λmax by 2–9 nm. Therefore, these anomalous trichromats have diminished color discrimination capacity due to reduced ratios of light absorption from the red and green cones at various wavelengths. There are rare cases of individuals who have no functional blue cones (tritanopes, <1:10,000) because of mutations in the blue-pigment gene on chromosome 7. In addition, there is a blue cone monochromacy, which is a severe defective color vision based on only blue cones during daylight. Such individuals may have residual dichromatic color vision based on rods and blue cones during twilight. Figure 6.1 shows how an image is perceived by both normal (central image) and color-deficient individuals.

Whereas dichromats have severe color vision defects, anomalous trichromats vary in the degree of loss of color discrimination capacity. The severity of color vision defects among anomalous trichromats is strongly correlated with the difference in λmax between the red and red-like pigments of deutans (deuteranopia and deuteranomaly), and the green and green-like pigments of protans (protanopia and protanomaly). The smaller the λmax separation, the more severe is the defect. As only the first two genes of the array are expressed in the retina, severity of anomalous trichromacy is determined by difference in λmax (Δλmax) between the two pigments encoded by these two genes. It is worth noting that polymorphism (e.g., Ser180Ala) plays an important role in the spectral separation between the red-green hybrid and normal pigments and therefore in the severity of both protan and deutan color vision defects.

Therefore, genetics and molecular basis of variation in human color vision is a complex scenario. You have learnt that variation in red-green color vision exists among both normal and color-deficient individuals. Differences at amino acids involved in tuning the spectra of the red and green cone pigments account for the majority of this variation. One source of variation is the very common Ser180Ala polymorphism that accounts for two spectrally different red pigments and that plays an important role in variation in normal color vision as well as in determining the severity of defective color vision. This polymorphism most likely resulted from gene conversion by the green-pigment gene. Another source of variation is the existence of various types of red-green pigment chimeras with different spectral properties. The red and green-pigment genes are arranged in a head-to-tail tandem array on the X-chromosome with one red-pigment gene followed by one or more green-pigment genes. The high homology between these genes has predisposed the locus to relatively common unequal recombination events that give rise to red-green hybrid genes and to deletion of the green-pigment genes. Such events constitute the most common cause of red-green color vision defects. The severity of red-green color vision defects is inversely proportional to the difference between the wavelengths of maximal absorption of the photopigments encoded by the first two genes of the array. For more information on various aspects of the genetics of variation in normal and defective color vision refer to the further reading list at the end of this chapter.

In general, the frequency of red-green color vision defects among humans is around 7% for males and 0.5% for females. It seems such values are lower (4–5%) for Asian and African origin males. Therefore, reported frequencies of color vision defects vary not only with evaluated population (with main variables being gender, origin, and age) and method of testing, but also in the presence of systemic and eye fatigue or damage, medical conditions or chronic illnesses (e.g., Alzheimer's and Parkinson's diseases, macular degeneration, diabetes mellitus, glaucoma, and leukemia), and side effect of medication (e.g., some antibiotics and barbiturates). In addition, it has been considered head trauma, deficient diet, great emotional situations, and air pollution.

Nevertheless, studies have shown that the gender influences on the accuracy of visual shade matching are controversial. Some studies reported a better performance from males, others favored females, and many studies showed no evidence of gender influence on visual shade matching (Table 6.1). Such controversy is mostly because of the low number of color-deficient individuals in the population and lack of study power to detect any difference within the examined population.

As mentioned, the measuring method influences on the reported frequency of color vision defects, which is slightly higher when detected by anomaloscopy than values reported using Ishihara or Farnsworth tests. Yet, the later tests, along with the test for color discrimination competency, are the most used to evaluate color competency in Dentistry.

The *Ishihara Color Blindness test* evaluates the red-green color deficiencies, but can be also used to detect some types of acquired dyschromatopsia. It consists of colored plates, each of which contains a circle made of many different sized dots of slightly different colors, spread in a seemingly random manner. Within the dot pattern, differentiated only by color, the observer sees either a number or an abstract illustration. The original and complete test consists of 38 plates, but the existence of a deficiency is usually clear after several plates and, therefore, many studies used a short version of it, containing a 25-plate test (Fig. 6.2). The test can detect observers with protanomaly, protanopia, deuteranomaly, and deuteranopia (Fig. 6.1).

The *Farnsworth Munsell 100 Hue test* was originally developed by Dean Farnsworth, in the 1940s, and it has been used as a standard testing for color

**Table 6.1** Studies reporting on the gender influence on the accuracy of visual shade matching

| | Gender best performing on color perception | | |
|---|---|---|---|
| Studies | Male | Female | No difference |
| Donahue et al. [1] | X | | |
| Milagres et al. [2] | X | | |
| Haddad et al. [3] | | X | |
| Gasparik et al. [4] | | X | |
| Pecho et al. [5] | | X | |
| Imbery et al. [6] | | X | |
| Barrett et al. [7] | | | X |
| Curd et al. [8] | | | X |
| Çapa et al. [9] | | | X |
| Poljak-Guberina et al. [10] | | | X |
| Silva et al. [11] | | | X |

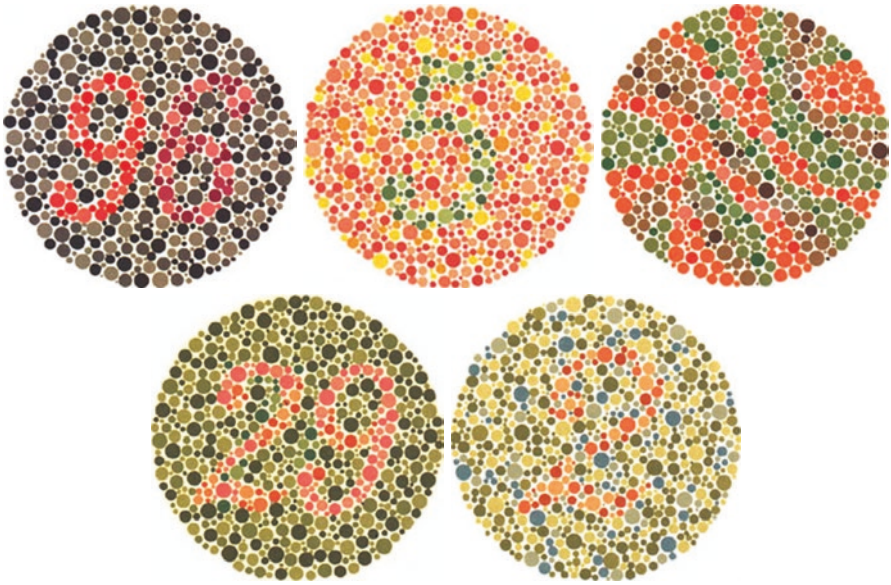

**Fig. 6.2** Five plates from the Ishihara Color Blindness test. *Top left circle*—Normal vision observers see number 96, an observer with protanopia sees number 6, and an observer with deuteranopia sees number 9. *Top middle circle*—Normal vision observers see number 5, an observer with red-green blindness sees number 2. *Top right circle*—It is an abstract illustration. *Bottom left circle*—Normal vision observers see number 29, an observer with red-green blindness sees number 10. *Bottom right circle*—Normal vision observers see number 2, an observer with red-green blindness does not recognize any number

discrimination, which is the ability to discriminate between various hues of a given color. It tests the ability to isolate and arrange small differences in color, having constant value and chroma, covering all the visual hues from the Munsell color system. The aim of the test is to order the colored tiles (usually round pieces of about an inch in diameter) in the correct order. They are arranged in four rows based on color hue. They are organized in order to cover orange/magenta, yellow/green, blue/purple, and purple/magenta hues (Fig. 6.3). The test trays, where the tiles have to be organized, have a black background to isolate and accentuate color hues. Any misplacement can point to some sort of color vision deficiency (Fig. 6.4). It has been used to detect congenital and acquired dyschromatopsias. The test determines if the observer has superior (up to five-pair errors), average (from five-pair to eight-pair errors), or poor (above eight-pair errors) color discrimination.

You may find online, digital derivatives of the test, which is far more popular given its easy access for little or no licensing fee, and an apparent level of accuracy for most audiences. Taking the physical hue test under experimentally sound conditions (e.g., light booth or cabin under controlled illumination) is far more accurate, but the high price of the physical test kit is often prohibitive.

In any case, the test software makes it possible to record, organize, and analyze the testing data. This software is also able to indicate the color discrimination index

**Fig. 6.3** The Farnsworth Munsell 100 Hue test

**Fig. 6.4** Observer taking the Farnsworth Munsell 100 Hue test under controlled conditions (light or viewing booth)

and the type of color vision deficiency based on the number and type of errors for each test participant.

To qualify as an adequate observer for dental color research, potential observers should undergo either Ishihara test or Farnsworth Munsell 100 Hue test and the results should demonstrate, respectively, normal color vision or superior or average color discrimination.

In the *test for color discrimination competency in Dentistry*, the observers should match pairs of shade tabs from two shade guides. One set of tabs should have original markings on tab holders (e.g., A1, B1, 1M2, and 2M2) while the original markings of the other set of tabs should be covered with custom letters, numbers, or symbols (e.g., M, N, 1, 2, and 3) (Fig. 6.5). VITA Classical and VITA Lumin Vacuum (Fig. 3.6) are examples of appropriate shade guides for this test. Visual comparisons should be made under the D65 illuminant of a viewing booth (the overhead/room lights should be turned off), at the distance of 25–33 cm, using 0°/45° or 45°/0°optical geometry. Tabs should be removed from joint tab holders,

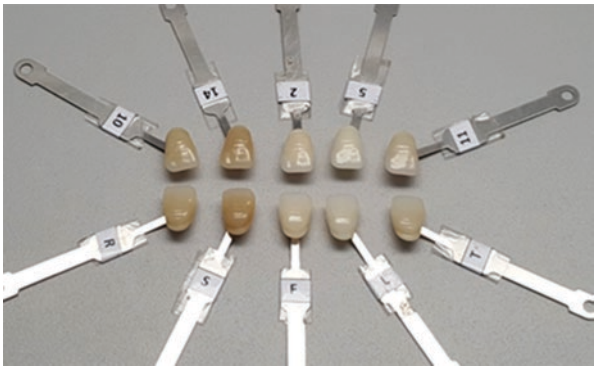

**Fig. 6.5** Original markings from shade guide tabs were covered with custom letters and numbers for the color discrimination competency test

placed on the floor of the viewing booth and mixed. After a period of adaptation by observing the walls of the viewing booth, the observers should begin tab arrangement. At least 12 pairs of tabs should be used for this test and one point should be assigned for each correctly matched pair. The test can be repeated with at least 7-day interval between the tests, in which case the higher of the two scores will be counted (ISO/TR 28642:2016 standard).

Thus, as an alternative to Ishihara and Farnsworth Munsell Hue tests, and to be considered competent for color matching in dentistry, an observer should have correctly assigned at least 60%, 75%, and 85% of the sample pairs presented in the test for poor, average, and superior color discrimination competency, respectively. At least twenty observers with superior- and average-color discrimination competency should participate in evaluation of perceptibility and acceptability visual judgments in dentistry (ISO/TR 28642:2016 standard).

## 6.2 Instruction and Experience to Apply Color Science in Dentistry

Formal color education is rarely present on the curriculum of dental schools. Teaching and training on dental color are usually only part of a lecture on esthetic dentistry and, therefore, color sciences in Dentistry is mostly abbreviated to shade-matching exercises during clinical practices. Chapter 2 presented enough information for dental students and dentists to learn the basics of color science and optical properties and, therefore, correctly apply such knowledge to Dentistry. Considering the information from previous chapters, it is expected that you know how to use dental shade guides (Chap. 2), instrumental shade determination (Chap. 4), and adequate color communication (Chap. 5) in Dentistry. So, it is time to further discuss the influence of color science instruction and experience on color selection and esthetic results in Dentistry.

It has been stated that in shade matching, the eye is the finest null detector. Despite of it, we have learnt that the human eye works as a complex light capture system and that ordinary visual determination of teeth shade is subjective and inconsistent because many observer related variables (e.g., gender, color deficiency, experience, and eye fatigue) can influence on color perception. Furthermore, color

perception does not only vary between people, but it also fluctuates for the same individual over time.

In addition to such human variables, historically, shade determination and communication, and color perception and harmonization are the main color components involved in esthetic dentistry. They are strongly associated with the shade-matching process, which is the most popular clinical approach, but it involves minimal knowledge of color science. Therefore, esthetic excellence is largely an art with primarily subjective interpretation.

In general, in vitro shade matching or any investigation on color and optical properties is associated with homogeneously colored objects (Fig. 6.6). However, teeth vary in color and translucency, and their color perception is mostly related to their surface texture, shape, arch location, adjacent teeth color, and some dental disorders (Fig. 6.7). Consequently, teeth are more difficult to shade match than regular, plain objects (Figs. 6.6 and 6.7). Thus, the ability to either reproduce the exact shade of natural teeth or reach the desired shade using restorative dental materials is one of the most challenging goals in clinical dentistry. Such clinical procedures are

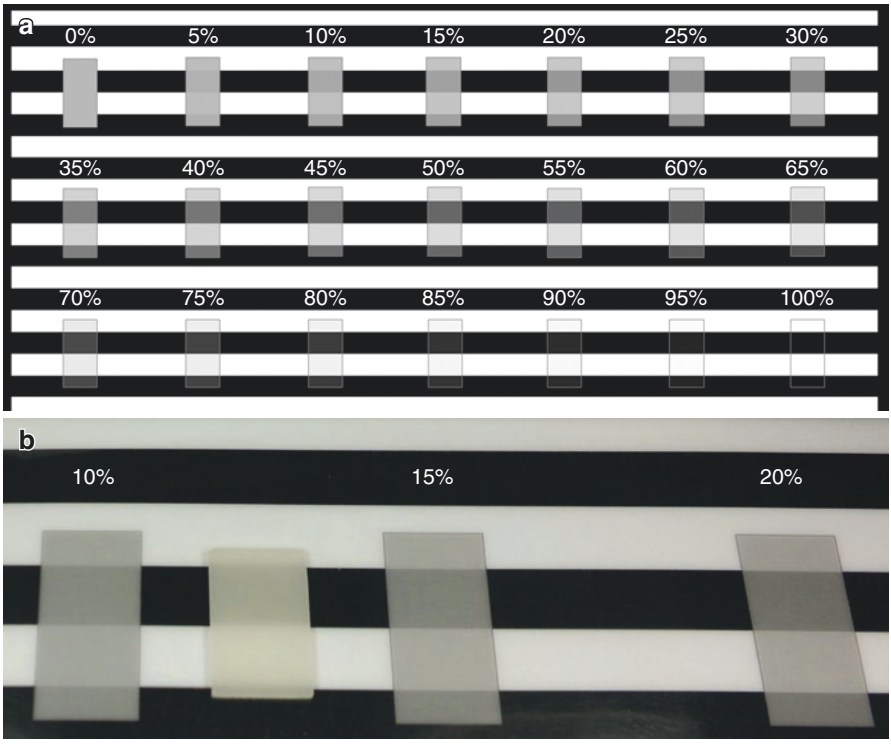


**Fig. 6.6** (**a**) Translucency can be visually evaluated over black and white backgrounds. (**b**) The percentage of translucency of esthetic dental materials (e.g., resin-based composite) can be compared using a visual scale (**a**). Since constant thickness is crucial, in vitro dental color research usually uses flat, plain geometric specimens

**Fig. 6.7** What would be the color of these teeth (top two images) with no mild–moderate dental fluorosis (a disorder of tooth enamel caused by overexposure to fluoride during enamel formation, resulting in opaque white patches/stripes on the enamel)? Impossible to say before removing the superficial intrinsic tooth discoloration using micro-abrasion (bottom image). In addition to usual challenges of visual dental shade determination, the subjectivity of color perception is also confronted by some dental disorders, as shown in this Figure. Patient authorized Dr. A Della Bona to use intra-oral images

traditionally performed by visual shade matching using commercially available shade guides (e.g., Vita Classical and Vita 3D-Master—Chap. 3). Yet, it is important to bear in mind key concepts from Chaps. 1 and 3, such as: *translucency*, which is the gradient between transparent and opaque; *fluorescence* that is the absorption of short wavelength light with the spontaneous emission of longer wavelength light; and *opalescence* that makes a material appear one color with reflected light and another color with transmitted light.

Thus, to perform adequate shade selection for esthetic dentistry, we have to consider several information on color science applied to Dentistry, optical properties of dental tissues and materials, physiological and pathological conditions, position of the observer, surrounding conditions, and illumination. Then, one should know how to adequately report and communicate the selected shade. Theoretical and practical principles on these topics were provided in previous chapters, so we are now able to suggest a *clinical protocol to shade selection for esthetic dentistry* as follows:

1. Watch out for the surrounding environment. The surround is defined as the field outside the background. Clinically, the surround is considered the entire environment in which the stimuli are viewed. Therefore, the surround should be matte and neutral (light grey), removing any bright color from the working field. It is often necessary to cover patient's bright clothing with neutral color apron (bib) and remove colored lipstick and makeup.

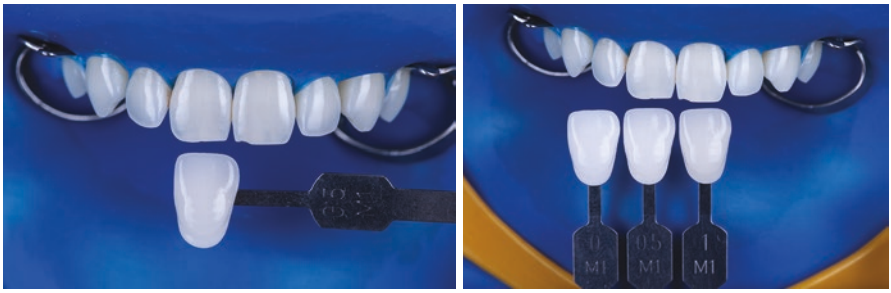


**Fig. 6.8** Despite correct shade tab position related to target tooth, these images show a common clinical *mistake* on shade matching. Shade selection should be done at the beginning of the patient's visit, right after cleaning the teeth. Thus, avoiding enamel dehydration as shown in these images. Pictures taken by Matheus Basegio

2. Teeth should be cleaned. It is usually necessary to clean the target teeth using prophylaxis paste. Avoid enamel dehydration since it reduces translucency and increases in value, having a great chance of misleading the clinician on shade selection. So, cleaned and hydrated teeth (target object) are essential to shade selection. It is worth noting that shade selection should be made at the beginning of a patient's visit (Fig. 6.8).
3. Adequate shade guide. Use the most appropriate shade guide for the clinical procedure. In case of direct resin-based composite restorations, use the shade guide provided with the restorative system or make your own with the restorative material to be used. In case of indirect restorations, most of the ceramic systems follow either Vita Classical or Vita 3D-Master shade designation and, therefore, you should follow the one corresponding to the ceramic system to be used (Fig. 6.9).
4. Position and distance from target. Patient should be viewed at eye level and at arm's length, so the most sensitive part of the retina will be used. It often means a clinician–patient distance of, approximately, 30 cm.
5. Adequate illumination. Visual shade comparisons should be made under different lighting conditions. Initial shade may be taken under a color corrected fluorescent light and then confirmed in natural daylight. For the latter, you may take the patient to an operatory window, in case of adequate daylight.
6. Avoid eye fatigue. Visual shade comparisons should take less than 5 s to avoid eye accommodation and hue sensitivity. The observer may look at a gray wall or patient's bib between each shade evaluation.
7. Shade tab position (Fig. 6.10). Place shade tabs either above or below the tooth to be match, never place shade tab over or adjacent to the tooth to avoid binocular effect. Shade tab should be at same level and inclination as the target tooth. This rationale also applies to shade selection of tooth preparations.
8. Value first. Focus on value first, followed by chroma and then hue. Such method is followed by recent shade guides (e.g., Vita 3D-Master system—Chap. 3).

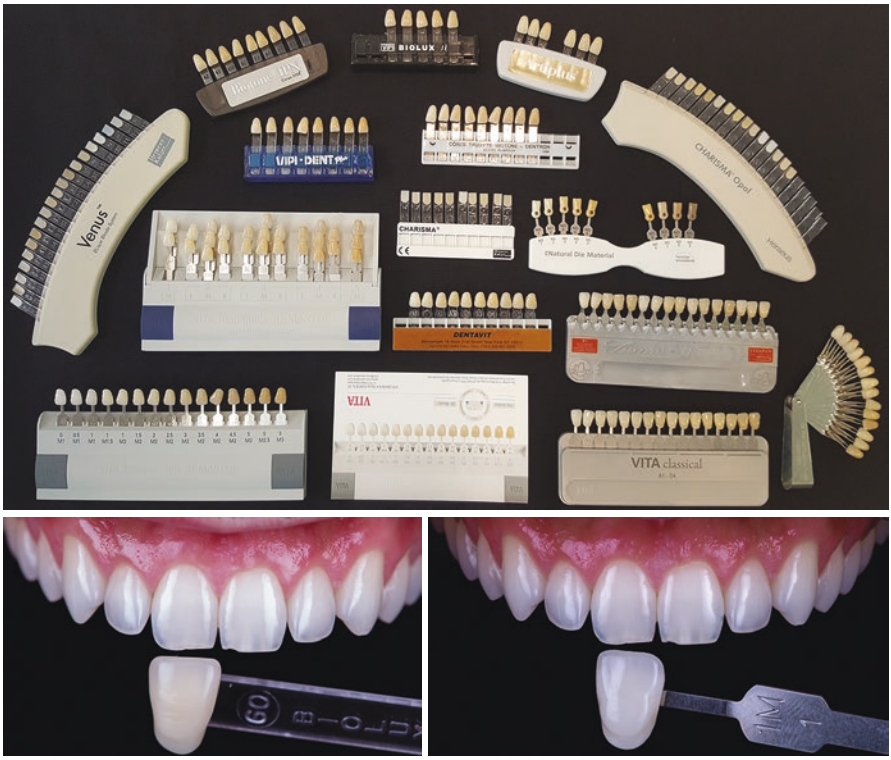


**Fig. 6.9** It should be used the most appropriate shade guide for the clinical procedure. Most direct resin-based composite systems provide their own shade guide for enamel and dentine colors. So, do not use shade guide tabs from different resin-based composites (bottom left image). Ceramic systems usually follow either Vita Classical or Vita 3D-Master shade guides (bottom right image). Pictures taken by Matheus Basegio

9. Esthetic features. The target tooth should be divided into three regions (gingival, middle, and incisal or occlusal thirds) to focus on specific features. The gingival area often offers accurate determination of dentinal chroma. Enamel is thicker in the middle and incisal/occlusal thirds, varying from translucent to transparent. Natural and acquired features should be recorded for replication.
10. Adequate recording and communication. Advances in high-quality digital imaging technology along with digital photography and drawing (Chap. 5) have facilitated recording, simulation, and communication of all clinical features in esthetic dentistry, including color and optical properties. So, use whatever imaging system you are more familiar with, but do not forget to record and communicate any relevant information or feature, especially the shade tab designation (Fig. 6.11). It is worth noting that shade selection should not be done immediately after bleaching, patient should be recalled after few weeks for shade determination.


**Fig. 6.10** Correct position of shade tab is shown at the top left image. The remaining images show common *mistakes* on positioning shade tabs for shade matching of a target tooth or preparation. Pictures taken by Matheus Basegio

**Fig. 6.11** Despite correct shade tab position related to target tooth, these images show a common *mistake* on shade communication: sending an image to dental laboratory with no shade tab designation. You may twist the tab handle so it fits in the image (as shown in the previous figure). Pictures taken by Matheus Basegio


**Fig. 6.12** Shade determination using a spectrophotometer (Vita Easyshade Advance)

Considering the innumerous aspects discussed in this textbook, color determination or dental shade matching is a subjective process. It is the subjectivity inherent in the visual shade-matching process that people try to overcome. Meaning, as the same color can be perceived differently among observers, it is feasible that instrumental shade identification may remove a certain subjectivity that arises from individual color perception. Thus, it has been reported that the main advantage of dental shade-matching instruments is their ability to reduce the imperfections and inconsistencies of visual shade matching. Yet, it has been demonstrated that instruments also have limitations, but color measuring instrumentation has facilitated and supported the clinician's shade selection to match the surrounding dentition and serve as an excellent tool to assist visual shade matching (Chap. 4).

11. Instrument shade selection assistance (Fig. 6.12). As mentioned, many factors can influence the perception of color and clinicians may take advantage of shade-matching technology and dental color measuring instruments

(e.g., spectrophotometers and colorimeters) to assist them on shade selection and communication (please refer to Chap. 4). It is recommended that instrumental color determination be always accompanied by experienced human visual perception.

To sum up, color is a psychophysical phenomenon that can be assessed by both visual and instrumental methods. Yet, additional elements including gloss, fluorescence, opalescence, and translucency affect esthetic dentistry and may influence the characterization of color appearance.

Therefore and despite the recent developments in industrial color difference evaluation, color matching still is largely dependent on visual perception. Although visual evaluation is highly subjective, shade-matching decisions exclusively based on instrumental color matching remain a desideratum far from resolution. With the incorporation of specific corrections on CIEDE2000 color difference formula (Chap. 1), the level of agreement between instrumental and visual color matching seemed to improve.

Similarly, recent developments on technology and materials have offered the chance to improve shade-matching skills in dentistry (Chap. 2). The ability to understand and distinguish color differences in visual shade matching is critical in clinical dentistry. Differences in shade perception due to observer variations can be minimized using additional observers and/or improving shade matching ability, mostly refer to experience. Thus, observers must be trained to optimize their color perception. Therefore, it is recommended that dental schools motivate students to study color sciences and the factors influencing shade matching. Such practicing skills can be learnt and trained clinically and online using the internet (Chap. 2).

Remember that one of the most important goals of any health care provider is restoring patient health, improving quality of life. Accurate shade selection that allows restorations to match the natural teeth positively influences the patient appearance and esthetic self-esteem, improving quality of life.

## 6.3 Management of Color Challenging Restorative Dentistry

The dental profession is experiencing great advances in materials and technology that positively influence the shade-matching process and color management in restorative dentistry. Yet, the overall shade replication process in indirect restorations, e.g., ceramic restorations, is more complicated than each part of the process suggests. In addition to all variables, mostly related to color science mentioned in previous chapters, there are further clinical and laboratory variables that can show single or cumulative effects on the final restoration. These additional variables include color of the substrate; composition, microstructure, thickness, and texture of the restoration; type of framework and veneering material, that is, the layering of

**Fig. 6.13** Esthetic dentistry challenge to mask different colored substrates using ceramic restorations. Image on bottom right shows the esthetic ceramic treatment for the case shown in the bottom left image. Pictures taken by Matheus Basegio

the ceramic system; firing cycles and their parameters; technical skills of the ceramist; and color and opacity of luting agents.

In clinical situations requiring restoration of non-vital discolored teeth or metal abutment structures, dentists are confronted to choose materials to mask the underlying color producing an adequate esthetic restoration. That is one of the greatest challenges in esthetic dentistry. Additionally, the ceramic framework translucency was recognized as a key factor determining the optical characteristics of all-ceramic restorations. The challenge of masking discolored substrates using esthetic restorations is illustrated by two clinical cases (Figs. 6.13 and 6.14).

There are many CAD-CAM ceramic systems combining strength and esthetics to cover different clinical situations. Lithium disilicate-based glass-ceramic has generated considerable interest for restorative dentistry mostly because of adequate strength (350–450 MPa) and optical properties. Yttria-stabilized tetragonal zirconia polycrystal (Y-TZP) is still the strongest and toughness ceramic ever used in dentistry, but its limited translucency and the veneer porcelain chipping are major disadvantages for veneered Y-TZP systems. Future research will show if such problems are solved with the recent introduced monolithic zirconia restorations using highly translucent Y-TZP or with new techniques and materials to produce multilayered all-ceramic restorations (e.g., CAD-on system).

The clinical challenge of masking an undesired discolored substrate has been presented and vastly discussed. Different parameters have been used to evaluate the masking ability of restorative materials, such as contrast ratio (CR) and translucency parameter (TP). In addition, we have seen in previous chapters that CIELAB color space and its associated CIELAB ( $\Delta E^*_{ab}$ ) and CIEDE2000 ($\Delta E_{00}$) total color difference formulas have been extensively used for color research in dentistry and, as a consequence, $\Delta E^*_{ab}$ or $\Delta E_{00}$ have also been used to evaluate the masking ability of restorative materials cemented on colored substrates (Table 6.2). Yet, the International Organization for Standardization (ISO/TR

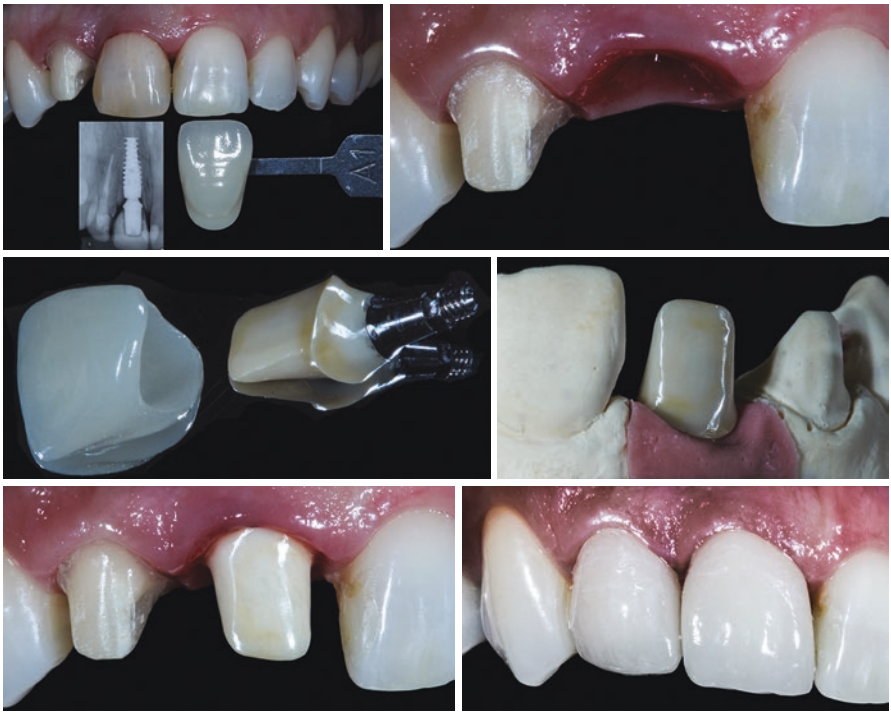

**Fig. 6.14** Esthetic dentistry challenge to mask different colored substrates. Six months after extraction of the central incisor due to root fracture and implant placement. Temporary restoration on the implant was made using the crown from extracted tooth. The abutment infrastructure was customized on zirconia-based ceramic to mask the implant metal substrate. Crowns were fabricated using a glass-ceramic (IPS e.max CAD). Final case right after cementation of ceramic restorations. Pictures taken by Matheus Basegio

28642:2016) states that color differences should be assessed on the basis of 50:50% acceptability (AT: $\Delta E^*_{ab}$ = 2.66 and $\Delta E_{00}$ = 1.77) and 50:50% perceptibility (PT: $\Delta E^*_{ab}$ = 1.22 and $\Delta E_{00}$ = 0.81) thresholds. Thus, if the color difference between two specimens is at or below PT, it represents an excellent match; if the difference is between PT and AT, it represents an acceptable match; and if the difference is above AT, it represents an unacceptable match [12]. So, natural-looking restorations require adequate shade matching and blending optical properties from adjacent natural teeth that need to be accepted by the patient.

**Table 6.2** Studies, in descending chronological order, and methods used to evaluate the masking ability in dentistry

| Studies | Methods |
|---|---|
| Basegio et al. [12] | $\Delta E^*_{ab}$, $\Delta E_{00}$ , TP and $TP_{00}$ |
| Tabatabaian et al. [13] | $\Delta E^*_{ab}$ |
| Basso et al. [14] | $\Delta E_{00}$ and TP |
| Tabatabaian et al. [15] | $\Delta E^*_{ab}$ |
| Dede et al. [16] | $\Delta E_{00}$ |
| Tabatabaian et al. [17] | $\Delta E^*_{ab}$ |
| Oh and Kim [18] | $\Delta E^*_{ab}$ and TP |
| Boscato et al. [19] | $\Delta E^*_{ab}$ and TP |
| Begum et al. [20] | $\Delta E^*_{ab}$ |
| Farhan et al. [21] | $\Delta E^*_{ab}$ |
| Choi and Razzoog [22] | $\Delta E^*_{ab}$ |
| Shono and Al Nahedh [23] | $\Delta E^*_{ab}$ |
| Chaiyabutr et al. [24] | $\Delta E^*_{ab}$ |
| Takenaka et al. [25] | $\Delta E^*_{ab}$ and TP |
| Kim et al. [26] | $\Delta E^*_{ab}$ and TP |
| Chu et al. [27] | $\Delta E^*_{ab}$ and CR |
| Okamura et al. [28] | $\Delta E^*_{ab}$ |
| Chu et al. [29] | $\Delta E^*_{ab}$ |

## Further Readings

1. Donahue JL, Goodkind RJ, Schwabacher WB, Aeppli DP. Shade color discrimination by men and women. J Prosthet Dent. 1991;65(5):699–703.
2. Milagres V, Teixeira ML, Miranda ME, Osorio Silva CH, Ribeiro Pinto JR. Effect of gender, experience, and value on color perception. Oper Dent. 2012;37(3):228–33.

3. Haddad HJ, Jakstat HA, Arnetzl G, Borbely J, Vichi A, Dumfahrt H, Renault P, Corcodel N, Pohlen B, Marada G, de Parga JA, Reshad M, Klinke TU, Hannak WB, Paravina RD. Does gender and experience influence shade matching quality? J Dent. 2009;37(Suppl 1):e40–4.
4. Gasparik C, Grecu AG, Culic B, Badea ME, Dudea D. Shade-matching performance using a new light-correcting device. J Esthet Restor Dent. 2015;27(5):285–92.
5. Pecho OE, Ghinea R, Perez MM, Della Bona A. Influence of gender on visual shade matching in dentistry. J Esthet Restor Dent. 2017;29(2):E15–23.
6. Imbery TA, Tran D, Baechle MA, Hankle JL, Janus C. Dental shade matching and value discernment abilities of first-year dental students. J Prosthodont. 2018;27(9):821–7.
7. Barrett AA, Grimaudo NJ, Anusavice KJ, Yang MC. Influence of tab and disk design on shade matching of dental porcelain. J Prosthet Dent. 2002;88(6):591–7.
8. Curd FM, Jasinevicius TR, Graves A, Cox V, Sadan A. Comparison of the shade matching ability of dental students using two light sources. J Prosthet Dent. 2006;96(6):391–6.
9. Çapa N, Malkondu O, Kazazoglu E, Calikkocaoglu S. Evaluating factors that affect the shade-matching ability of dentists, dental staff members and laypeople. J Am Dent Assoc. 2010;141(1):71–6.
10. Poljak-Guberina R, Celebic A, Powers JM, Paravina RD. Colour discrimination of dental professionals and colours deficient laypersons. J Dent. 2011;39(3):17–22.
11. Silva MA, Almeida TE, Matos AB, Vieira GF. Influence of gender anxiety and depression symptoms, and use of oral contraceptive in color perception. J Esthet Restor Dent. 2015;27(Suppl 1):S74–9.
12. Basegio MM, Pecho OE, Ghinea R, Perez MM, Della Bona A. Masking ability of indirect restorative systems on tooth-colored resin substrates. Dent Mater. 2019;35(6):e122–30.
13. Tabatabaian F, Taghizade F, Namdari M. Effect of coping thickness and background type on the masking ability of a zirconia ceramic. J Prosthet Dent. 2018;119:159–65.
14. Basso GR, Kodama AB, Pimentel AH, Kaizer MR, Della Bona A, Moraes RR, Boscato N. Masking colored substrates using monolithic and bilayer CAD-CAM ceramic structures. Oper Dent. 2017;42:387–95.
15. Tabatabaian F, Shabani S, Namdari M, Sadeghpour K. Masking ability of a zirconia ceramic on composite resin substrate shades. Dent Res J (Isfahan). 2017;14:389–94.
16. Dede DÖ, Armağanci A, Ceylan G, Celik E, Cankaya S, Yilmaz B. Influence of implant abutment material on the color of different ceramic crown systems. J Prosthet Dent. 2016;116:764–69.
17. Tabatabaian F, Masoomi F, Namdari M, Mahshid M. Effect of three different core materials on masking ability of a zirconia ceramic. J Dent (Tehran). 2016;13:340–48.
18. Oh SH, Kim SG. Effect of abutment shade, ceramic thickness, and coping type on the final shade of zirconia all-ceramic restorations: in vitro study of color masking ability. J Adv Prosthodont. 2015;7:368–74.
19. Boscato N, Hauschild FG, Kaizer MR, Moraes RR. Effectiveness of combination of dentin and enamel layers on the masking ability of porcelain. Braz Dent J. 2015;26:654–9.
20. Begum Z, Chheda P, Shruthi CS, Sonika R. Effect of ceramic thickness and luting agent shade on the color masking ability of laminate veneers. J Indian Prosthodont Soc. 2014;14:46–50.
21. Farhan D, Sukumar S, von Stein-Lausnitz A, Aarabi G, Alawneh A, Reissmann DR. Masking ability of bi- and tri- laminate all-ceramic veneers on tooth-colored ceramic discs. J Esthet Restor Dent. 2014;26:232–9.
22. Choi YJ, Razzoog ME. Masking ability of zirconia with and without veneering porcelain. J Prosthodont. 2013;22:98–104.
23. Shono NN, Nahedh HN. Contrast ratio and masking ability of three ceramic veneering materials. Oper Dent. 2012;37:406–16.
24. Chaiyabutr Y, Kois JC, LeBeau D, Nunokawa G. Effect of abutment tooth color, cement color, and ceramic thickness on the resulting optical color of a CAD/CAM glass-ceramic lithium disilicate-reinforced crown. J Prosthet Dent. 2011;105:83–90.
25. Takenaka S, Wakamatsu R, Ozoe Y, Tomita F, Fukushima M, Okiji T. Translucency and color change of tooth-colored temporary coating materials. Am J Dent. 2009;22:361–65.

26. Kim SJ, Son HH, Cho BH, Lee IB, Um CM. Translucency and masking ability of various opaque-shade composite resins. J Dent. 2009;37:102–07.
27. Chu FC, Chow TW, Chai J. Contrast ratios and masking ability of three types of ceramic veneers. J Prosthet Dent. 2007;98:359–64.
28. Okamura M, Chen KK, Kakigawa H, Kozono Y. Application of alumina coping to porcelain laminate veneered crown: part 1 masking ability for discolored teeth. Dent Mater J. 2004;23:180–83.
29. Chu FC, Sham AS, Luk HW, Andersson B, Chai J, Chow TW. Threshold contrast ratio and masking ability of porcelain veneers with high-density alumina cores. Int J Prosthodont. 2004;17:24–8.
30. Brewer JD, Wee A, Seghi R. Advances in color matching. Dent Clin N Am. 2004;48:341–58.
31. Deeb SS. The molecular basis of variation in human color vision. Clin Genet. 2005;67:369–77.
32. Della Bona A, Barrett AA, Rosa V, Pinzetta C. Visual and instrumental agreement in dental shade selection: three distinct observer populations and shade matching protocols. Dent Mater. 2009;25(2):276–81.
33. Della Bona A. Bonding to ceramics: scientific evidences for clinical dentistry. Artes Médicas: São Paulo; 2009. 310p.
34. Della Bona A, Nogueira AD, Pecho OE. Optical properties of CAD-CAM ceramic systems. J Dent. 2014;42(9):1202–9.
35. Della Bona A, Pecho OE, Ghinea R, Cardona JC, Pérez MM. Colour parameters and shade correspondence of CAD-CAM ceramic systems. J Dent. 2015;43(6):726–34.
36. Ghinea R, Pérez MM, Herrera LJ, Rivas MJ, Yebra A, Paravina RD. Color difference thresholds in dental ceramics. J Dent. 2010;38(Suppl 2):e57–64.
37. Neitz M, Neitz J. Molecular genetics of human color vision and color vision defects. In: Chalupa LM, Werner J, editors. The visual sciences, vol. 2. Cambridge: MIT Press; 2004. p. 974–88.
38. Nogueira AD, Della Bona A. The effect of a coupling medium on color and translucency of CAD-CAM ceramics. J Dent. 2013;41(Suppl 3):e18–23.
39. Pecho OE, Ghinea R, Alessandretti R, Pérez MM, Della Bona A. Visual and instrumental shade matching using CIELAB and CIEDE2000 color difference formulas. Dent Mater. 2016;32(1):82–92.
40. Pérez MM, Herrera LJ, Carrillo F, Pecho OE, Dudea D, Gasparik C, Ghinea R, Della Bona A. Whiteness difference thresholds in dentistry. Dent Mater. 2019b;35(2):292–7.
41. Pérez MM, Ghinea R, Pecho OE, Pulgar R, Della Bona A. Recent advances in color and whiteness evaluation in dentistry. Curr Dent. 2019a;1(1):23–9.
42. Pulgar R, Lucena C, Espinar C, Pecho OE, Ruiz-López J, Della Bona A, Pérez MM. Optical and colorimetric evaluation of a multi-color polymer-infiltrated ceramic-network material. Dent Mater. 2019;35(7):e131–9.
43. Salas M, Lucena C, Herrera LJ, Yebra A, Della Bona A, Pérez MM. Translucency thresholds for dental materials. Dent Mater. 2018;34(8):1168–74.
44. Sharpe LT, Stockman A, Jagle H, Nathans J. Opsin genes, cone photopigments, color vision, and color blindness. In: Gegenfurtener KR, Sharpe LT, editors. Color vision, from genes to perception. Cambridge: Cambridge University Press; 1999. p. 3–51.

# Future Developments Using Artificial Intelligence (AI) in Dentistry

7

Luis Javier Herrera Maldonado, Francisco Carrillo Pérez, María del Mar Pérez Gómez, and Alvaro Della Bona

## Contents



## 7.1 Artificial Intelligence in Dentistry

It is well known the huge impact that computational intelligence is having on our entire environment, not only on our daily lives (e.g., autonomous cars, facial recognition systems for security, inference of behavior in social networks, and influence on social and electoral movements in the world), but also in all major areas of research. Distinctively, medical sciences are experiencing challenges on many

L. J. Herrera Maldonado (✉) · F. Carrillo Pérez
Department of Computer Architecture and Technology, Higher Technical School of Information Technology and Telecommunications Engineering, University of Granada, Granada, Spain
e-mail: jherrera@ugr.es; franciscocp@ugr.es

M. del M. Pérez Gómez
Optics Department, Faculty of Science, University of Granada, Granada, Spain
e-mail: mmperez@ugr.es

A. Della Bona
Dental School, Postgraduate Program in Dentistry, University of Passo Fundo, Passo Fundo, RS, Brazil
e-mail: dbona@upf.br



A. Della Bona (ed.), *Color and Appearance in Dentistry*,
https://doi.org/10.1007/978-3-030-42626-2_7

high-tech and scientific frontiers, introducing complex questions in areas like surgery (e.g., intelligent systems to support surgery and video-surgery) and untimely diagnosis of diseases (e.g., decision support diagnosis systems from images and other sources, identification of genetic signature for many tumors, and predisposition to diseases). Precise and individualized medicine is closer to reality, thanks to a massive data storage (e.g., medical images, clinical history, and genetic profile) from patients throughout the world, and their subsequent treatment generating a gigantic network of heterogeneous databases, both public and private.

The advances in computational intelligence techniques are distinct. The resurgence in recent years of neural networks under the new paradigm of deep learning, the incursion of fuzzy systems for the treatment of uncertainty and the labeling of data through "linguistic" terms, and the boom of kernel methods are just some of the most important milestones to emphasize. Particularly in the area of fuzzy systems, the so-called color naming (i.e., color designation) techniques based on fuzzy logic have bridged the gap between the representation of color in computers and the human subjective perception of color. Fuzzy colors allow semantics to be introduced in the description of color using linguistic labels, taking into account the fuzzy boundaries between different color terms.

Finally, deep learning has allowed, in some highly complex problems, for equalizing or even improving the human performance of very complex tasks in areas such as image processing (e.g., object detection and facial identification) and sound processing (e.g., speech synthesis and processing). In dentistry, the first models based on convolutional networks and 2D and 3D photography are emerging for 3D design of dental prostheses, improving their performance. It is also worth noting some industrial initiatives to virtually store information from loads of cases for subsequent processing, building knowledge to optimize treatments using artificial intelligence (Fig. 7.1).

In this current context of high-speed changes, advanced techniques offered by artificial intelligence have opened up a wide range of possibilities in the area of color and esthetic dentistry, including the optimal use of esthetic restorative materials.

## 7.2 Fuzzy Dental Color Spaces: Overcoming the Problem of the Association Between Objective and Subjective Shade Matching

Color perception by human visual system is eminently fuzzy. Color is usually represented by a three-dimensional space such as CIELAB (CIE1976), while the association of every possible point in a color space to a known color name perceived by a human does not always provide a single answer [1, 2]. So, this subjectivity of human color perception depends mostly on the observer and on the environmental conditions (e.g., illuminant and orientation of the illuminant). As presented and described throughout this book, the visual color matching is the most popular dental color assessment method.

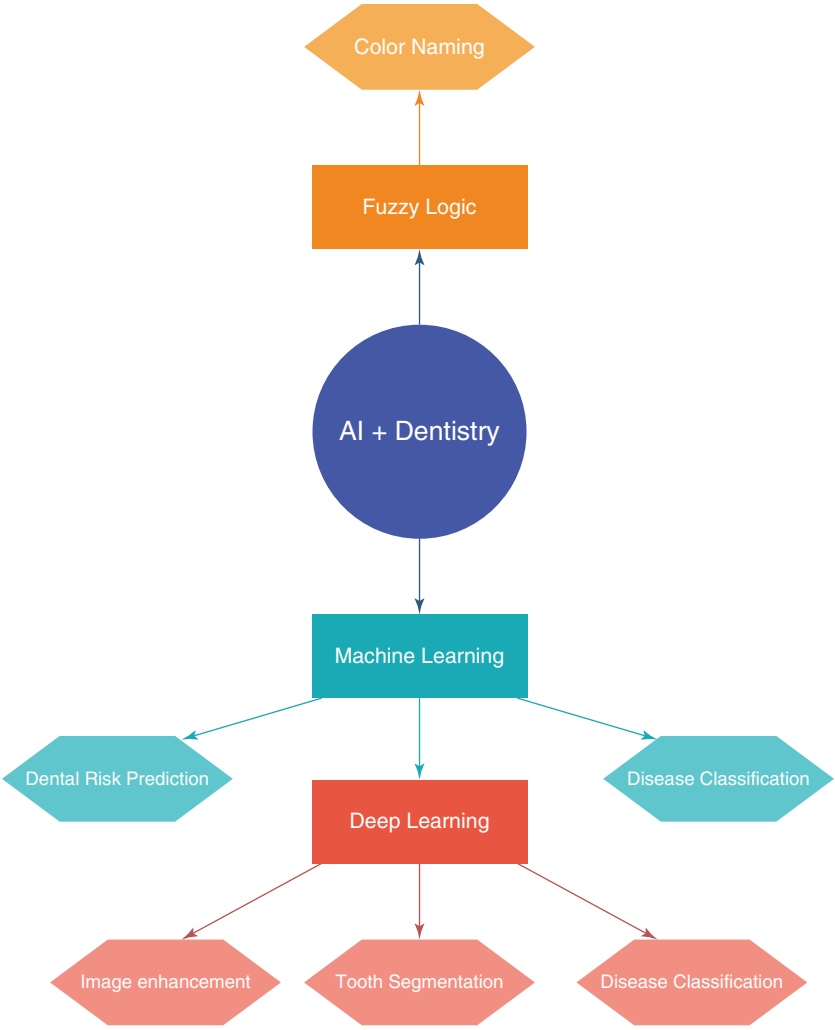


**Fig. 7.1** Schematic representation of how artificial intelligence (AI) can be applied to Dentistry

As most esthetic dental materials use VITA shade designation, color assessment in Dentistry should be standardized, and color differences between the target teeth and the restoration materials should be within the acceptability thresholds. Nevertheless, it has been reported that different manufacturers present material colors that differ from the original VITA shades [3, 4].

It was learnt in this book that human visual system can detect little differences in color; however, the ability to detect these differences in terms of magnitude and nature is limited. Having that in mind, some studies reported on color naming processes in which a fuzzy association was performed between a CIELAB subspace, corresponding to the dental color space, and the VITA shade guides [5]. Thus,

psychophysical experiments were performed, in which experienced observers used the VITA shade tabs to assess a set of dental samples from different manufacturers. Colorimetric measurements using spectroradiometry and the subjective information from the psychophysical experiments were used to create the CIELAB subareas, as fuzzy sets, that the observers associated with each VITA shade. Later this fuzzy set system was associated with the colorimetric measurements of different tooth-shaped pieces and to the VITA Classical shades. Composites taken from two different manufacturers (a VITA-based and a non-VITA-based shade) were used in this second stage of the study to show the applicability of the color designation system to dental clinics.

Another study aimed to provide a set of fuzzy rules to describe the efficacy of a bleaching treatment through VITA shades changes [6]. Human tooth color was determined using a spectroradiometer before and after bleaching. Concurrently, clinical experts performed subjective associations of the objective measurements to the VITA Bleaching shade guide. Then fuzzy sets were optimally estimated according to the objective and subjective measurements, and a set of rules in the form: *if pre-bleaching shade is XX then post-bleaching shade will be XXX*, were provided. It generated a methodology able to model both the uncertainty of the bleaching process and the subjectivity of the color naming (designation) in clinics. Furthermore, confidence values and different possible post-bleaching shades were provided.

## 7.3 Applied Research on Neural Networks and Other Machine Learning Techniques in Dentistry

The use of machine learning (ML) techniques in Dentistry has shown promising results. Some studies have used ML algorithms for the diagnosis and detection of dental diseases. Deep convolutional neural networks (CNNs) were used with 3000 dental radiographic images for diagnosis of dental caries in premolar and molar human teeth [7]. Usually, a larger dataset is required to train a deep convolutional neural network. However, authors used transfer learning where pre-trained weights of a network (trained in another problem domain with sufficient samples) are applied for fine-tuning it in a small dataset. In that case, the pre-trained weights of GoogLeNet Inception v3 CNN network were used. Diagnosis accuracy of dental caries were 89.0% (80.4–93.3) for premolar and 88.0% (79.2–93.1) for molar teeth. In a follow-up study [8], the authors again used transfer learning to train a CNN for diagnosis and prediction of periodontally compromised teeth (PCT). With the deep learning algorithm, the diagnostic accuracy for PCT was 81.0% for premolars and 76.7% for molars.

Another study [9] used a number of machine learning methods to indicate the presence/absence of root caries. Several variables fed the machine learning models, but four of them were relevant: age, income, date of last dental visit, and hours of television watching. The support vector machine showed the best performance to detect root caries with an accuracy of 97.1%, precision of 95.1%, sensitivity of 99.6%, and specificity of 94.3%.

Authors from another study [10] manually extracted features as inputs to an extreme learning machine (ELM) to diagnose gingivitis. The features extracted were based on contrast-limited adaptive histogram equalization (CLAHE) and the gray-level co-occurrence matrix (GLCM). The dataset used by authors contained 93 images, where 58 images were from gingivitis cases and 35 images were from healthy patients (control). Methodology was built upon previous work improving the results obtained, reaching 74% accuracy, 75% sensitivity, and 73% specificity.

In addition to the prediction of dental diseases, predicting of dental care need has been reported using a regression model with LASSO feature selection [11]. Eight features were selected but the most relevant were the following: gum health, demographics, healthcare access, and general health variables. These variables were used as input for different models such as logistic regression, support vector machine, random forest, and classification and regression tree. Random forest outperforms the other models in terms of accuracy (84.1%).

A CNN model was also used for 3D dental segmentation where authors [12] extracted manually a set of geometry features as face feature representations. In the training step, the network was fed with those features, producing a probability vector where each element indicated the fitting probability of a face to the corresponding model part. Authors presented a two-level hierarchical CNNs structure for tooth segmentation: one for teeth-gingiva labeling and other for inter-teeth labeling. Following, Tian et al. [13] proposed a new approach for segmenting and classifying tooth types on 3D dental models. This new approach is based on the sparse voxel octree and 3D convolution neural networks (CNNs). Initially, a two-level hierarchical feature learning was used to solve the problem of misclassification in highly similar tooth categories. Then, a three-level hierarchical segmentation method based on the deep convolutional features was used to conduct segmentation of teeth-gingiva and inter-teeth, respectively, and lastly the conditional random field model was used to refine the boundary of the gingival margin and the inter-teeth fusion region. Results presented in Level-1 network were 95.96% for classification accuracy, whether in Level-2 and Level-3 networks were 88.06% and 89.81%, respectively, being this last one the tooth segmentation accuracy. When it comes to the segmentation of gingival diseases, Rana et al. [14] used a CNN trained with annotations from dental professionals that successfully provides pixel-wise inflammation segmentations of color-augmented intraoral images. The classifier presented obtained an area under the curve (AUC) of 0.746, a precision of 0.347, and a recall of 0.621 in the task of distinguishing between inflamed and healthy gingiva.

The use of image enhancing techniques has been reported to improve low resolution or defective images. Hatvani et al. [15] presented a deep learning-based method for enhancing the resolution of dental computed tomography (CT) images using two CNN architectures (a subpixel network and the U-net network). Different metrics (peak signal-to-noise ratio, structure similarity index, and other objective measures estimating human perception) were used to evaluate the model. CNN approach improved the CT images, allowing better detection of features, such as the size, shape, or curvature of the root canal. Similarly, Hu et al. [16] used Wasserstein generative adversarial networks for artifact correction of low-dose dental CT imaging.

Authors trained a generative adversarial network (GAN) with Wasserstein distance (WGAN) and mean squared error (MSE) loss, called m-WGAN, to remove artifacts and obtain high-quality CT dental images. Peak signal-to-noise ratio (PSNR), structural similarity (SSIM), and statistical properties were used for metrics. The m-WSGAN outperformed general GAN.

## 7.4 A Glance to the Future

Further characterization of tooth color should address the characterization of chromatic map, mainly for the buccal surface of teeth, for different gradients, and the association of different objective color measurements to subjective assessments. This will require a first phase of complex data collection and a second phase of colorimetric map modeling using intelligent systems (diffuse models and convolutional neural networks). Finally, using a color designation process, it will be possible to characterize the tooth chromatic map using dental images. The fusion of these techniques with 3D reconstruction of the teeth will boost the efficacy of restorative dentistry in terms of mechanical and colorimetric properties. Every single step performed on those areas will allow for developing methodological solutions to efficiently obtain accurate information from dental restorations, enhancing communication between dentists and dental laboratory technicians.

## Further Readings

1. Benavente R, Vanrell M, Baldrich R. Parametric fuzzy sets for automatic color naming. J Opt Soc Am A. 2008;25(10):2582–93.
2. Menegaz G, Le Troter A, Sequeira J, Boi J-M. A discrete model for color naming. Eurasip J Adv Signal. 2007;1:1–11.
3. Browning WD, Contreras-Bulnes R, Brackett MG, Brackett WW. Color differences: polymerized composite and corresponding Vitapan classical shade tab. J Dent. 2009;37(Suppl 1):e34–9.
4. Della Bona A, Pecho OE, Ghinea R, Cardona JC, Pérez MM. Colour parameters and shade correspondence of CAD-CAM ceramic systems. J Dent. 2015;43(6):726–34.
5. Herrera LJ, Pecho O, Ghinea R, Rojas I, Pomares H, Guillen A, Ionescu A, Cardona J, Pulgar R, Perez MM. Color fuzzy set design for dental applications. 13th International Conference on Intelligent Systems Design and Applications (ISDA) 2013;281:277–82.
6. Herrera LJ, Pulgar R, Santana J, Cardona JC, Guillén A, Rojas I, Perez MM. Prediction of color change after tooth bleaching using fuzzy logic for vita classical shades identification. Appl Opt. 2010;49(3):422–9.
7. Lee JH, Kim DH, Jeong SN, Choi SH. Detection and diagnosis of dental caries using a deep learning-based convolutional neural network algorithm. J Dent. 2018;77:106–11.
8. Lee JH, Kim DH, Jeong SN, Choi SH. Diagnosis and prediction of periodontally compromised teeth using a deep learning-based convolutional neural network algorithm. J Periodontal Implant Sci. 2018b;48(2):114–23.
9. Hung M, Voss MW, Rosales MN, Li W, Su W, Xu J, Bounsanga J, Ruiz-Negrón B, Lauren E, Licari FW. Application of machine learning for diagnostic prediction of root caries. Gerodontology. 2019a;36(4):395–404.

10. Li W, Chen Y, Sun W, Brown M, Zhang X, Wang S, Miao L. A gingivitis identification method based on contrast-limited adaptive histogram equalization, gray-level co-occurrence matrix, and extreme learning machine. Int J Imaging Syst Technol. 2019;29(1):77–82.
11. Hung M, Xu J, Lauren E, Voss MW, Rosales MN, Su W, Licari FW. Development of a recommender system for dental care using machine learning. Appl Sci. 2019b;1(7):785.
12. Xu X, Liu C, Zheng Y. 3D tooth segmentation and labeling using deep convolutional neural networks. IEEE Trans Vis Comput Graph. 2018;25(7):2336–48.
13. Tian S, Dai N, Zhang B, Yuan F, Yu Q, Cheng X. Automatic classification and segmentation of teeth on 3D dental model using hierarchical deep learning networks. IEEE Access. 2019;7:84817–28.
14. Rana A, Yauney G, Wong LC, Gupta O, Muftu A, Shah P. Automated segmentation of gingival diseases from oral images. In: IEEE Healthcare Innovations and Point of Care Technologies (HI-POCT). Piscataway: IEEE; 2017. p. 144–7.
15. Hatvani J, Horváth A, Michetti J, Basarab A, Kouamé D, Gyöngy M. Deep learning-based super-resolution applied to dental computed tomography. IEEE Trans Radiat Plasma Med Sci. 2018;3(2):120–8.
16. Hu Z, Jiang C, Sun F, Zhang Q, Ge Y, Yang Y, Liang D. Artifact correction in low-dose dental CT imaging using Wasserstein generative adversarial networks. Med Phys. 2019;46(4):1686–96.

The last word is part of the future history.
The last page is the start of a new development.

Comments are welcome at dbona@upf.br. Please use the subject heading "Color and Appearance in Dentistry book." Your comments will be appreciated.

"The noblest pleasure is the joy of understanding."
Leonardo da Vinci

"We must learn to live together as brothers or perish together as fools."
Martin Luther King, Jr.